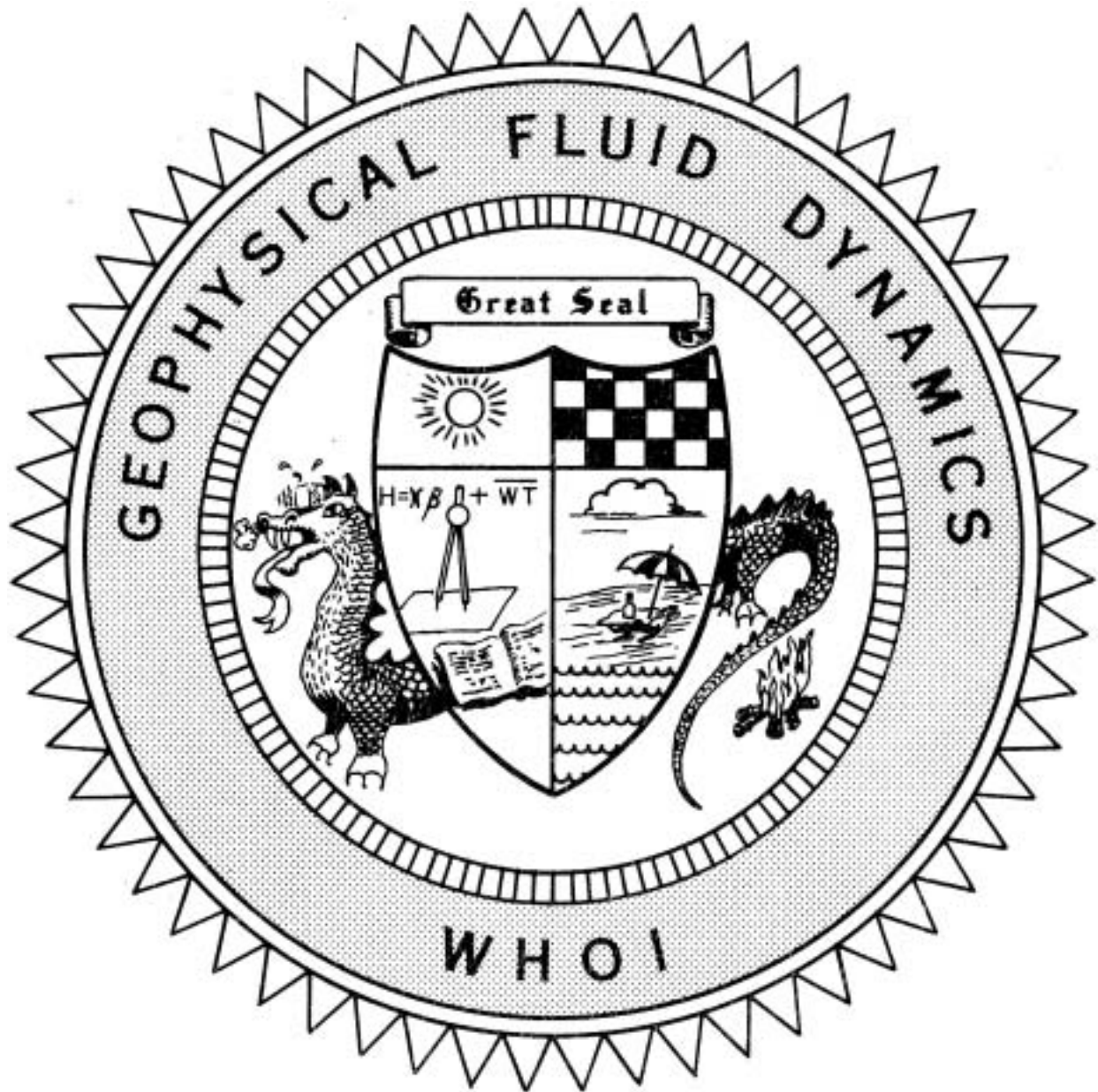


1973  
VOLUME



COURSE LECTURES

SEMINARS

ABSTRACTS

Notes on the 1973  
Summer Study Program  
in  
GEOPHYSICAL FLUID DYNAMICS  
at  
THE WOODS HOLE OCEANOGRAPHIC INSTITUTION

Reference No. 73-41

Contents of the Volumes

- Volume I Course Lectures, Seminars and Abstracts
- Volume II Fellowship Lectures

Participants and Staff Members

Benney, David J.	Massachusetts Institute of Technology
Busse, Friedrich H.	University of California at Los Angeles
Childress, Stephen	Courant Institute of Mathematical Sciences
Davis, Russ E.	Scripps Institution of Oceanography
Howard, Louis N.	Massachusetts Institute of Technology
Huppert, Herbert E.	University of Cambridge, England
Ingersoll, Andrew P.	California Institute of Technology
Keller, Joseph B.	Courant Institute of Mathematical Sciences
Lindzen, Richard S.	Harvard University
Malkus, Willem V.R.	Massachusetts Institute of Technology
Monin, Prof. Andrei	P.P.Shirshov Institute of Oceanology, U.S.S.R.
Mork, Martin T.	University of <b>Bergen</b> , Norway
Phillips, Owen M.	The Johns Hopkins University
Rhines, Peter B.	Woods Hole Oceanographic Institution
Simmons, William F.	Woods Hole Oceanographic Institution
Spiegel, Edward A.	Columbia University
Stern, Melvin E.	University of <b>Rhode Island</b>
Veronis, George	Yale University
Wunsch, Carl	Massachusetts Institute of Technology

Fellows

<b>Bergholz</b> , Robert F.	University of <b>Michigan</b>
Desautel, Richard D.	Stanford University
<b>Fitzjarrald</b> , Daniel E.	University of California at Los Angeles
Frese, Michael H.	Massachusetts Institute of <b>Technology</b>
<b>Gammelsrød</b> , Tor	University of <b>Bergen</b> , Norway
Kimura, Ryuji	University of Tokyo, <b>Japan</b>
Petersen, Erik L.	<b>Technical University of Denmark</b>
St-Maurice, Jean-Pierre	Yale University
Smith, Ronald B.	The Johns Hopkins University
Tupaz, Jesus B.	USN <b>P.G.School</b> , Monterey, California
Wang, Dong-Ping	University of Miami, Florida

### Editor's Preface

Nonlinear wave interactions formed the theme of the fifteenth summer program in Geophysical Fluid Dynamics at the Woods Hole Oceanographic Institution. Owen Phillips was our principal lecturer on this subject. He chose to emphasize interactions among small numbers of discrete wave modes, including both internal and surface gravity waves in his discussions. His lectures provided a stimulating introduction to this important subject.

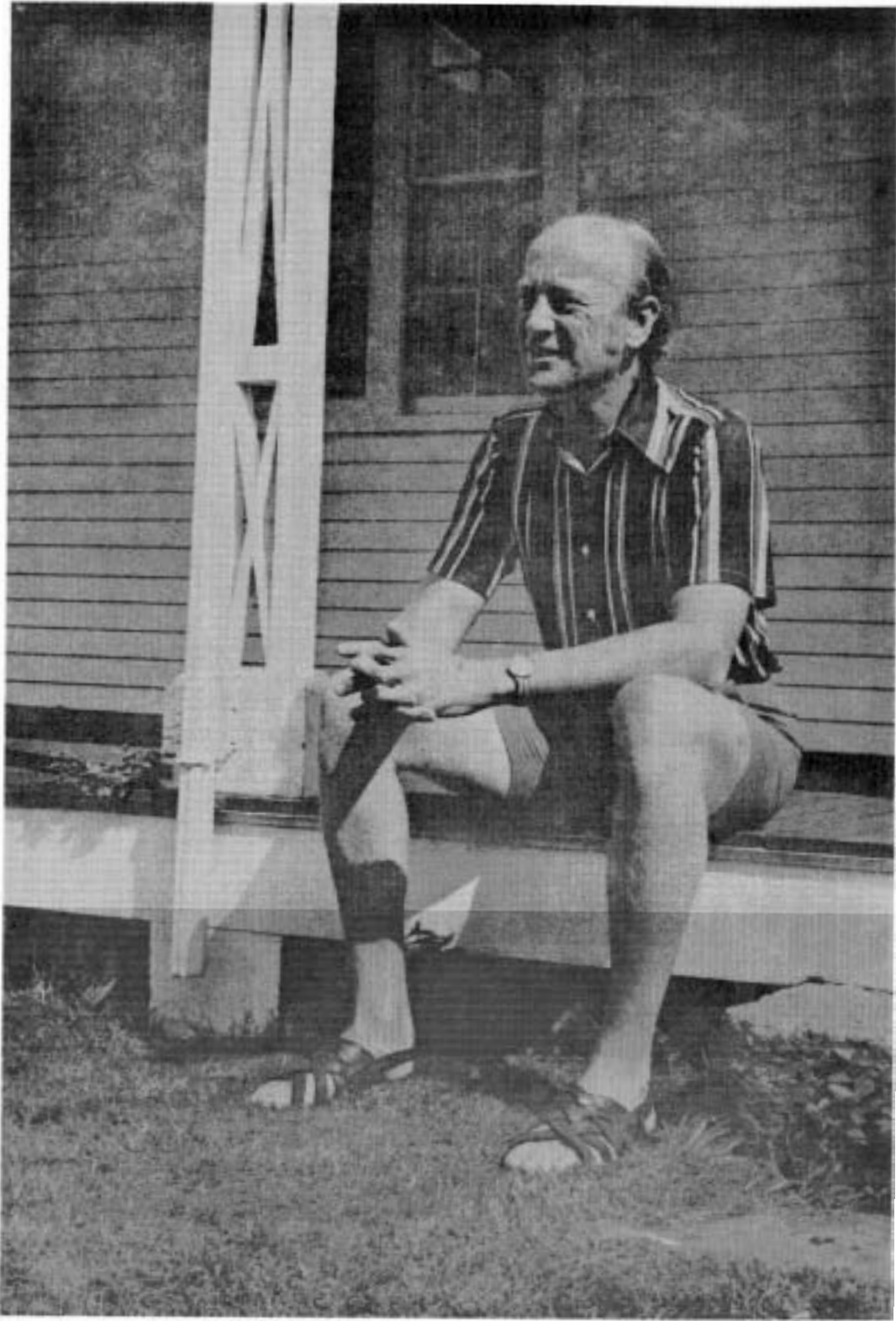
Phillips' lectures were supplemented by a lecture by William Simmons on experiments with interacting internal waves, and a lecture by Carl Wunsch on internal waves in the ocean. Later in the summer, Wunsch gave us a lecture series on practical time-series analysis. Although of a pedagogic nature, these lectures were well-attended and well-received.

There were 11 fellows in the summer program this year. As in previous years, each of the fellows was expected to contribute to the notes from the principal lecture series and to present the results of his summer project in oral and written form. The notes from the principal lectures, as well as abstracts of research seminars follow in Volume I. The papers on the fellows' summer projects are in Volume II.

This year the program was again supported by the National Science Foundation. We thank the N.S.F. for their continuing support.

We all express our thanks to Mary Thayer, who once again has applied her enormous talents and enthusiasm to managing the program. She helped us all, in many ways, both large and small,

Andrew P. Ingersoll.



Owen M. Phillips, Principal Lecturer (waving internally).

CONTENTS OF VOLUME I

Course Lectures, Seminars and Abstracts

COURSE LECTURES

Page No.

by

Owen M. Phillips  
The Johns Hopkins University

NONLINEAR WAVE INTERACTIONS

Lecture #1	WAVES AND WAVE INTERACTIONS - INTRODUCTION.	1
Lecture #2	Resonance Conditions . . . . .	5
Lecture #3	Gravity-Capillary Waves . . . . .	11
Lecture #4	Internal Gravity Waves . . . . .	15
Lecture #5	Interactions of Surface Gravity Waves	21
Lecture #6	Internal-Surface Wave Interactions . . . . .	27
Lecture #7	A Theory of Wave Breaking . . . . .	33

SEMINARS

Experiments with Internal Waves - Resonant Interactions	41
William F. Simmons	
Internal Waves in the Ocean . . . . .	45
Carl I. Wunsch	

TIME SERIES ANALYSIS

Carl I, Wunsch

Lecture #1	Introduction to Practical Time Series Analysis	48
Lecture #2	A Band Limiting Process . . . . .	52
Lecture #3	Examples of Random Signals . . . . .	58
Lecture #4	The Power Density Spectrum . . . . .	60
Lecture #5	Model of an Instrument . . . . .	63

CONTENTS OF VOLUME I (continued)

	Page No.
ABSTRACTS	
Long Waves . . . . .	71
David J. Benney	
A Simple Magnetostatic Model of Sunspots .	72
Friedrick H. Busse	
Transition to Turbulence	73
Friedrick H. Busse	
Bioconvection . . . . .	74
Stephen Childress	
Perturbed Turbulence and Eddy Viscosity	81
Russ Davis	
Dust Devils - Movies and Slides .	82
Daniel B. FitzjarraId	
Plane Wave Solutions to Reaction-Diffusion Equations .	82
Louis N. Howard	
The Effect of Bottom Topography in Rotating Stratified Systems	84
Herbert E. Huppert	
Jupiter's Great Red Spot: A Free Atmospheric Vortex?	88
Andrew P. Ingersoll	
Ray Theory of Wave Propagation	89
Joseph B. Keller	
Asymtotic Theory of Wave Propagation .	90
Joseph B. Keller	
Forced Periodic Vibrations of Nonlinear Systems .	90
Joseph B. Keller	
An Experiment on "Heat Island" Convection .	91
Ryuji Kimura	



CONTENTS OF VOLUME I (continued)

	Page No.
Cumulus Convection and Equatorial Waves in the Atmosphere Richard S. Lindzen	94
Macrodynamics of Planetary Dynamos W.V.R.Malkus and M.R.E.Proctor	95
Wind-induced Internal Waves in a Stratified Ocean Martin T. Mork	99
Models of Eddies and Waves Peter B. Rhines	99
Archimedean Instabilities in Two-phase Flows Edward A. Spiegel	100
Diabatic and Wind Stress Adjustments of Rotating Currents Melvin E. Stern	100
Thermocline in a Rotating Annulus Melvin E. Stern	101
Model of World Ocean Circulation George Veronis	102
Oceanic Microstructure Andrei S. Monin	104

COURSE LECTURES  
by  
Owen M. Phillips  
The Johns Hopkins University

NONLINEAR WAVE INTERACTIONS

(All references are listed at end of course - p.38)

Lecture #1. WAVES AND WAVE INTERACTIONS - INTRODUCTION

1. A wave can be defined somewhat loosely as a disturbance or pattern which moves through a medium without propagation of the medium as a whole. There are a large variety of waves that are of interest in geophysical fluid dynamics, for example:

- a. surface gravity waves (deep water, and shallow water)
- b. capillary waves
- c. internal gravity waves in media with either continuous or discontinuous density distribution
- d. inertial waves
- e. Rossby waves
- f. edge waves
- g. and others.

2. For waves with infinitesimal amplitude, we can approximate the full equations of motion by linear equations. In symbolic form we can write

$$\mathcal{L}(p) = 0, \quad (1)$$

where  $\mathcal{L}$  is some linear operator whose precise form depends upon the type of wave in question and  $p$  is some property of the waves, such as pressure, or the free surface displacement,

The solution may be expressed in the form

$$p = a(\epsilon x, \epsilon t) e^{i\chi}, \quad (2)$$

where  $\epsilon \ll 1$ ,  $a$  is a slowly varying amplitude, and  $\chi$  is the phase function.  $e^{i\chi}$  then represents the oscillatory part of the wave. The amplitude is assumed to vary only slightly over a wavelength. The time scale of the amplitude variation is large compared to a period.

For example, the wave may have the form shown in Fig.1



Fig.1

Much of the phenomena associated with waves are well-described by a solution of this type. This suggests that the nonlinear terms are not crucial to the wave dynamics, even though they may be important in some cases. This is in contrast to turbulence, where the interactions are much faster and inherently nonlinear.

3. We may define a local wave number vector  $\underline{k}$  as

$$k_i \equiv \frac{\partial \chi}{\partial x_i} \quad (i = 1, 2, 3), \quad (3)$$

where  $k_i = (k_1, k_2, k_3)$  are the components of  $\underline{k}$  in  $(\underline{x}) = (x_1, x_2, x_3)$ , the frequency is defined as

$$\eta \equiv -\frac{\partial \chi}{\partial t}. \quad (4)$$

If the wave number and frequency are constant, the phase function will have form

$$\chi \sim \underline{k} \cdot \underline{x} - \eta t. \quad (5)$$

A simple kinematical relation can be derived which relates the time rate of change of the wave number density (or number of waves/unit length) to the number of wave crests which pass by a particular point/unit time, This is,

$$\frac{\partial k_i}{\partial t} + \frac{\partial \eta}{\partial x_i} = 0 \quad (6)$$

This relation is sometimes called the equation for the conservation of waves.

4. The form of the equation  $\mathcal{L}(p) = 0$  will vary according to the type of wave motion. Substitution of operation (2) into equation (1) gives a condition which must be satisfied if the solution is to have the assumed form. This is called the dispersion relation which relates the frequency to the wave number,

$$n = n(\underline{k}) \tag{7}$$

We can define the phase velocity as

$$v_p \equiv \frac{n}{k} \underline{\hat{k}} \quad \text{where} \tag{8}$$

$\underline{\hat{k}}$  is a unit vector in the direction of the wave number vector,

(Notes submitted by Robert Bergholz)

Second Half of Lecture #1

Consider the energy density in real space of a modulated monochromatic wave, that is, a wave  $p(\underline{x}, t) = \int a(\underline{k}) e^{i(\underline{k} \cdot \underline{x} - n(\underline{k})t)}$  where  $a(\underline{k})$  is sharply peaked near  $\underline{k}_0 = \underline{k}_0$  and zero elsewhere. If the energy density is proportional to  $p^2$  then we can show that it has the form

$$p^2 \approx F(\underline{x} - \underline{c}_g(\underline{k}_0)t)$$

where  $\underline{c}_g = \nabla_{\underline{k}} n$ . Since  $p$  is real

$$p^2 = pp^* = \iint a(\underline{k}_1) a(\underline{k}_2) e^{i[(\underline{k}_1 - \underline{k}_2) \cdot \underline{x} - (n(\underline{k}_1) - n(\underline{k}_2))t]} d\underline{k}_1 d\underline{k}_2$$

and since only those  $\underline{k}$ 's near  $\underline{k}_0$  contribute to this integral (because of the nature of  $a$ ) we may write with reasonable accuracy that

$$n(\underline{k}_1) - n(\underline{k}_2) = \underline{c}_g(\underline{k}_0) \cdot (\underline{k}_1 - \underline{k}_2).$$

Therefore

$$p^2 \approx \iint a(\underline{k}_1) a(\underline{k}_2) e^{i(\underline{k}_1 - \underline{k}_2)(\underline{x} - \underline{c}_g(\underline{k}_0)t)} d\underline{k}_1 d\underline{k}_2 \approx F(\underline{x} - \underline{c}_g(\underline{k}_0)t)$$

Similarly, the wave momentum propagates at the group velocity,

Given below are some of the relevant formulae for some of the types of waves mentioned above,

	$\mathcal{L}(p)$	$n = n(k)$	$\underline{c}_g$
surface gravity waves (deep water)]	$\frac{\partial \phi}{\partial t^2} + g \frac{\partial \phi}{\partial z} = 0 \text{ at } z=0$	$n = (gk)^{1/2}$	$\frac{1}{2} \left( \frac{g}{ k } \right)^{1/2} \frac{k}{ k }$

	$\mathcal{L}(\rho)$	$n = n(k)$	$\mathcal{L}g$
Capillary waves	-	$n = \left(\frac{Tk^3}{\rho}\right)^{1/2}$	$\frac{3}{2} \left(\frac{Tk^3}{\rho}\right)^{1/2} \frac{k}{ k }$
internal waves ( $\rho(z)$ linear)	$\left(\frac{\partial^2}{\partial t^2} \nabla^2 + N^2 \frac{\partial^2}{\partial z^2}\right) w = 0$ $N^2 = -\frac{g}{\rho} \frac{\partial \rho}{\partial z}$	$n = N \frac{k_z}{ k }$ $v = N \cos \theta$	EXERCISE FOR READER $\mathcal{L}g \perp k$
	$\nabla_k^2 = \frac{\partial^2}{\partial x^2} + \frac{\partial^2}{\partial y^2}$	$\mathcal{L} \frac{\mathbf{i}}{ \mathbf{i} }$ a horizontal unit vector parallel to the horizontal part of	

A simple calculation shows that the phase velocity of gravity waves is twice the group velocity, and this is verified by the pebble-in-the-pool experiment in which a wave group is produced whose individual waves propagate through the group from back to front. For capillary waves, the group velocity is 3/2 the phase velocity. The standing waves in front of a fishing line entering a flowing stream are capillary waves whose phase velocity equals the stream velocity, and they are radiating energy ahead of the line into the stream at the group velocity.

The dispersion relation for internal waves shows that these waves are anisotropic (waves are isotropic if  $n = n(|k|)$ ). Waves propagating horizontally have the largest frequency, and they correspond to vertical columns of fluid bobbing up and down.

It is physically reasonable that the group velocity for internal waves should be perpendicular to the wave vector. Since the fluid is incompressible  $\nabla \cdot (\mathbf{u} e^{i(\mathbf{k} \cdot \mathbf{x} - n(\mathbf{k})t)}) = 0$  and this implies  $\mathbf{k} \cdot \mathbf{u} = 0$ . Therefore, the energy flux being  $\overline{p \mathbf{u}}$ , where  $p$  is the pressure and  $\mathbf{u}$  the velocity, it must be parallel to  $\mathbf{u}$  and hence perpendicular to  $\mathbf{k}$ . (This argument can lead one astray in certain cases, in particular in the case of Rossby waves!)

Waves are said to be dispersive if the phase velocity is a non-constant function of wave vector magnitude. Both surface gravity waves and capillary waves are dispersive,

The nonlinear effects which are to be discussed are of two distinct types:

- 1) the effect of large amplitude on a single wave train,
- 2) the effect of two or more wave trains upon each other,

Some examples of the first class are:

- a) the distortion and change of phase speed of a single wave train of finite amplitude (Stokes),
- b) the instability of a train of Stokes waves to small changes in envelope (Benjamin and Feir),
- c) the interaction of waves and currents (Longuet-Higgins and Stewart),
- d) the cresting and breaking of waves,

As for the second, such questions as possibility of energy exchange and rate of energy exchange will be discussed. The papers of Hasselmann on surface waves, of McEwan and of Martin, Simmons and Wunsch on internal waves, and of McGoldrick on capillary waves will guide us in some of our studies in this area.

(Notes submitted by Michael H. Frese)

## Lecture #2. RESONANCE CONDITIONS

The general equation of motion for weak interactions has the form

$$\begin{aligned} \mathcal{L}(p) &= \text{nonlinear terms} \\ \text{or} \\ \mathcal{L}(p) &= \epsilon N(p) \end{aligned} \tag{2.1}$$

where  $N$  = nonlinear operator

and

$\epsilon$  is a small ordering parameter whose magnitude is described by the ratio of magnitudes of nonlinear and linear terms,

For the most simple case we consider the problem of the spatially homogeneous interaction of two uniform wave trains.

Assume the solution  $p$  has the form

$$p = \sum_{n=1}^m a_n(\epsilon t) \cos [k_n \cdot x - \omega_n t + \delta_n(\epsilon t)] \tag{2.2}$$

$$p = \sum_{n=1}^m a_n(\epsilon t) \cos \chi_n \quad (2.3)$$

$$\text{where } \chi_n = k_n \cdot \underline{x} - n_n t + \delta_n(\epsilon t)$$

and  $m$  denotes the number of interacting wave trains.

Question: Under what conditions does the solution  $p$  vary significantly with time?

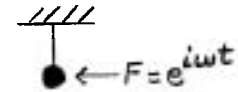
For analogy, we consider the simple problem in mechanics of free and forced oscillations of a pendulum:

$$\ddot{x} + \mu^2 x = 0 \quad \text{free oscillations}$$

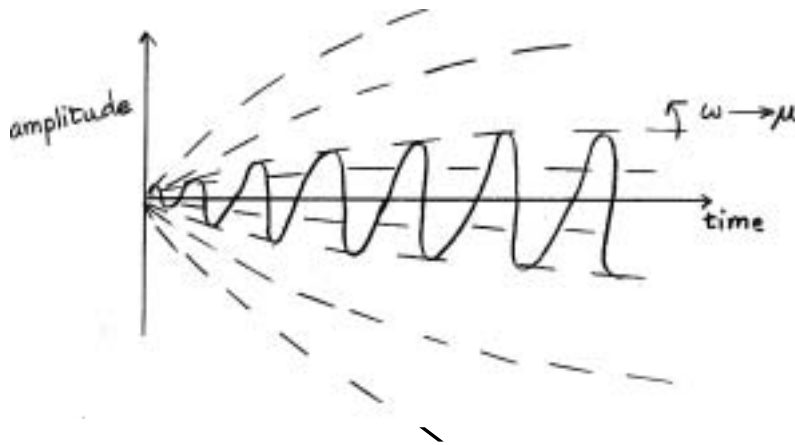


$$\ddot{x} + \mu^2 x = \epsilon e^{i\omega t} \quad \text{forced oscillations with initial conditions}$$

$$x = \dot{x} = 0 \quad \text{at } t = 0.$$



Then the general solution for the forced oscillation problem is oscillations at the forcing frequency with amplitude dependent on the relative values of  $\omega$  and  $\mu$ , i.e. forcing frequency and system natural frequency.



Note that for  $a_n = \text{constant}$  and  $\delta_n = 0$ ,

$$\mathcal{L}(a \cos \chi_n) = 0.$$

Substitution of the expected solution form  $p$  given by (2.3) into (2.1) produces L.H.S. and R.H.S. terms of the following forms ( $n = 1, 2$ ):

$$\text{L.H.S. } \mathcal{L} [a(\epsilon t) \cos \chi_n] = \epsilon \dot{a}_n \cos \chi_n + \epsilon \delta \sin \chi_n + O(\epsilon^2) \quad (2.5)$$

and

$$\text{R.H.S. } \epsilon N [a(\epsilon t) \cos \chi_n] = \epsilon a_1 a_2 \cos \chi_1 \cos \chi_2 + O(\epsilon^2 a^2) \quad (2.6)$$

The R.H.S. terms (2.6) may be rewritten in terms of sum and difference component terms:

$$\text{R.H.S.} \rightarrow \epsilon a^2 \cos(\chi_1 + \chi_2) \mp \epsilon a^2 \cos(\chi_1 - \chi_2).$$

Clearly the initial two waveforms combine in the nonlinear forcing function to produce two new waveforms.

With the definition

$$\hat{\chi}_n = k_n \cdot x - n t$$

it is seen that the two wave trains considered here will be resonant with a third wave train  $(k_3, n_3)$  if

$$\hat{\chi}_1 \pm \hat{\chi}_2 \pm \hat{\chi}_3 = 0$$

This relation and the definition  $\hat{\chi}_n$  lead to the relations

$$\left. \begin{aligned} k_1 \pm k_2 \mp k_3 &= 0 \\ n_1 \pm n_2 \mp n_3 &= 0 \end{aligned} \right\} \quad (2.7)$$

Also, for each  $n$ , we have the dispersion relation

$$n_n = n_n(k_n).$$

These relations are the conditions for exact resonance,

This interaction is very selective and is a weak interaction since

interaction time scale,  $T = O(\epsilon^{-1})$  in general.

Note: for surface gravity waves,  $T \sim O(\epsilon^{-2})$ .

Questions: 1) Do solutions exist?

2) If so, what about variations with time?

Answers: 1) Depends on the problem.

One of the simplest ways to determine existence of a solution in many cases is by geometric means.



Example: For capillary-gravity waves, we have

$$n = (gk + \gamma k^3)^{1/2}$$

$$\text{where } \gamma = \frac{T}{\rho}.$$

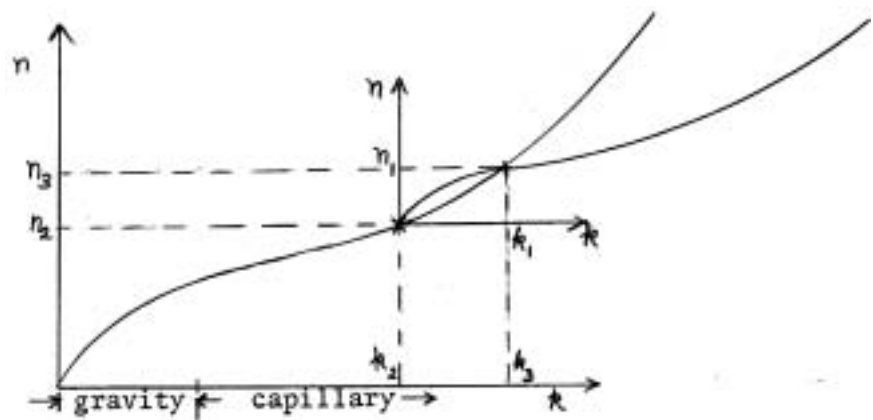
We want to find solutions for which

$$k_1 + k_2 = k_3$$

$$\text{and } n_1 + n_2 = n_3.$$

The geometric determination is

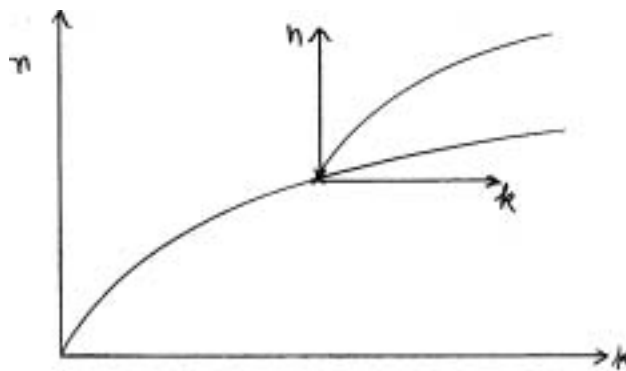
Capillary-Gravity Waves



Thus such a  $(k_3, n_3)$  solution exists. For two-dimensional  $\mathbb{R}^2$ , the two curves in this diagram become two surfaces whose intersection is a locus of  $(k_3, n_3)$  points rather than a single point.

A similar determination for pure gravity waves at the order  $\mathcal{E}$  shows that no resonant solution exists:

Pure Gravity Waves



Thus no intersection of the two curves exists, There is no non-trivial solution to the triplet interaction case.

Answers: 2) To determine time variations of solutions to the triplet interaction problem, one may either sort out the terms in the governing equations or use a variational approach to save work (Simmons 1969).

We define  $p$  such that the wave energy

$$E = \beta p^2,$$

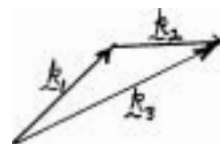
where  $\beta$  is independent of  $k$  and For surface gravity waves,  $p$  could be surface displacement. For internal gravity waves,  $p$  could be the velocity.

Then we have to lowest order in  $\epsilon$

$$\underline{k}_1 + \underline{k}_2 = \underline{k}_3 \quad (2.8)$$

and

$$n_1 + n_2 = n_3 \quad (2.9)$$



In analogy to the theory of vibrations of coupled oscillators, we utilize the concept of interaction coefficients to write

$$\dot{a}_1 = n_1 C a_2 a_3 \quad (2.10)$$

$$\dot{a}_2 = n_2 C a_3 a_1 \quad (2.11)$$

$$\dot{a}_3 = -n_3 C a_1 a_2 \quad (2.12)$$

where  $C = C(\underline{k}_n)$  = interaction coefficient and all the  $C$ 's turn out to be the same because

$$E \propto p^2.$$

These relations imply energy conservation for the triplet as is shown by

$$E_i \propto a_i^2$$

and from (2.10-2.12)

$$a_1 \frac{da_1}{dt} = n_1 C a_1 a_2 a_3$$

$$a_2 \frac{da_2}{dt} = n_2 C a_1 a_2 a_3$$

$$a_3 \frac{da_3}{dt} = -n_3 C a_1 a_2 a_3$$

or

$$\frac{dE}{dt} = \frac{d}{dt} (a_1^2 + a_2^2 + a_3^2) = C a_1 a_2 a_3 (n_1 + n_2 - n_3).$$

Since  $(n_1 + n_2 - n_3) = 0$  by (2.9), it follows

$$\frac{dE}{dt} = 0.$$

Note: The energy conservation relation will determine a relation for  $C_1, C_2, C_3$  when the C's are different, i.e.  $E \neq p^2$ .  
Bretherton (1969) discusses how to fix  $\beta$  for various cases.

Partition Integrals:

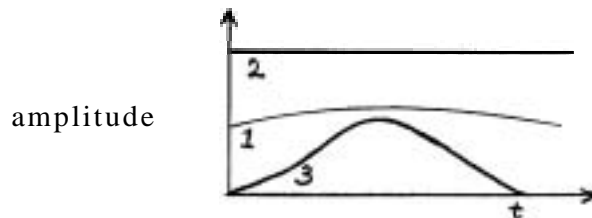
We obtain two energy partitioning relations by cross-multiplying and integrating (2.12) with (2.10) and with (2.11). The two resulting partition relations are:

$$\left. \begin{aligned} \frac{a_1^2}{n_1} + \frac{a_2^2}{n_2} &= \text{constant} \\ \frac{a_1^2}{n_1} + \frac{a_3^2}{n_3} &= \text{constant} \end{aligned} \right\} \quad (2.13)$$

Conclusions:

1)  $a_1, a_2$   $\left\{ \begin{array}{l} \text{increase} \\ \text{decrease} \end{array} \right\}$  as  $a_3$   $\left\{ \begin{array}{l} \text{decreases} \\ \text{increases} \end{array} \right\}$

2) Solutions are in the form of  
Jacobi Elliptic Functions.



3) Suppose  $a_1, a_2 \ll a_3$   
then from (2.10 - 2.12)

$$\begin{aligned} \dot{a}_3 \sim 0 &\longrightarrow a_3 \sim \text{constant} \\ \left\{ \begin{array}{l} \dot{a}_1 = (n_1 C a_3) a_2 \\ \dot{a}_2 = (n_2 C a_3) a_1 \end{array} \right\} &\longrightarrow \left\{ \begin{array}{l} \ddot{a}_1 = (n_1 n_2 C^2 a_3^2) a_1 \\ \ddot{a}_2 = (n_1 n_2 C^2 a_3^2) a_2 \end{array} \right\} \end{aligned}$$

Since  $(n_1 n_2 C^2 a_3^2) > 0$ , the  $a_1, a_2$  solutions are of the form

$$\left. \begin{array}{l} a_1 \\ a_2 \end{array} \right\} \propto e^{\lambda t}, e^{-\lambda t}$$

where  $\lambda = (n_1 n_2 C^2 a_3^2)^{1/2}$ .

Thus exponentially growing solutions are possible for the perturbation waves; they increase until condition (a) is violated. Note the integrals say that  $a_1^2 = \text{const} - (\text{small constant}) e^{2\lambda t}$ .

Thus, any wave train  $(k_3, \omega_3)$  is unstable to lower frequency disturbances  $(k_1, \omega_1)$  and  $(k_2, \omega_2)$  at wave numbers which form a resonant triad (Hasselmann, 1967).

Notes submitted by  
Richard D. Desautel  
and Erik L. Petersen

### Lecture #3. GRAVITY-CAPILLARY WAVES

#### Introduction

We saw in the last lecture that for gravity-capillary waves the dispersion relation is given by

$$\omega = (gk + \gamma k^3)^{1/2}$$

It was also shown that gravity-capillary waves can form resonant triads. The interactions between three gravity-capillary waves were recently studied by Valenzuela and Laing (1972). They found that energy was denuded from a wavelength of 1.7 cm in both directions of the spectrum and they could in that manner explain an apparent dip in the observed energy-wavelength diagrams. McGoldrick (1965) also studied these interactions.

#### 1. Harmonic Resonance Theory

The phase velocity  $C$  of gravity-capillary waves is given by

$$C = \sqrt{\frac{g}{k} + \gamma k}$$

and has a minimum for  $k_m = \sqrt{g/\gamma}$ . A plot of  $C$  versus  $k$  is given on Fig. 1.

#### First Harmonic

It is easy to see that for

$$k_1 = \sqrt{\frac{g}{2\gamma}} = \frac{k_m}{\sqrt{2}}$$

we can form a resonant triad of the wave interacting with itself and its first harmonic. The reason is that

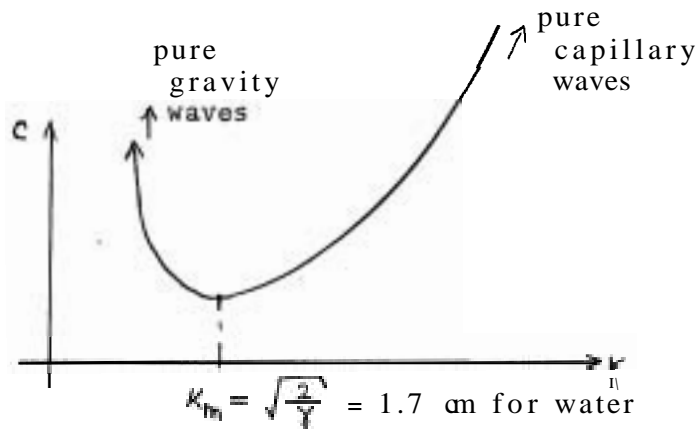


Fig. 1

$$k_1 + k_1 = k_2 = \sqrt{\frac{2g}{\gamma}} = 2k_1$$

while at the same time

$$n_1 + n_1 = n_2 = 2 \left( \frac{2\sqrt{2}}{2\sqrt{2}} \right)^{1/2} \frac{g^{3/4}}{\gamma^{1/4}} = 2n_1$$

Therefore, if  $k_1$  is generated it will interact with itself and form  $k_2$ . From the equations for the growth rates we have

$$\begin{aligned} \dot{a}_1 &= -n_1 C a_1 a_2 \\ \dot{a}_2 &= n_2 C a_1^2 \end{aligned}$$

The solution for these amplitudes is shown in Fig. 2. It is readily seen that  $a_2$  grows at the expense of  $a_1$ . In that sense, there is no possible steady state for  $a_1$ , to second order. Thus the wave with wave-

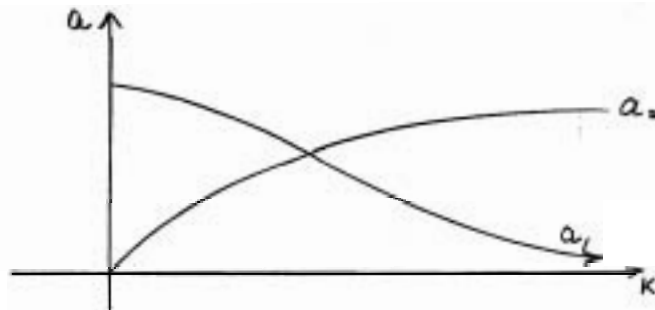


Fig. 2

length 2.4 cm (corresponding to  $k_1$ ) goes into a wave with wavelength 1.2 cm (corresponding to  $k_2$ ). On Fig. 1 we then have waves on the

"gravity" side that are converted to the "capillary" side when taking into consideration higher order interaction. The fact that waves with wave number  $k_1$  evolve in this way is reflected in the singularity in the 2nd order steady state solution of Wilton (1915) at a wavelength of 2.4 cm - a steady state solution does not exist at this wavelength.

### Higher Harmonic Resonance

If we choose  $k_1 = \sqrt{\frac{g}{\lambda_1}}$  it can again be shown that  $k_1$  can interact " $n$ " times with itself to form the wave of wave number  $k_n$ , where

$$k_n = \sqrt{\frac{n^2 g}{\lambda_1}}$$

This means that  $n_n = n k_1$ , as is easily verified. McGoldrick's (1972) experiments demonstrate these higher resonances clearly.

This result suggests that as  $k_1$  is produced, capillary waves of the same phase velocity are formed on top of it (as  $n \rightarrow \infty$ ,  $k_1$  is a "pure" gravity wave and  $k_n$  a "pure" capillary wave). In fact ratios between  $k_1$  and  $k_n$  are sometimes observed to be like (15:1) or (30:1).

However, problems arise in this theory. As " $n$ " is increased the resonances become more closely spaced, and ultimately the idea of a discrete resonance is lost. We will now use a very different approach that takes into account the fact that  $\lambda_g \gg \lambda_c$ . We will call it the "Parasitic capillary" approach, and it was developed by Longuet-Higgins (1963) and Crapper (1970).

## 2. Parasitic Capillary Theory

Assume that the velocity field of the orbital velocity of the associated gravity wave,  $\underline{U}$ , is, with respect to the capillary wave,

1. slowly varying
2. independent of depth.

We need the equation for the "conservation of waves" in the moving frame (lecture #1).

$$\frac{\partial k_\alpha}{\partial t} + \underline{a} \cdot \left( n - \underline{k} \cdot \underline{U} \right) = 0$$

One can also derive the equation for the energy balance of the fluctuation motion of the capillary waves (Longuet-Higgins and Stewart (1961), (1962))

$$\frac{\partial E}{\partial t} + \frac{\partial}{\partial x_\alpha} \left\{ (c_{g\alpha} + U_\alpha) E \right\} + S_{\alpha\beta} \frac{\partial U_\beta}{\partial x_\alpha} = -E.$$

$E$  is the energy of the capillary wave

$S_{\alpha\beta}$  is the "radiation stress"!

$E = 4\nu K^2 E$  represents the viscous dissipation.

In the limit of pure capillary waves in deep water and with the use of our two assumptions the last equation can be written as

$$\frac{\partial}{\partial \Delta} \{E(C_g - U)\} - \frac{3E}{2} \frac{\partial U}{\partial \Delta} = -4\nu K^2 E$$

where  $\Delta$  represents the distance along the surface from the primary wave crest.

With these same assumptions it can be shown from the conservation of waves that

$$K = U^2(\Delta) / \gamma$$

$$\text{and } C_g - U = U(\Delta) / 2$$

The integration of the energy equation then yields

$$\frac{E(\Delta)}{E_0} = \frac{a^2 K^2}{a; K_0^2} \frac{U^2(\Delta)}{U^2(\Delta_0)} \exp\left(-\frac{8\nu}{\gamma^2} \int_0^\Delta U^3(\Delta) d\Delta\right)$$

We then found that the wavelength decreases along " $\Delta$ " as  $U$  is increased and that the amplitude is given by the last equation which yields the plot of Fig.3.

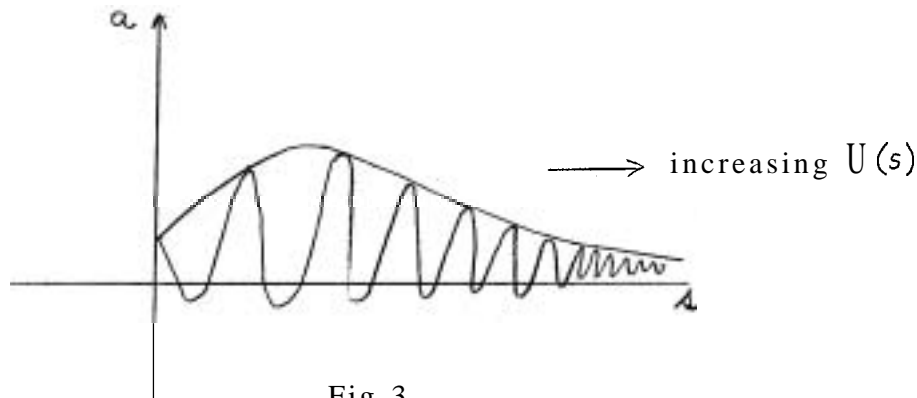


Fig. 3

The capillary wave gains energy from the gravity wave and loses it to viscous dissipation. That trend is similar to what we found in the first part of this lecture,

### 3. Summary

These two methods differ in many respects. In Table 1, we show a summary of these differences.

Table 1

Harmonic Resonance Theory (McGoldrick)	Parasitic Capillary Theory (Longuet-Higgins and Crapper)
$\frac{\lambda_g}{\lambda_c} = \text{integer}$	$\frac{\lambda_g}{\lambda_c} \gg 1$
Resonance	Continuous response
No spatial localness	Local excitation and energy exchange
Harmonic analysis works	Harmonic analysis is ill-conditioned representation of sharp crests.

Notes submitted by

Jean Pierre St-Maurice  
and Tør Gammelsrød.

### Lecture #4. INTERNAL GRAVITY WAVES

1. Using the Boussinesq approximation and neglecting the earth's rotation, the momentum equation can be written as:

$$\frac{\partial u_i}{\partial t} + u_j \frac{\partial u_i}{\partial x_j} + \frac{1}{\rho_0} \frac{\partial p_i}{\partial x_i} + g m_i \frac{\bar{p}(z) + p'}{\rho_0} = 0 \quad (1)$$

where  $\underline{m}$  is a unit vector vertically upward. Since water is considered incompressible, we get

$$\frac{\partial u_i}{\partial x_i} = 0, \quad \text{and} \quad (2)$$

$$\frac{dp}{dt} = \frac{\partial p'}{\partial t} + u_j \frac{\partial p'}{\partial x_j} + w \frac{\partial \bar{p}}{\partial z} = 0 \quad (3)$$

where  $p'$  is the fluctuation from the mean,  $\bar{p}(z)$ . Using Eqns. (1)-(3), a simple equation to describe the motion of a stratified fluid is obtained, i.e.

$$\frac{\partial^2 w}{\partial t^2} \nabla^2 w + N^2(z) \nabla_n^2 w = Q(\underline{x}, t) \quad (4)$$



where " $\omega$ " is the vertical velocity, " $Q(x,t)$ " represents the nonlinear terms, and " $N(z)$ " is the Brünt-Väisälä frequency, defined by

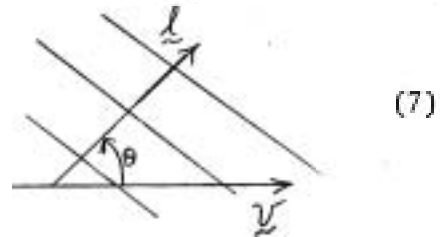
$$N^2(z) = -\frac{g}{\rho_0} \frac{\partial \bar{\rho}(z)}{\partial z} \quad (5)$$

For infinitesimal disturbances in the absence of mean shear,  $Q(x,t)$  of Eqn.(4) is negligible, hence, the governing equation becomes linear, i.e.

$$\frac{\partial^2}{\partial t^2} \nabla^2 \omega + N^2(z) \nabla_n^2 \omega = 0 \quad (6)$$

Let us consider  $N(z)$  to be constant, hence, the solution to Eqn. (6) can be written in the form of

$$\omega \propto \exp\{i(\underline{k} \cdot \underline{x} - \omega t)\}$$



where  $\omega = N \underline{k} \cdot \underline{z} = N \cos \theta$

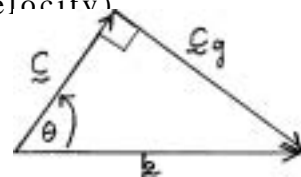
(frequency)

$$c = \frac{\omega}{k} \underline{\underline{z}}$$

(phase velocity)

$$c_g = \underline{\underline{k}} \times (\underline{\underline{b}} \times \underline{\underline{z}})$$

$$\underline{\underline{b}} = \frac{N}{k} \underline{\underline{v}}$$



a. These waves are anisotropic giving unusual properties,

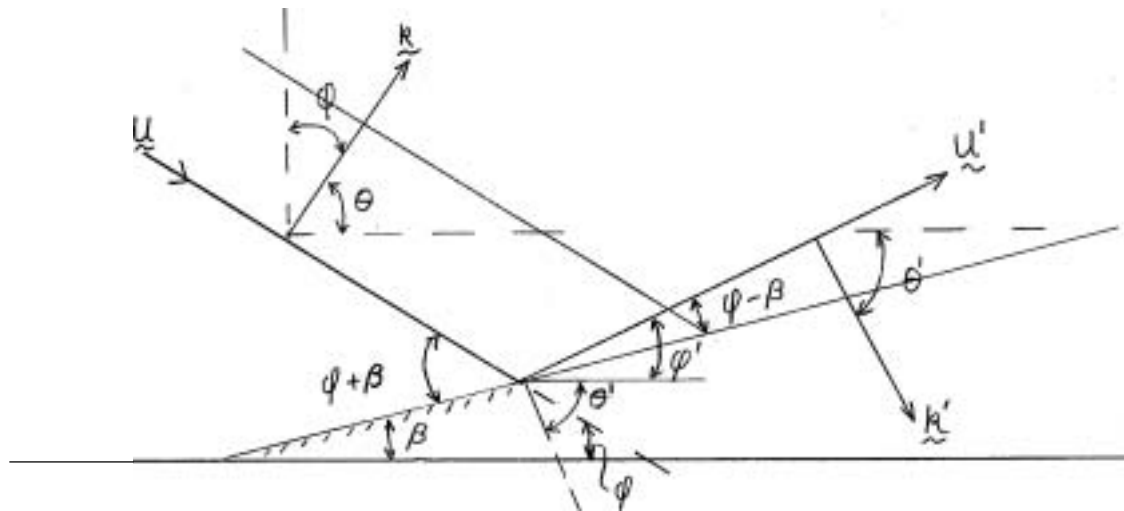


Fig.1. Reflections of an Internal Gravity Wave from a Sloping Bottom.

Let us consider an internal gravity wave  $(\omega, k)$  that is incident on a sloping bottom (with slope  $\beta$ ), Fig.1.

The reflected wave  $(\omega', k')$  must satisfy the following conditions:

1. frequency of the incident and reflected waves must be equal, i.e.

$$\omega = \omega' \quad \text{or} \quad \cos \theta = \cos \theta'$$

2. there is no normal velocity across the bottom surface, or the components of the two wave numbers in the plane (sloping surface Fig.1) must be equal, and

$$k \sin(\varphi + \beta) = k' \sin(\varphi - \beta), \quad (8)$$

where

$\varphi + \beta$  is the angle of incidence

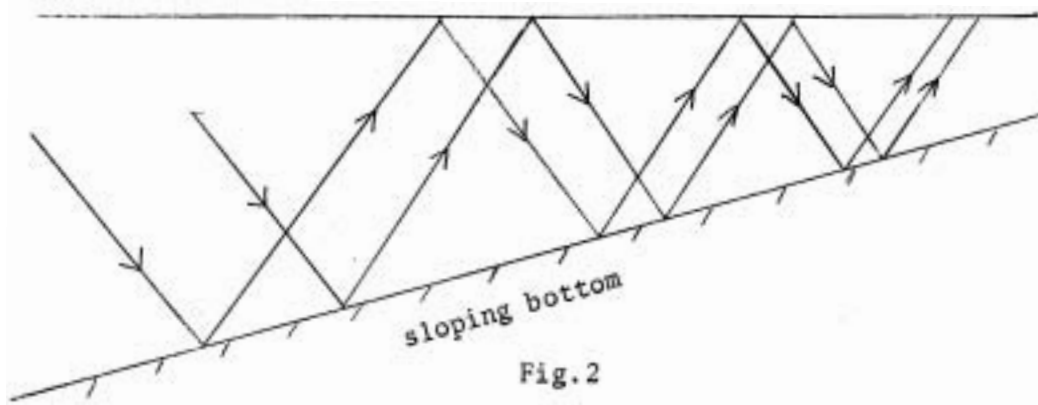
$-\beta$  is the angle of reflection

In addition,, the particle speeds of the incident ( $\alpha$ ) and reflected ( $\alpha'$ ) waves must satisfy the same kinematic condition,, i.e.

$$\frac{\alpha}{k} = \frac{\alpha'}{k'} \quad (9)$$

b. As the wave propagates onshore (up-slope) as depicted in Fig.2, its wave number increases, that is, the energy per unit volume of the wave increases as it propagates onshore. This effect is also given by the relation

$$\frac{E'}{E} \sim \frac{\alpha'^2}{\alpha^2} \sim \frac{k'^2}{k^2} \quad (10)$$



## 2. Wave Interactions

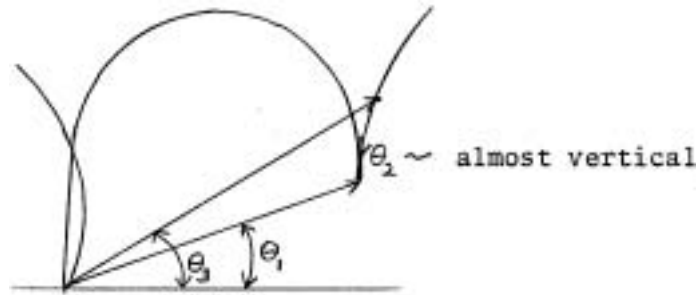
We now consider the effects of the nonlinear terms that were neglected previously. Certain binary interactions between components and wave numbers  $\underline{k}_1$  and  $\underline{k}_2$  form resonant triads, i.e.

$$\begin{cases} \underline{k}_1 \pm \underline{k}_2 = \underline{k}_3 & \text{and} \\ \omega_1 \pm \omega_2 = \omega_3, \end{cases} \quad (11)$$

and since  $\omega = N \cos \theta$ , and  $N$  is assumed to be constant, we also get

$$\cos \theta_1 \pm \cos \theta_2 = \cos \theta_3$$

a. A special case where  $\theta_1 \approx \theta_3$  is illustrated below:



b. The interaction of resonant triads can be described by the following:

$$\begin{aligned} \text{When } \underline{k}_1 + \underline{k}_2 = \underline{k}_3 \\ \dot{a}_1 = \omega_1 \zeta a_2 a_3 \\ \dot{a}_2 = \omega_2 \zeta a_1 a_3 \\ \dot{a}_3 = -\omega_3 \zeta a_1 a_2 \end{aligned} \quad (12)$$

where " $\zeta$ " is the interaction coefficient, and  $\dot{a} = \frac{da(t)}{dt}$

(i) Let us consider the special case where  $\underline{k}_1$  is vertical, or  $\omega_1 = 0$ , thus, we get

$$\begin{aligned} \dot{a}_1 &= 0 \\ \dot{a}_2 &= \omega_2 \zeta a_1 a_3 \\ \dot{a}_3 &= -\omega_3 \zeta a_1 a_2 \end{aligned}$$

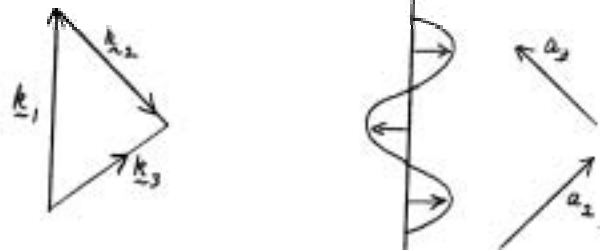


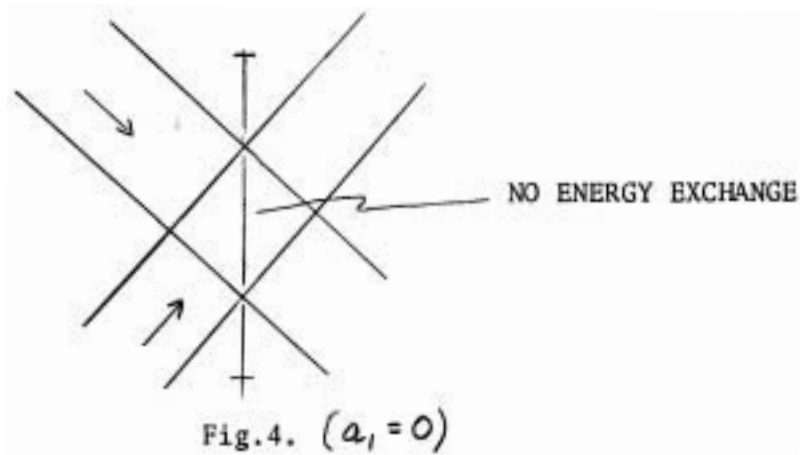
Fig. 3

The wave with vertical wave number merely scatters the waves  $k_1$  and  $k_2$ , but does not partake of the energy exchange. In this sense it is catalytic to the interaction.

(ii) If  $k_1$  is still vertical, but now  $a_1 = 0$ , we get

$$\dot{a}_1 = \dot{a}_2 = \dot{a}_3 = 0$$

Thus, there is no energy exchange between two internal waves of the same wave number which propagate through each other. This is depicted in Fig.4.



This effect can also be depicted by the standing internal wave modes that can exist in a channel,

### 3. Experiments of Resonant Interactions of Standing Internal Gravity Waves:

McEwan (1971) performed these experiments in a tank filled with linearly stratified salt solutions (i.e.  $N(z)$  was constant). With the constraint of sidewall boundary conditions, only standing modes were generated by an oscillatory paddle system as shown in Fig.5.

Hence, the associated wave numbers must satisfy the following integer relations:

$$\begin{aligned} m1 \text{ (horizontal wave number)} &= \frac{M_1 \pi}{L} \\ n1 \text{ (vertical wave number)} &= \frac{N_1 \pi}{H} \end{aligned} \quad (13)$$

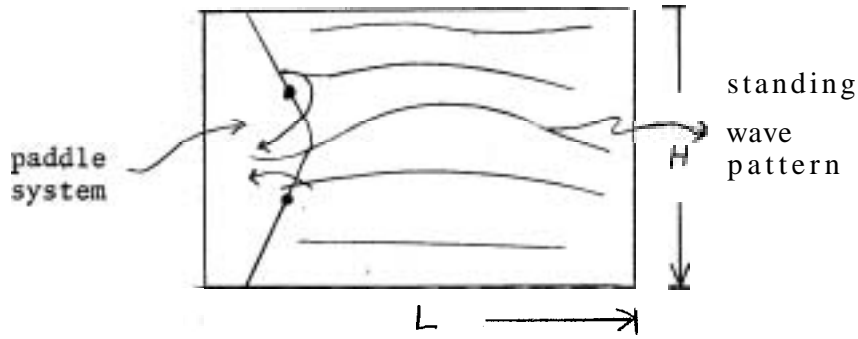


Fig.5

where "L" is the width and "H" is the depth of the tank, respectively,

The resonant conditions imply that

$$\begin{aligned}
 M_1 \pm M_2 \pm M_3 &= 0 \\
 N_1 \pm N_2 \pm N_3 &= 0 \\
 \omega_1 \pm \omega_2 \pm \omega_3 &= 0
 \end{aligned}
 \tag{14}$$

The governing equation set is given by

$$\begin{aligned}
 \dot{a}_1 &= \omega_1 \zeta a_2 a_3 - \tau_1 a_1 \\
 \dot{a}_2 &= \omega_2 \zeta a_1 a_3 - \tau_2 a_2 \\
 \dot{a}_3 &= -\omega_3 \zeta a_1 a_2 - \tau_3 a_3 + \delta
 \end{aligned}
 \tag{15}$$

where  $(\tau_i)$  terms are the dissipation rates of the individual modes due to the viscous dissipation effect mainly in the side walls. These dissipation terms were determined by direct measurement, " $\delta$ " is the "driving" term due to the oscillatory paddle system which generates the fundamental mode (denoted by subscript 3).

a. Let us consider the special case where the amplitude of the fundamental mode is much larger than the resonant waves, hence, it is approximately constant throughout the interaction, i.e.

$$\begin{aligned}
 a_3 & \text{ (approx. constant) } \gg a_1, a_2 \text{ and} \\
 a_1 &= A_1 e^{\lambda t} \\
 a_2 &= A_2 e^{\lambda t}
 \end{aligned}
 \tag{16}$$

The resonant waves will not grow (i.e. no turbulence can be generated), if frictional dissipation dominates. This decay of the disturbance is given by

$$a_3 < \left( \frac{\tau_1 \tau_2}{\omega_1 \omega_2 \zeta^2} \right)^{\frac{1}{2}}
 \tag{17}$$

b. If, on the other hand, the amplitude of the fundamental mode is larger than the critical amplitude, the wave becomes unstable, and turbulence is subsequently generated. This effect is depicted in Fig.6 and Fig.7.

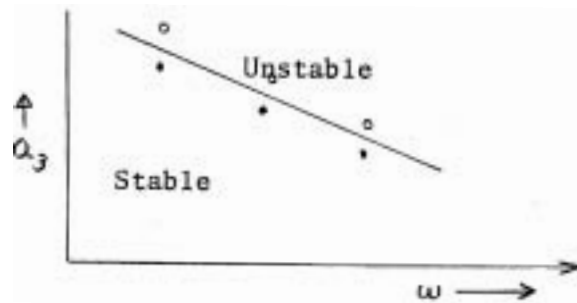


Fig. 6 Dissipation effect ( $a_3$  vs.  $\omega$ )

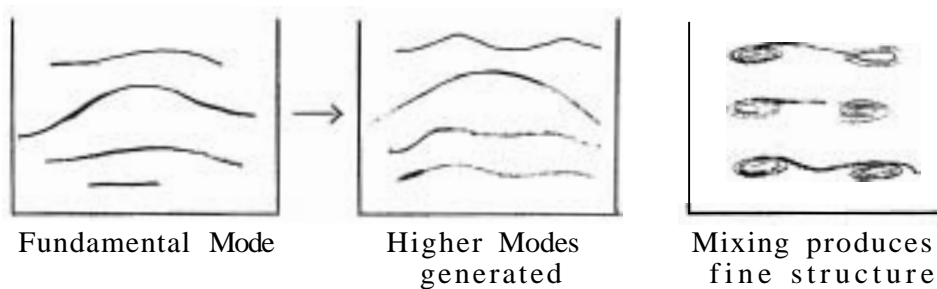


Fig. 7 Unstable Waves

Notes submitted by  
J. B. Tupaz  
and D. P. Wang

### Lecture #5. INTERACTIONS OF SURFACE GRAVITY WAVES

Recall that the boundary condition for surface gravity waves can be written

$$\phi_H + g\phi_z = Q + C + \dots \quad (5.1)$$

where  $Q$  and  $C$  represent the quadratic and cubic terms respectively. Dropping all the nonlinear terms results in sinusoidal solutions with the dispersion relation  $\eta = (gk)^{1/2}$  (in deep water). Retaining only  $Q$  on the right-hand side of Eq. (5.1) results in a modification of the wave profile (i.e. sharpening of the wave crests) but no wave interactions.

In this sense, surface gravity waves are pathological as there are no solutions to the triplet resonance conditions. Interactions can occur however from the cubic terms (C) but these will involve a quartet of waves, The resonant conditions are

$$\begin{aligned} k_1 \pm k_2 \pm k_3 \pm k_4 &= 0 \\ \text{and} \qquad \qquad \qquad n_1 \pm n_2 \pm n_3 \pm n_4 &= 0 \end{aligned} \tag{5.2}$$

There exist solutions of (5.2) together with the surface gravity wave dispersion relation. Such a solution is shown geometrically in Fig-5-1 for the choice of signs in (5.2) such that

$$\begin{aligned} k_1 + k_2 &= k_3 + k_4 \\ n_1 + n_2 &= n_3 + n_4 \end{aligned}$$

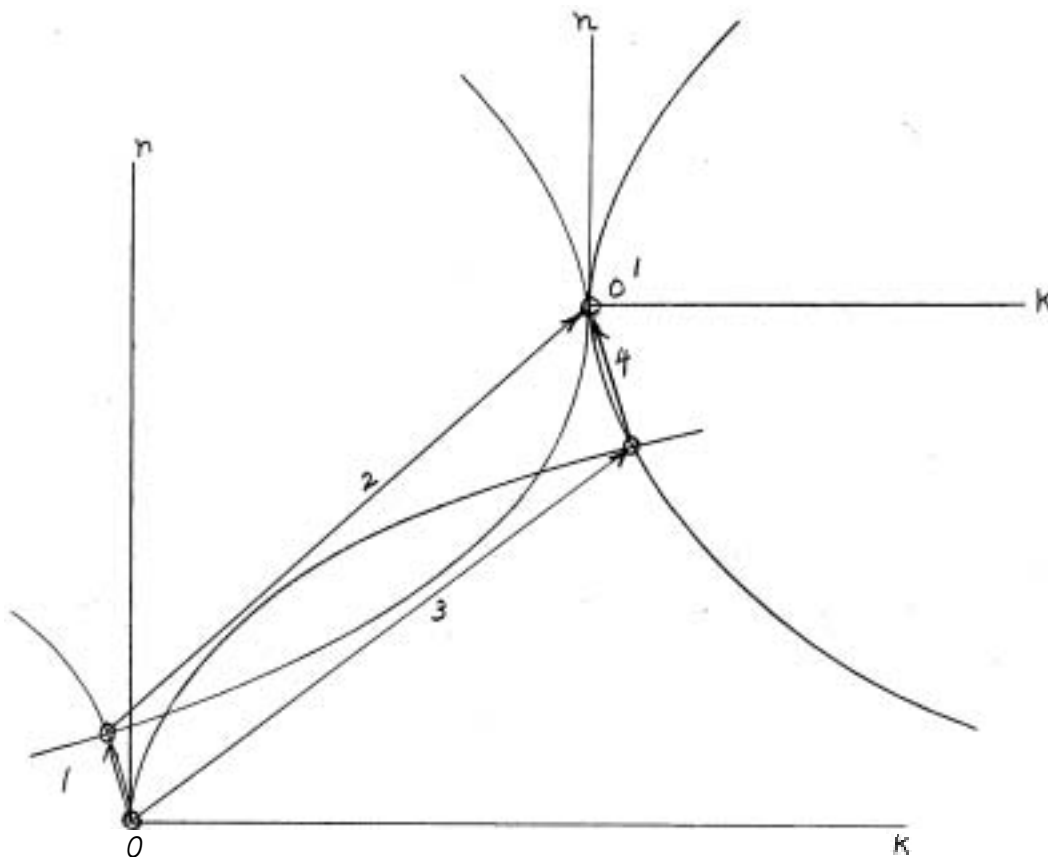


Fig. 5-1

The projection of this structure on the plane of wave numbers (Fig.5-2)

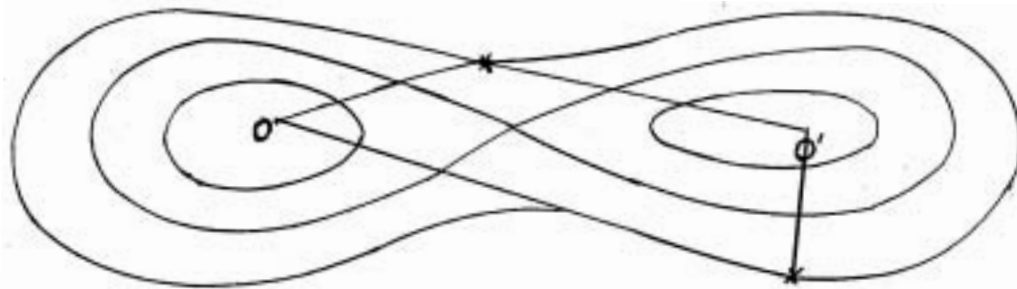


Fig.5-2

shows the two-dimension locus of the interacting wave numbers, On this diagram any two points on the same curve can be connected with the points 0 and 0' to form a resonant quartet.

Two degenerate cases had been studied without the interaction formalism.

$$1) k_1 = k_2 = k_3 = k_4$$

This is the case of self-interaction which is equivalent to the 3rd order Stokes expansion

$$2) k_1 = k_3 \quad k_2 = k_4$$

This is the interaction of two wave trains at 3rd order (Longuet-Higgins and Phillips, 1962) in which there is only a change in the phase speed of the waves with no energy transfer.

The interaction equations:

$$\text{if } \zeta = \frac{1}{2}(a e^{i k x} + a^* e^{-i k x}) \text{ the surface displacement}$$

then

$$\begin{aligned} \dot{\bar{a}}_1 &= , \quad \left( \overbrace{g_{11} a_1 a_1^*}^{\text{I}} + \overbrace{g_{12} a_2 a_2^* + \dots + g_{14} a_4 a_4^*}^{\text{II}} \right) \\ &\quad + i h n_1 a_1 a_1^* \\ \dot{\bar{a}}_2 &= i a_2 (g_{21} a_1 a_1^* + \dots + i h n_2 a_1 a_2 a_3 a_4^* ) \\ \dot{\bar{a}}_3 &= i a_3 ( \dots + i h n_3 a_1 a_2 a_4^* ) \\ \dot{\bar{a}}_4 &= i a_4 ( \dots + i h n_4 a_1 a_2 a_3^* ) \end{aligned} \tag{5.3}$$

where  $g_{ij}$  and  $h$  are real coefficients, functions of the four wave numbers.



The amplitude functions  $(a_i(\epsilon t))$  are complex and contain all information concerning the relative phases of the interacting waves.

Notes

1) The terms of the type marked I are the self-interaction terms. As the resulting  $\dot{a}_1 \perp a_1$ , this represents only a change in the wave frequency, and therefore the phase velocity

$$C = \left(\frac{\omega}{k}\right)^{1/2} \left(1 + \frac{1}{2} (\alpha k)^2 + \dots\right)$$

2) The terms marked II result in a modification of the phase velocity of a wave train by interaction with another, without energy transfer.

3) Partition Integrals (for  $k_1 + k_2 = k_3 + k_4$ )

Multiplying the  $\dot{a}_1$  equation by  $a_1^*$  and the complex conjugate of the  $\dot{a}_1$  equation by  $a_1$  and adding together with the  $\dot{a}_2$  equations,

results in 
$$\frac{a_1 a_1^*}{n_1} - \frac{a_2 a_2^*}{n_2} = \text{constant}$$

similarly

$$\begin{aligned} n_1 + n_2 &= \text{constant} \\ \frac{a_1 a_1^*}{n_1} + \frac{a_2 a_2^*}{n_2} &= \text{constant} \end{aligned}$$

Thus energy is gained/lost by wave 1 and 2 together as it is lost/gained by 3 and 4 together.

It may also be shown that

$$\sum_{r=1}^4 a_r a_r^* = \text{energy density} = \text{constant}$$

and

$$\sum_{r=1}^4 \frac{k_r a_r a_r^*}{n_r} = \text{momentum density} = \text{constant}$$

(recall that  $\frac{k_r}{n_r} = 1/C_r$ , the phase speed and momentum density =  $E/C$ ).

4) As we have already seen, the third-order interaction of the gravity waves produces the frequency change of interacting waves. Then, the frequencies of the wave trains no longer satisfy the resonance condition (2). However, if we choose the group of wave numbers which is not in the exact resonance relation, but shifts slightly from the resonance loop, the equation (5) can be modified so that the change of the frequency by inter-

action is cancelled out by the modified terms introduced by the "de-tuning". In such a situation the resonance is preserved among finite-amplitude gravity waves. Figure 3 shows the "de-tuning" region in case of  $k_1 = k_2$  (i.e. the figure-of-eight region).

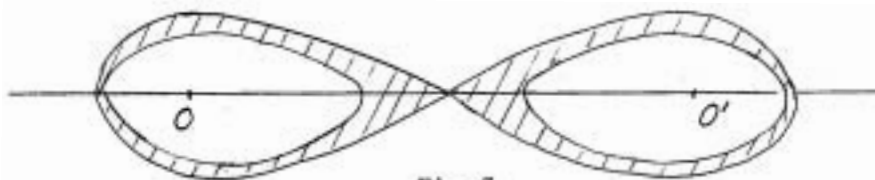


Fig. 3

Experiments:

1) Longuet-Higgins and Smith (1966) and McGoldrick *et al.*, (1966) performed laboratory experiments to observe nonlinear interaction of gravity waves in resonance conditions.

Giving  $k_1, k_2 (= k_1)$  and  $k_3 (\perp \tau)$ , they observed amplitude growth of  $k_4 (= 2k_1 - k_3)$ . Their results are reproduced in Fig.4.

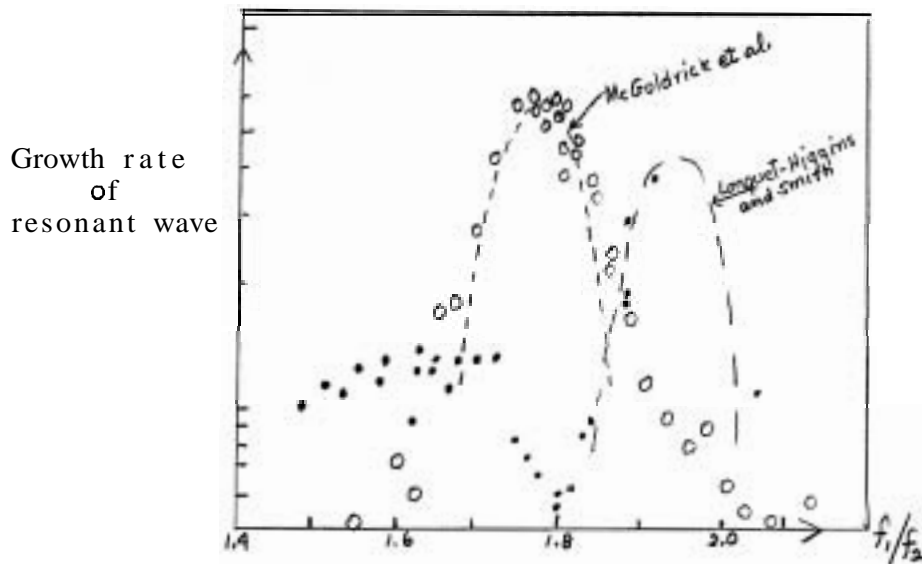


Fig. 4

The abscissa represents the frequency ratio of the primary waves,  $k_1$  and  $k_3$ , and the ordinate represents the growth rate of the resonant wave. In these experiments the resonance condition (2) gives

Notice that the observed frequency ratios shift from this value, The amount of shift in the Longuet-Higgins and Smith's experiment is greater than that in the McGoldrick *et al.*'s experiment. This may be explained by the fact that the amplitudes of the primary waves in the Longuet-Higgins and Smith's experiment are larger than those in the McGoldrick *et al.*'s experiment. Longuet-Higgins and Smith (1966) tried a detailed analysis of the response near resonance and found that

$$a_4 \propto \frac{\sin(\delta k x)}{\delta k x}$$

where  $\delta k$  expresses the amount of "mismatch" in the wave number plane and is the resonant distance,

## 2) Wave train instability (Benjamin and Feir, 1967).

This experiment considers the stability of a single finite amplitude wave train. It is found experimentally that the wave train is unstable and breaks down into groups of waves,



In terms of wave interactions this is a wave ( $K_1$ ) interacting with itself and with a small amplitude perturbation wave with  $K_3 \approx K_1$ . In this case, all three wave numbers  $K_1$ ,  $K_2 = K_1$ , and  $K_3$  are colinear, and the interaction locus must be broadened by amplitude dispersion to obtain the energy transfer.

Notes submitted by  
Ryuji Kimura and  
Roland B. Smith.

Lecture #6. INTERNAL-SURFACE WAVE INTERACTIONS

The present topic, the interaction of internal waves with relatively short wavelength surface waves, is of theoretical interest because it offers a point of contact between two bodies of theory concerned with finite amplitude effects in waves. One theory treats slowly varying wave trains, the second is concerned with resonant wave interactions.

A possible practical interest for this topic lies in the explanation for several observations at sea of the apparent modification of short, wind-generated surface waves by long internal gravity waves, e.g. Perry and Schimke.

1. Slowly varying surface wave train

Suppose an internal wave sets up a known surface current

$$U = U(x - C_i t)$$

where  $C_i$  = internal wave phase speed.

We wish to find the resultant modification to a short surface wave train; that is, to find

$$\text{phase velocity } c = c(x)$$

$$\text{group velocity } c_g = \frac{1}{2} c(x)$$

$$\text{and wave number } k = k(x)$$

The energy equation for the surface wave train is

$$\frac{\partial E}{\partial t} + \frac{\partial}{\partial x} [E(\frac{1}{2}c + U)] + \frac{1}{2} E \frac{\partial U}{\partial x} = 0, \tag{6.1}$$

$$\text{since } c_g = \frac{1}{2} c.$$

The surface wave conservation equation and frequency are

$$\frac{\partial k}{\partial t} + \frac{\partial}{\partial x} (n + kU) = 0 \tag{6.2}$$

and

$$n = (gk)^{1/2}. \tag{6.3}$$

a) Kinematics

If we fix our axes to the internal wave, we have

$$\frac{\partial}{\partial t} = -C_i \frac{\partial}{\partial x} \tag{6.4}$$

$$\text{and } U = U(x).$$

Substitution of (6.4) in (6.2) allows the latter to be integrated as a function of  $x$ , giving

$$n - k(c_i - U) = \text{constant}$$

or

$$n - k(c_i - U) = n_0 - k_0 c_i \quad (6.5)$$

where  $n_0, k_0$  are the values at the point where  $U(x) = 0$ .

Substitution of the dispersion relation (6.3) into (6.5) gives

$$k(c + U - c_i) = k_0(c_0 - c_i)$$

since  $\frac{k_0}{k} = \left(\frac{c}{c_0}\right)^2$ , we have

$$\left(\frac{c}{c_0}\right)^2 = \frac{c + U - c_i}{c_0 - c_i}$$

Solving this quadratic relation for  $\left(\frac{c}{c_0}\right)$ :

$$\frac{c}{c_0} = \frac{c_0 + (c_0 - 2c_i) \left\{ 1 + \frac{4U(c_0 - c_i)}{(c_0 - 2c_i)^2} \right\}^{1/2}}{2(c_0 - c_i)} \quad (6.6)$$

where we have determined the sign of the radical by imposing the condition

$$\frac{c}{c_0} \rightarrow 1 \text{ as } U \rightarrow 0$$

Case 1. Suppose  $c_i = 0$  (stationary current pattern: Longuet-Higgins and Stewart)

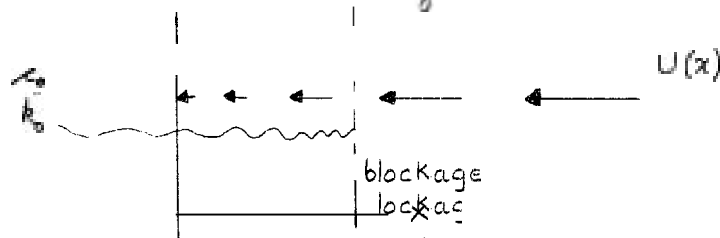
$$\text{then } \frac{c}{c_0} = \frac{1}{2} + \frac{1}{2} \left( 1 + \frac{4U}{c_0} \right)$$

and no real solution exists if an adverse current exists

$$U < -\frac{1}{4}c_0$$

$$\text{when } U = -\frac{1}{4}c_0, \frac{c}{c_0} = \frac{1}{2}$$

and  $\frac{U}{c} = -\frac{1}{2}$  i.e.  $U = c_g$ , energy propagation speed.



Surface wave phase speed and wavelength decrease, wave number increases.

At blockage,

energy propagation speed = adverse current.

Case 2.  $C_i \neq 0$

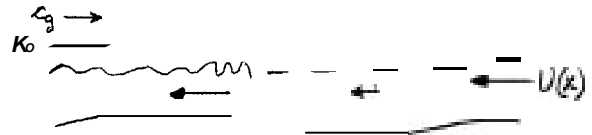
For  $C_i > c_0$ , no real solution exists if

$$U < - \frac{(c_0 - 2C_i)^2}{4(c_0 - C_i)} \quad (6.7)$$

In general, three situations of interest exist as viewed in a reference frame fixed to the internal wave.

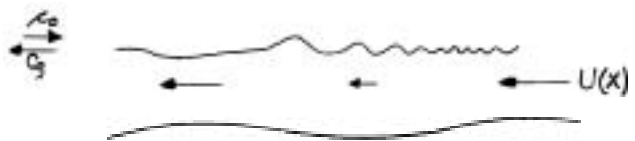
i)  $C_i < \frac{1}{2} c_0$

Here, blockage can occur for a sufficiently strong adverse current  $U$ . Phase velocity and wavelength are decreased, wave number increased.



ii)  $\frac{1}{2} c_0 < C_i < c_0$

Wavelength increases,  $C_d$  increases to balance  $U$ .



iii)  $\frac{C_i}{c_0} > \frac{1}{2}; U \rightarrow C_i$  (6.8)

This situation is not applicable to real internal waves; maybe long surface waves of large slope. Then

$$\frac{c}{c_0} = \frac{c_0 + (c_0 - 2C_i) \left\{ 1 + \frac{4C_i(c_0 - C_i)}{(c_0 - 2C_i)^2} \right\}^{1/2}}{2(c_0 - C_i)}$$

or

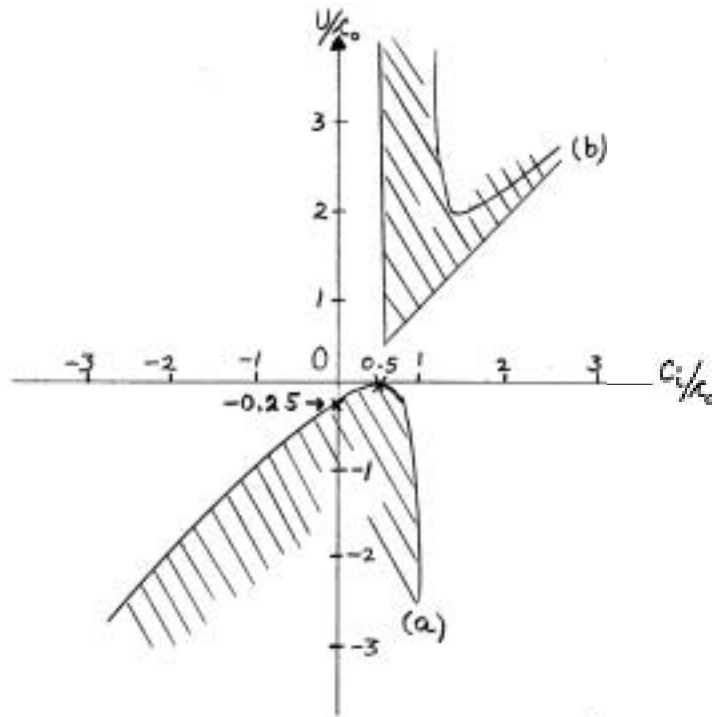
$$\frac{c}{c_0} = \frac{c_0 \left\{ 1 + \frac{c_0 - 2C_i}{|c_0 - 2C_i|} \right\}}{2(c_0 - C_i)}$$

Thus  $\frac{c}{c_0} = 0$  if  $c_0 < 2C_i$ .

In this limit, as  $U \rightarrow C_i$ , the surface wave wave number becomes infinite,

$$k \rightarrow \infty.$$

The plot on the following page shows the regions and blockage conditions noted here.



Case (1) blockage

$$C_i = 0 \quad \frac{U}{c_0} = -\frac{1}{4}$$

is a special point on the whole curve (a) representing blockage according to Eq. (6.7). A second special point on this curve is

$$U = 0, \quad (C_i/c_0) = \frac{1}{2}.$$

Here, even an infinitesimal adverse current is sufficient to cause blockage. Curve (b) corresponds to the theoretical blockage produced by conditions given in (6.8).

(b) Energy

i) steady state solution

Using  $\frac{\partial}{\partial t} \rightarrow \frac{\partial}{\partial t} - C_i \frac{\partial}{\partial x}$  in (6.1) and seeking the steady state solution, we have

$$\frac{\partial}{\partial x} [E(U - C_i + \frac{1}{2} \kappa)] + \frac{1}{2} E \frac{\partial U}{\partial x} = 0 \quad (6.9)$$

where  $\kappa = \kappa(U)$ , a known function of  $U$  (and thus  $x$ ) from the foregoing kinematics discussion.

In solving (6.9), the following lemma is used:

$$\text{Lemma: Prove } \frac{1}{2} \kappa \frac{\partial U}{\partial x} = \left( \frac{1}{2} \kappa + U - C_i \right) \frac{\partial \kappa}{\partial x}.$$

Substitution of this result into (6.9) allows immediate integration in  $x$ , giving

$$E \kappa (U - C_i + \frac{1}{2} \kappa) = \text{constant}$$

or

$$E \kappa (U - C_i + \frac{1}{2} \kappa) = E_0 \kappa_0 (-C_i + \frac{1}{2} \kappa_0). \quad (6.10)$$

The left-hand side of this relation must remain finite and constant (= right-hand side) even when either of two special conditions occur at some point  $x$  in the flow:

$$\kappa \rightarrow 0 \quad (c)$$

$$\text{or } (U - C_i + \frac{1}{2} \kappa) \rightarrow 0 \quad (d).$$

In either of these cases,  $E(x)$  must tend to  $\infty$  to maintain the left-hand side constant. In these cases, the time-dependent solution of the energy equation will show energy accumulation.

ii) time-dependent solution

The time dependent version of (6.1) using (6.4) is

$$\frac{\partial E}{\partial t} + \frac{1}{2} E \frac{\partial U}{\partial x} + \frac{\partial}{\partial x} [E(U - C_i + \frac{1}{2} \kappa)] = 0.$$

thus, with condition (d)

$$\frac{\partial E}{\partial t} = -\frac{1}{2} E \frac{\partial U}{\partial x}$$

indicating the general solution

$$E \propto E_0 e^{\alpha t}$$

where  $\alpha$  = rate of convergence (divergence) of energy.

Ex:  $t = 0$



$t > 0$



## 2. Resonant interaction problem.

Consider two short surface waves with neighboring wave numbers,



$$k_1 = k_i \quad n_1 = n_i$$

$$k_2 = k + \delta k \quad n_2 = n_i + \delta n$$

and an internal wave  $k_i, n_i$ .

From the exact resonance conditions,

$$k_2 - k_1 = k_i$$

$$n_2 - n_1 = n_i$$

we have

$$\delta k = k_i$$

$$\delta n = n_i$$

or

$$\frac{\delta n}{\delta k} = \frac{n_i}{k_i}$$

Thus the resonance conditions reduce to  $C_i = C_g = \frac{1}{2} c$ .

This condition  $C_i = \frac{1}{2} c_g$  is the point of contact between the resonant interaction theory and the preceding slowly varying wave treatment.

### Comparison of Methods

We may form a tabular comparison of the two methods as follows:

<u>Slowly Varying Wave Train</u>	<u>Resonant Interaction</u>
1. Assumed current $U = U(x - c_i t)$ (any configuration)	Periodic $U$ given $a_1, a_2$ at $t=0$ find $a_1(t), a_2(t)$
2. Both give $\dot{a}_2(t)$ at $t=0$	
3. Valid for $\epsilon t \ll 1$	$\epsilon t < 1$
4. Can work out off resonance case.	Exchange between 3 components.

A critique of the relation of this discussion to observations at sea (e.g. Perry and Schimke) includes:

- i) in the observations many surface wave numbers are present, i.e. the process is untuned, and
- ii) winds present at the observations might overpower the process discussed here and prevent development of the quiescent regions over the internal wave troughs.

### References

Perry, R.B. and G.R. Schimke 1965 Large amplitude internal waves observed the northwest coast of Sumatra. J. Geophys. Res. 70(10): 2319.

Notes submitted by  
Erik Petersen and  
Richard Desautel.

## Lecture #7. A THEORY OF WAVE BREAKING

### Introduction

Very little is known about wave breaking. It is however important because it is involved in the exchange of heat, water, oxygen, etc. with the atmosphere,

There exists some semi-empirical work dealing with breakers on beaches. But this is intrinsically a transient phenomenon. Recently Longuet-Higgins (1973) has published a paper where he wanted to study the properties of already-broken waves: a dividing streamline was between one region where the flow was assumed irrotational and another where it was turbulent, with a very small Reynolds number. A stagnation point was assumed to exist at the origin of the dividing streamline; a constant eddy viscosity was assumed too. But this work appears to be irrelevant. The free surface is not steady so that the assumed stagnation point does not exist.

Stokes had predicted wave breaking when the wave crest made an angle of 120 degrees. This was for an irrotational motion; in the ocean, waves are seen to break long before the formations of a sharp crest with an angle of 120 degrees and because of the wind stress the motion can not be considered irrotational. This leads to the present work where that effect will be considered.

### The Model

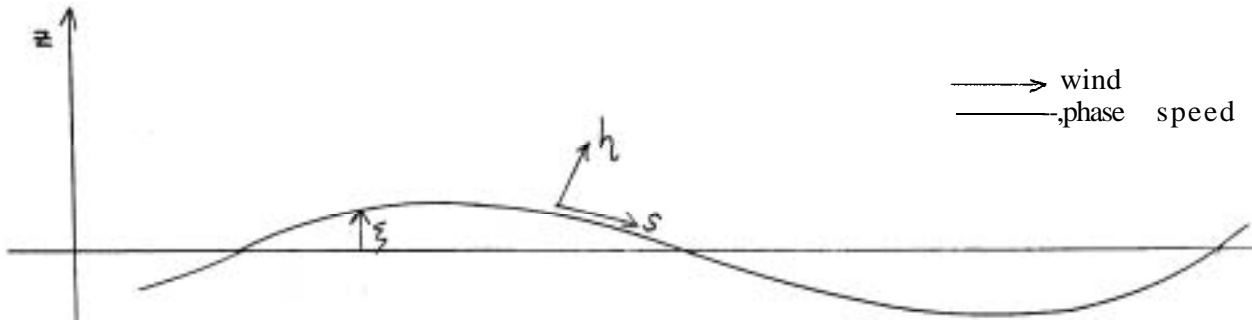
We will assume a two-dimensional geometry. Because of the shear due to the wind a thin vortex layer exists near the surface. There will be no capillary effects. The time for the vortex layer to be formed will be much longer than the period of the wave.

### Theory

Consider a wave with phase speed  $C$  and work the problem in the rest frame of the wave. The various coordinates are shown in Fig.1(a).

Let  $\underline{u} = (u, w)$  be the velocity of the fluid and  $\underline{\omega} = \nabla \times \underline{u}$  be the vorticity. Assume  $\frac{\partial}{\partial t} = 0$  in the moving frame of reference. From the equations of motion we have

$$-\underline{u} \times \underline{\omega} = \nabla \left( \frac{P}{\rho} + \frac{u^2}{2} + g z \right)$$



,  $c =$  phase speed

Fig.1(a)

Since the vorticity is perpendicular to  $u$  (see Fig.1(b)) we then have along the surface

$$\frac{P}{\rho} + \frac{1}{2} u_{\xi}^2 + g \xi = c t$$

where  $u_{\xi}$  is the velocity at  $\xi = \xi$ .

But  $P$  is a constant at the surface. This implies

$$\frac{1}{2} u_{\xi}^2 + g \xi = \frac{1}{2} u_{\xi}^2 (\xi = 0) \quad (1)$$

where  $u_{\xi} (\xi = 0)$  represents the surface speed at the mean sea level.

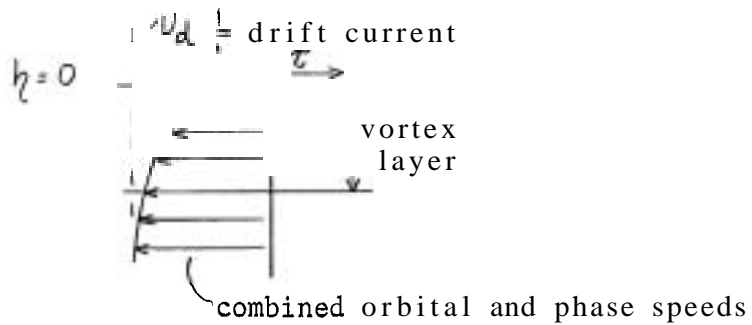


Fig.1(b): The thin vortex layer.

We now assume that the condition for wave breaking is that a stagnation point is formed on the surface. Then the maximum wave crest without breaking is

$$\xi_{max} = \frac{u^2 (\xi = 0)}{2g} \quad (2)$$

For the surface velocity we may write

$$u_{\xi} = u_0 - c + u_d$$

where  $u_0 =$  orbital velocity taken in the reference frame

$u_d =$  the drift velocity resulting from the wind.

Let us define  $\underline{U} = \underline{u}_0 - \underline{c}$ , the velocity below the vorticity layer.

Then

$$\underline{u}_\xi = \underline{U} + \underline{u}_d \quad (3)$$

Our assumption about the time scales and inviscidity of the flow means that there is no source of vorticity, Then vorticity is conserved along the streamlines and

$$\underline{u} \cdot \nabla |\omega| = \mu \frac{\partial \omega}{\partial s} + \omega \frac{\partial \omega}{\partial \eta} = 0$$

Now using the incompressibility condition, this becomes

$$\frac{\partial}{\partial s} (\mu \omega) + \frac{\partial}{\partial \eta} (\omega \omega) = 0$$

Integrating across the surface layer gives

$$\frac{\partial}{\partial s} \int_{\text{lower layer}}^{\eta=0} (\mu \omega) d\eta + \omega \omega \Big|_{\text{lower layer}}^{\eta=0} = 0$$

But  $\omega = 0$  in lower layer

$$\omega = 0 \text{ at } \eta = 0.$$

Therefore

$$\int (\omega \omega) d\eta = c t \text{ along } s.$$

So the flux of vorticity is independent of  $s$ .

But

$$\omega = |\nabla \times \underline{u}| = \frac{\partial \mu_d}{\partial \eta} (1 + \theta(\epsilon^2))$$

where  $\epsilon^2 =$  boundary layer thickness/wavelength.

Therefore we can write

$$\frac{1}{2} \mu_\xi^2 - \frac{1}{2} U^2 = \frac{1}{2} B \text{ when } B \text{ is yet undetermined.}$$

With (3) this becomes

$$\mu_d^2(0) + 2 U \mu_d(0) - B = 0$$

where  $\mu_d(0)$  is the drift current at the surface  $\eta = 0$ .

Then

$$\mu_d(\eta=0) = -U(s) \pm \sqrt{U^2(s) + B}.$$

But when  $\omega = 0$  (no vorticity),  $\mu_d = 0$ . Thus only the + sign has to be kept.

The tangential surface speed is then

$$\mu_\xi = \mu_d(0) + U(s) = \sqrt{U^2 + B} \quad (4)$$

To find B we use the result from Levi-Civita (Lamb, p.420) that at  $\xi = 0$  we have

$$v = -c \quad (\mu_0 = 0)$$

Let  $q$  be the value of the surface drift at  $\xi = 0$

$$q = \mu_d(\xi = 0)$$

Then we have

$$q = c + \sqrt{c^2 + B}$$

and

$$B = -q(2c - q) \quad (5)$$

At the crest  $\underline{\mu}_0$  is horizontal and one can write

$$v = \mu_0 - c$$

Using (4) and (5) we may then write

$$\mu_\xi(s_1) = \sqrt{(\mu_0 - c)^2 - q(2c - q)}$$

where  $s_1$  is at the crest. Therefore the condition for no breaking is

$$(\beta - 1)^2 > \gamma(2 - \gamma)$$

where

$$\beta = \frac{\mu_0}{c}$$

$$\gamma = \frac{q}{c}$$

This result is illustrated in Fig. 2 for  $\beta, \gamma \leq 1$ . When  $\gamma = 0$  we recover the well-known Stokes result with breaking occurring at  $\mu_0 = c$

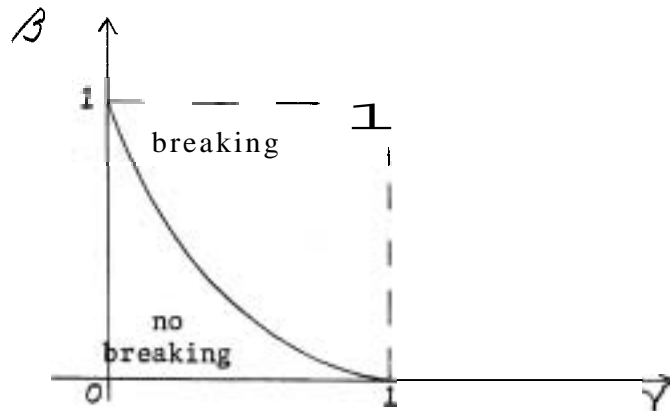


Fig. 2

We already stated that the maximum possible value for  $\xi$  at the crest is given by

$$\xi_{\max} = \frac{1}{2g} \mu_\xi^2(\xi = 0)$$

since  $u_{\xi}(\xi=0) = -c + q$ , we then have  $\xi_{max} = \frac{c^2}{2g} (\gamma - 1)^2$

This relation is illustrated in Fig.3 for  $\gamma \leq 1$ .

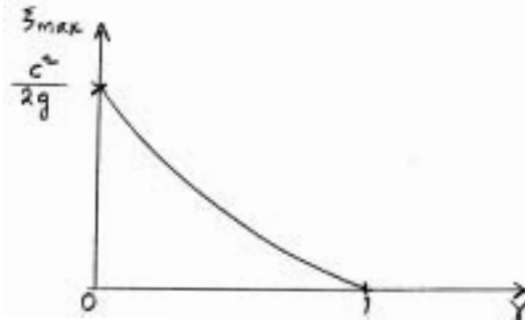


Fig.3

EXAMPLE

The surface drift speed may be estimated by equating the stress in the air to the stress in the water

$$\rho_a u_*^2 \sim \rho_w w_*^2$$

But

$$\frac{\rho_a}{\rho_w} \sim \frac{1}{900} \rightarrow \frac{u_*}{w_*} \sim 30$$

and the surface drift layer is about 3% of the wind speed,

Then for a 20 knot wind,  $q = 30$  cm/sec for a 30 cm wavelength  $c \sim 68$  cm/sec. Then  $\gamma = 0.44$  and it can be shown that breaking will occur at  $\frac{u_*}{c} = 0.3$  instead of 1, according to Stokes' theory.

Streak photographs of a broken wave show (a) an irregular forward (tumbling) face, (b) a very small region where the mean flow recirculates, with a (divergence) stagnation point in the mean flow near the wave crest, and (c) a turbulent wake trailing the broken region whose thickness is of order the wave height.

Notes submitted by  
Jean-Pierre St-Maurice  
and Tør Gammelrød.

## References

- Ball, F. K. Energy transfer between external and internal gravity waves. *J.Fluid Mech.*, 19 (1964), 465.
- Benjamin, T. Brooks Internal waves of finite amplitude and permanent form. *J.Fluid Mech.*, 25 (1966), 241.
- Internal waves of permanent form in fluids of great depth. *J.Fluid Mech.*, 29 (1967), 559.
- Instability of periodic wave trains in nonlinear dispersive systems. *Proc.Roy.Soc.*, A, 299 (1967), 59.
- and Feir, J. E. The disintegration of wave trains on deep water, Part I, Theory, *J.Fluid Mech.*, 27 (1967), 417.
- Benney, D. J. Nonlinear gravity wave interactions. *J.Fluid Mech.*, 14 (1962), 577.
- and Saffman, P. G. Nonlinear interactions of random waves in a dispersive medium. *Proc.Roy.Soc.*, A, 289 (1966), 301.
- Booker, J. R. and Bretherton, F. P. The critical layer for internal gravity waves in a shear flow, *J.Fluid Mech.*, 27 (1967), 513.
- Bretherton, F. P. Resonant interactions between waves. The case of discrete oscillations, *J.Fluid Mech.*, 20 (1964), 457.
- Bryatt-Smith, J. G. B. An exact integral equation for steady surface waves, *Proc.Roy.Soc.*, A, 315 (1970), 405.
- Cox, C. S. Measurements of slopes of high-frequency wind waves. *J.Mar.Res.*, 16 (1958), 199.
- Crapper, G. D. Nonlinear capillary waves generated by steep gravity waves. *J.Fluid Mech.*, 40 (1970), 149.
- Nonlinear gravity waves on steady non-uniform currents, *J.Fluid Mech.*, 52 (1972), 713.
- Davis, Russ E. and Acrivos, A. Solitary internal waves in deep water. *J.Fluid Mech.*, 29(1967), 593.
- and ----- The stability of oscillatory internal waves, *J.Fluid Mech.*, 30 (1967), 723.
- Fenton, J. A ninth-order solution for the solitary wave. *J.Fluid Mech.*, 53 (1972), 257.
- Gargett, A. E. and Hughes, B. A. On the interaction of surface and internal waves. *J.Fluid Mech.*, 52 (1972), 179.
- Hasselmann, K. On the nonlinear energy transfer in a gravity-wave spectrum. Part I, General Theory, *J.Fluid Mech.*, 12 (1962), 481.
- On the nonlinear energy transfer in a gravity-wave spectrum. Part II. Conservation theorem; wave-particle analogy; irreversibility, *J.Fluid Mech.*, 15 (1963), 273.
- On the nonlinear energy transfer in a gravity-wave spectrum, Part III. Evaluation of the energy flux and swell-sea interaction for a Neumann spectrum. *J.Fluid Mech.*, 15 (1963), 385.

References (continued)

- Hasselmann, K. A criterion for nonlinear wave stability.  
J.Fluid Mech., 30 (1967), 737,
- Nonlinear interactions treated by the methods of theoretical physics (with application to the generation of waves by wind).  
Proc.Roy.Soc., A, 299 (1967), 77,
- On the mass and momentum transfer between short gravity waves and larger scale motions, J.Fluid Mech., 50 (1971), 189,
- Kim, Y. Y. and Hanratty, T. J. Weak quadratic interactions of two-dimensional waves. J.Fluid Mech., 50 (1971), 107.
- Longuet-Higgings, M. S. Resonant interactions between two trains of gravity waves. J.Fluid Mech., 12 (1962), 321,
- The generation of capillary waves by steep gravity waves, J.Fluid Mech., 16 (1963), 138,
- On the form of the highest progressive and standing waves in deep water. Proc.Roy.Soc., A, 331 (1972), 445.
- and Phillips, O. M. Phase velocity effects in tertiary wave interactions. J.Fluid Mech., 12 (1962), 333.
- and Smith, N. D. An experiment on third-order resonant wave interactions, J.Fluid Mech., 25 (1966), 417,
- and Stewart, R. W. Changes in the form of short gravity waves on long waves and tidal currents. J.Fluid Mech., 8 (1960), 565.
- and ----- The changes in amplitude of short gravity waves on steady non-uniform currents, J.Fluid Mech., 10 (1961), 529,
- and ----- Radiation stress and mass transport in gravity waves, with application to 'surf beats', J.Fluid Mech., 13 (1962), 481.
- Martin, S., Simmons, W. F. and Wunsch, C. I. Resonant internal wave interactions. Nature, 224 (1969), 1014,
- McGoldrick, L. F. Resonant interactions among capillary-gravity waves. J.Fluid Mech., 21 (1965), 305.
- An experiment on second-order capillary-gravity resonant interactions, J.Fluid Mech., 40 (1970a), 251.
- An experiment on second-order capillary-gravity resonant interactions, J.Fluid Mech., 40 (1970b), 251,
- On Wilton's ripples: a special case of resonant interactions. J.Fluid Mech., 42 (1970), 193,
- On the rippling of small waves: a harmonic nonlinear nearly resonant interaction, J.Fluid Mech., 52 (1972), 725,
- , Phillips, O. M., Huang, N. E. and Hodgson, T. H. Measurements of third-order resonant wave interactions. J.Fluid Mech., 25 (1966), 437,



References (continued)

- McEwan, A. D. Degeneration of resonantly-excited standing internal gravity waves. *J.Fluid Mech.*, 50 (1971), 431.
- Mander, D. W. and Smith, R. K. Forced resonant second-order interaction between damped internal waves, *J.Fluid Mech.*, 55 (1972), 589.
- Mitchell, J. H. The highest waves in water. *Phil.Mag.* (5), 36 (1893), 430.
- Nayfeh, A. H. Third-harmonic resonance in the interaction of capillary and gravity waves. *J.Fluid Mech.*, 48 (1971), 385.
- Perry, R. B. and Schimke, G. R. Large amplitude internal waves observed off the Northwest coast of Sumatra, *J.Geophys.Res.*, 70 (1965), 2319.
- Phillips, O. M. On the dynamics of unsteady gravity waves of finite amplitude, Part 1, The elementary interactions, *J.Fluid Mech.*, 9 (1960), 193,
- The Dynamics of the Upper Ocean. Cambridge University Press (1966), 261 pp.
- Theoretical and experimental studies in gravity wave interactions. *Proc.Roy.Soc.*, A, 299 (1967), 104.
- The interaction trapping of internal gravity waves. *J.Fluid Mech.*, 34 (1968), 407.
- Saffman, P. G. Discussion (to a paper by K. Hasselmann), *Proc.Roy.Soc.*, A, 299 (1967), 101,
- Simmons, W. F. A variational method for weak resonant wave interactions. *Proc.Roy.Soc.*, A, 309 (1969), 561,
- Smith, R. An instability of internal gravity waves. *J.Fluid Mech.*, 52 (1972), 393.
- Thorpe, S. A. On wave interactions in a stratified fluid, *J.Fluid Mech.*, 24 (1966), 737.
- On standing internal gravity waves of finite amplitude, *J.Fluid Mech.*, 32 (1968), 489.
- Valenzuela, G. R. and Laing, M. B. Nonlinear energy transfer in gravity-capillary wave spectra, with applications. *J.Fluid Mech.*, 54 (1972), 507.
- Whitham, G. B. Mass momentum and energy flux in water waves. *J.Fluid Mech.*, 12 (1962), 135,
- A general approach to linear and nonlinear dispersive waves using a Lagrangian. *J.Fluid Mech.*, 22 (1965), 273,
- Nonlinear dispersion of water waves. *J.Fluid Mech.*, 27 (1967), 399.
- Variational methods and applications to water waves. *Proc.Roy.Soc.*, A, 299 (1967), 6.

References (continued)

Wilton, J. R. On ripples. *Phil-Mag.* (6) 29 (1915), 173.  
 Woods, J. D. Wave-induced shear instability in the summer thermocline. *J.Fluid Mech.*, 32 (1968), 791,

EXPERIMENTS WITH INTERNAL WAVES - RESONANT INTERACTIONS

William F. Simmons

The experiments described below were performed to determine the answers to two questions:

- 1) Is a resonance possible? and if so
- 2) Where does the energy go?

I. Review of the theory

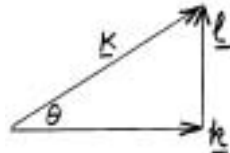
With stratification such that  $N^2 = -\frac{g}{\rho} \frac{\partial \rho}{\partial z} = \text{constant}$  solutions are obtained which have the form

$$\psi = a \cos(\underline{k} \cdot \underline{x} - \omega t + \eta) \sin \ell z \quad \text{where } \omega = \frac{\partial \psi}{\partial x}.$$

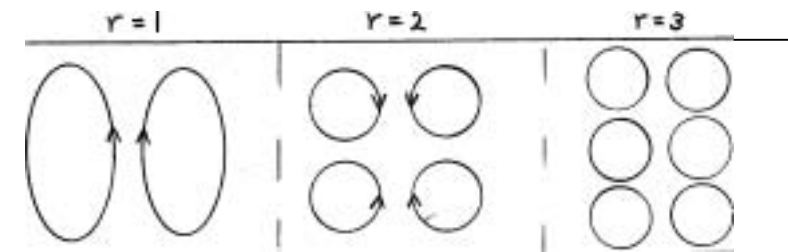
This solution leads to the dispersion relation

$$\frac{\omega^2}{N^2} = \cos^2 \theta = \frac{|\underline{k}|^2}{|\underline{k}|^2 + |\underline{\ell}|^2} \quad \text{where } \underline{k} \text{ and } \underline{\ell} \text{ are}$$

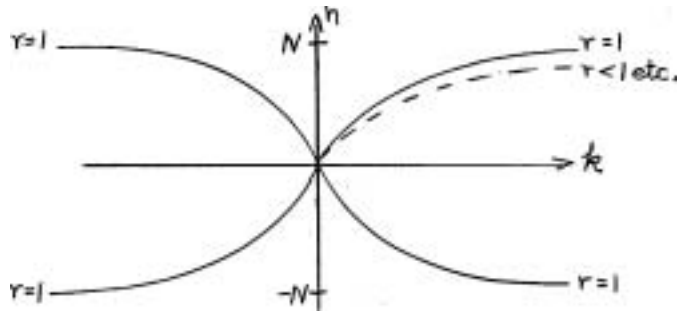
the horizontal and vertical wave numbers.



Using  $\ell = \frac{r\pi}{D}$ , where  $r = \text{integer}$  and  $D$  is the channel depth, the first three vertical modes have the following appearance:



The dispersion relation has the form



For a 2nd order triad interaction

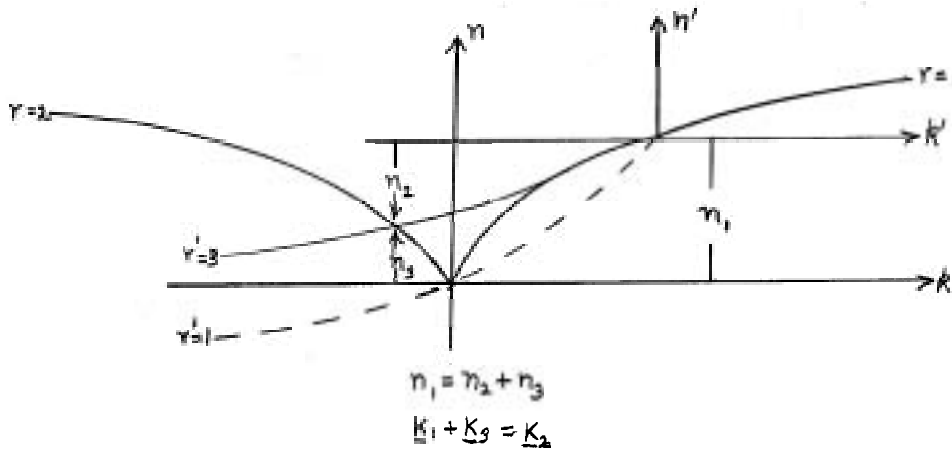
(a)  $n, 4n_2 \pm n_3 = 0$

(b)  $k_{H1} \pm k_{H2} \pm k_{H3} = 0$

where  $K_H$  is the horizontal component of  $K$ . ( $k \equiv K_H$ )

(c)  $r_1 \pm r_2 \pm r_3 = 0$  must be satisfied.

If we start with  $r=1$  and  $r=3$ , waves of  $r=2$  or  $r=4$  are needed to complete the triad. So that a graphical construction for the 1, 2, 3 triad is as follows:



Using the solution above and allowing both the amplitude and phase to be slowly varying functions of time, the relations governing the amplitudes and phases of the resonant waves are

$$\begin{aligned} \frac{D_1 a_1}{Dt} &= n_1 c a_2 a_3 \sin \eta \\ \frac{D_2 a_2}{Dt} &= n_2 c a_3 a_1 \sin \eta \\ \frac{D_3 a_3}{Dt} &= n_3 c a_1 a_2 \sin \eta \\ a_1 \frac{D_1 \eta_1}{Dt} &= n_1 c a_2 a_3 \cos \eta \\ a_2 \frac{D_2 \eta_2}{Dt} &= n_2 c a_3 a_1 \cos \eta \\ a_3 \frac{D_3 \eta_3}{Dt} &= n_3 c a_1 a_2 \cos \eta \end{aligned}$$

where  $\eta = \sum_{i=1}^3 \eta_i$

The operator

$$\frac{D_i}{Dt} = \frac{\partial}{\partial t} + (C_{gx})_i \nabla_H + (C_{gz})_i \frac{\partial}{\partial z}$$

where  $C_{gx}$  is the group velocity in the horizontal direction  $\frac{d\mathbf{k}}{dt} = C_{gx}$ . ( $C_{gz}$  will be neglected for the channel flow experiment to be described below.)

The appearance of  $C_g$  in  $\frac{D_i}{Dt}$  is due to the slowly varying  $\eta$ . The relation between these results and those of Professor Phillips is seen by putting  $\frac{\partial}{\partial t} = 0$ .

$$\frac{\partial}{\partial x} a_i = \frac{n_i}{C_{gx_i}} C a_2 a_3 \sin \eta.$$

So the two methods give the same result with  $k$  replacing  $f$ . Now the member of the triad with the largest  $k$  is unstable.

Aside: From equations for  $a_i$  we can get

$$a_1 a_2 a_3 \cos \eta = \text{constant} = Q$$

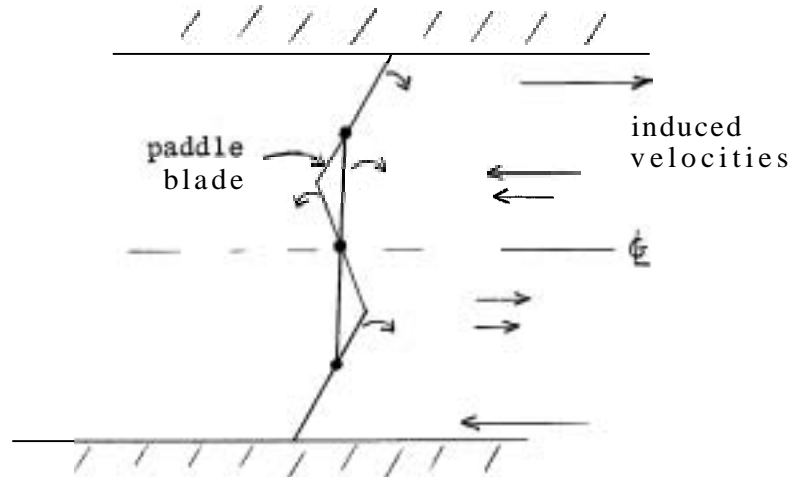
if  $Q=0$  initially, then  $Q=0$  always.

$$\therefore \eta = \pi/2.$$

So with phase angles constant, the interaction manifests itself only in the amplitude.

## II. Description of Experiment

A paddle blade capable of generating both the 1-wave and 3-wave was operated in a 1.2 m x 1.2 m x 21 m tank with a linear vertical salt stratification. A wave-absorbing beach was placed at the opposite end,



The experimental procedure was to set  $n_1$ , tune  $n_3$  into resonance, and look for  $n_2$  and  $n_4$ .

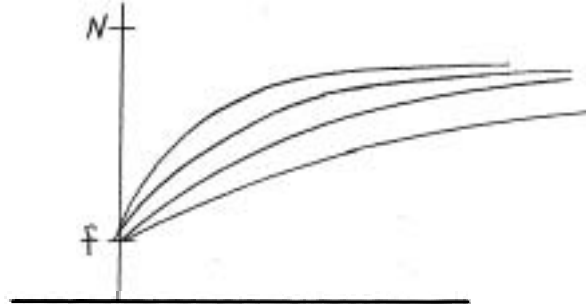
The results of this experimental procedure were given in the form of periodograms of wave amplitudes at various stations down the tank from the wave generator. With  $\eta_3$  tuned to the 1-3-4 triad the energy in the 4-wave had grown to be nearly equal to the 1-3 input at the station 11 m from the generator. See Ref.1.

Since the wave of largest  $\eta$  is unstable to two others in each triad, there are an infinite number of pairs to which  $\mathbf{a}_r$  can send its energy. So if a 1-wave is generated, it will find enough 2-3 in the noise and feed energy to them.

If we take  $\mathbf{a}_1 = \alpha_0$ ,  $\mathbf{a}_r = \alpha_{0r} e^{\lambda t}$ ,  $\mathbf{a}_r = \alpha_{0r} \exp(\alpha_0 C(\eta_1 \eta_r + 1) t)$ . So the initial growth rate of the  $r$ -th wave depends upon the initial noise  $\alpha_{0r}$  and the amount of forcing  $\alpha_0$ .

The experiment described above was done using only the 3-wave as forcing and five different waves which were members of various triads were observed. See Ref.2. The experiment was done with more initial noise and the observed interaction wave amplitudes were greater.

Aside: If rotation  $f$  is added the dispersion curve becomes



For any wave  $\omega_1$  we can find several triads, one of which is  $f$  and  $f \pm \omega$ , so that energy can go directly to  $f$ -scale motions without a long cascade through intermediate frequencies. This is a possible explanation for the spike in current meter data at frequency  $f$ , which gets energy from many internal waves.

The above experiments were instrumented with conductivity probes (see Ref.2). Since the probe Reynolds number is nearly one, the time response of these probes limits the results obtained, Later designs have been improved to minimize this difficulty.

References

1. Martin, S., Simmons, W.F., and Wunsch, C. 1969. Resonant internal wave interactions. Nature, 224: 1014,
2. Martin, S., Simmons, W.F., and Wunsch, C. 1972. The excitation of resonant triads by single internal waves. J. Fluid Mech., 53: 17-44.

Notes submitted by  
Daniel E. Fitzjarrald.

INTERNAL WAVES IN THE OCEAN

Carl Wunsch

We will consider first some general properties of internal gravity waves propagating in an inviscid, stably stratified fluid. We will assume that the motion is of small enough amplitude so that the linear theory applies and that the motion is simple harmonic in time, expressed by the factor  $e^{-i\sigma t}$ . A single equation for any dependent variable can be derived. For a rotating system this is (for the two-dimensional case),

$$-\frac{1}{c^2} \nabla_{xx}^2 p = 0,$$

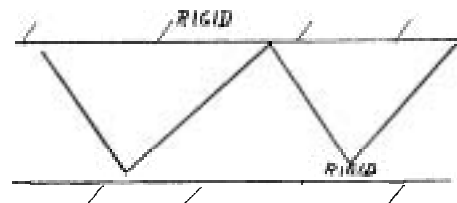
where  $c^2 = \frac{N^2(z) - \sigma^2}{\sigma^2 - f^2}$ ,  $x, y$  are the horizontal and vertical coordinates, respectively, and  $p$  is the perturbation pressure. Note that the equation is hyperbolic, which leads to some of the peculiar properties of internal waves,

$N(z) = \left[ -\frac{g}{\rho_0} \frac{\partial \rho(z)}{\partial z} \right]^{1/2}$  is the Brunt-Väisälä frequency, and  $f$  is the Coriolis parameter.

The existence of internal modes requires that the wave frequency  $\sigma$  satisfy  $f \leq \sigma \leq N$ .

For the geometry shown in Fig.1, the solution can be written as, for the case of constant  $N$  and  $f$ ,

$$p_n = A \cos\left(\frac{n\pi z}{D}\right) e^{\pm i \frac{n\pi}{D} cx}, \quad n = 1, 2, 3, \dots$$



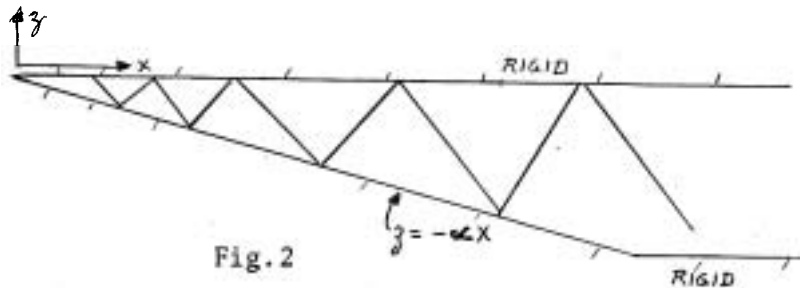
The general solution has the form

$$p = F(cx - z) + G(cx + z),$$

as would be expected from a simple application of the theory of characteristics to the hyperbolic system. Influence then propagates along the characteristic curves

$$cx \pm z = \text{constant}.$$

A more interesting problem is that of internal waves propagating into a wedge-shaped region, shown in Fig. 2.



The solution is composed of the sum of two progressive waves. The solution for the stream function is

$$\psi_n = A_n \left[ e^{i \frac{2n\pi}{\Delta} (cx - z)} - e^{-i \frac{2n\pi}{\Delta} (cx + z)} \right] e^{-i\sigma_n t},$$

$$\text{where } \Delta = \frac{c + \alpha c}{c - \alpha c}, \quad n = 1, 2, 3, \dots$$

and  $n$  is the mode number. For  $\alpha < c$ , the solution is singular at  $x = 0 = z$ . This problem is a special case of what have been called "spagetti" problems, where  $x$  is taken to be a time-like variable. The actual motion can break down at the wedge corner in three different ways:

- (1) if the motion is slow enough, it is just dissipated by viscosity,
- (2) there can be a surge or bore along the bottom,
- (3) if the motion is strong enough, internal wave breaking can occur.

The above solution is actually the inviscid interior solution away from the boundaries. There are Stokes boundary layers near the walls of thickness  $\sim \left(\frac{\nu}{\sigma}\right)^{1/2}$ . The bottom boundary layer exhibits an instability in the form of regularly spaced vortices as an incident characteristic becomes nearly parallel to the bottom.

Also, since there is a mean Stokes drift associated with the wave motion, it is possible to produce "sets" (i.e. a mean displacement) in the isopycnics. These sets act to drive a flow in the opposite direction to cancel the mean drift.

If rotation is included, internal wave energy may feed onto inertial modes of oscillation, through a similar mechanism.

In the three-dimensional case, the equation is

$$p_{zz} - \frac{1}{c^2} (p_{xx} + p_{yy}) = 0$$

which can be separated as  $p = F(z) G(x, y)$  to give

$$F''(z) + \lambda^2 \frac{[N^2(z) - \sigma^2]}{\sigma^2 - f^2} F = 0$$

which is just an eigenvalue problem for the vertical mode structure, and

$$G_{xx} + G_{yy} + \lambda_n^2 G = 0.$$

If the restriction  $\sigma > f$  is removed, we may now have internal Kelvin waves, Poincare waves, etc.

For the case of  $\sigma < f$ , trapped modes have been observed around islands. Peaks in the energy vs. frequency spectra are seen somewhat as shown in Fig.3.

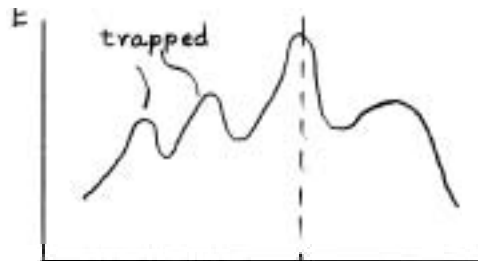


Fig.3

'Leaky' modes are also observed for  $\sigma > f$ , in which the energy is slowly radiated away. Similar phenomena might be expected to occur around submerged sea mounts,

Consider now some aspects of time series data taken in the deep ocean, i.e. 300 meters or more below the surface, Figure 4 is such a spectrum, in particular a spectrum of a current meter time series. Note that it shows fairly distinct peaks at  $f$  and at the semidiurnal frequency. It does not show any signs of a cutoff at either  $f$  or  $N$ . The curve between  $N$  and  $f$  seems to be roughly  $\sigma^{-2}$ , though one cannot say that it is not  $\sigma^{-1}$ . Figure 5 is another



LOG POWER DENSITY (CM/SEC)<sup>2</sup>/CPH VS LOG FREQUENCY (CPH)

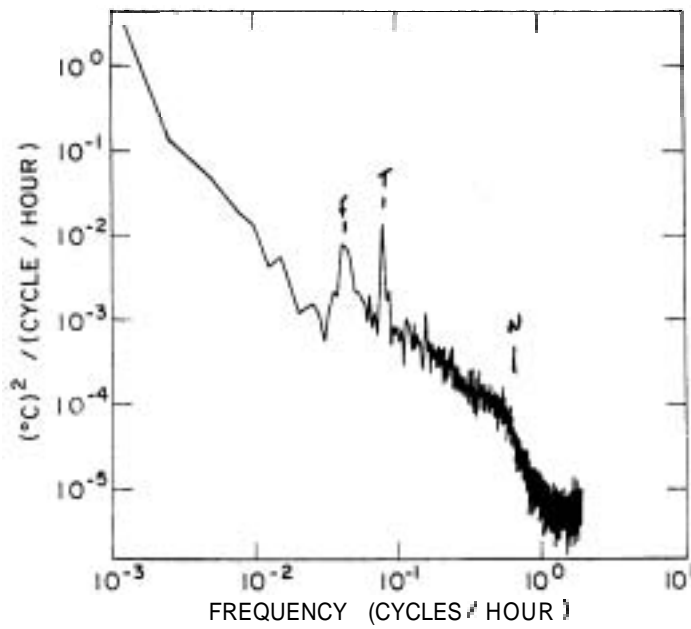


Fig.4 Spectrum of velocity made north of the Gulf Stream. f is inertial frequency, T is semidiurnal tide, and N is buoyancy frequency.

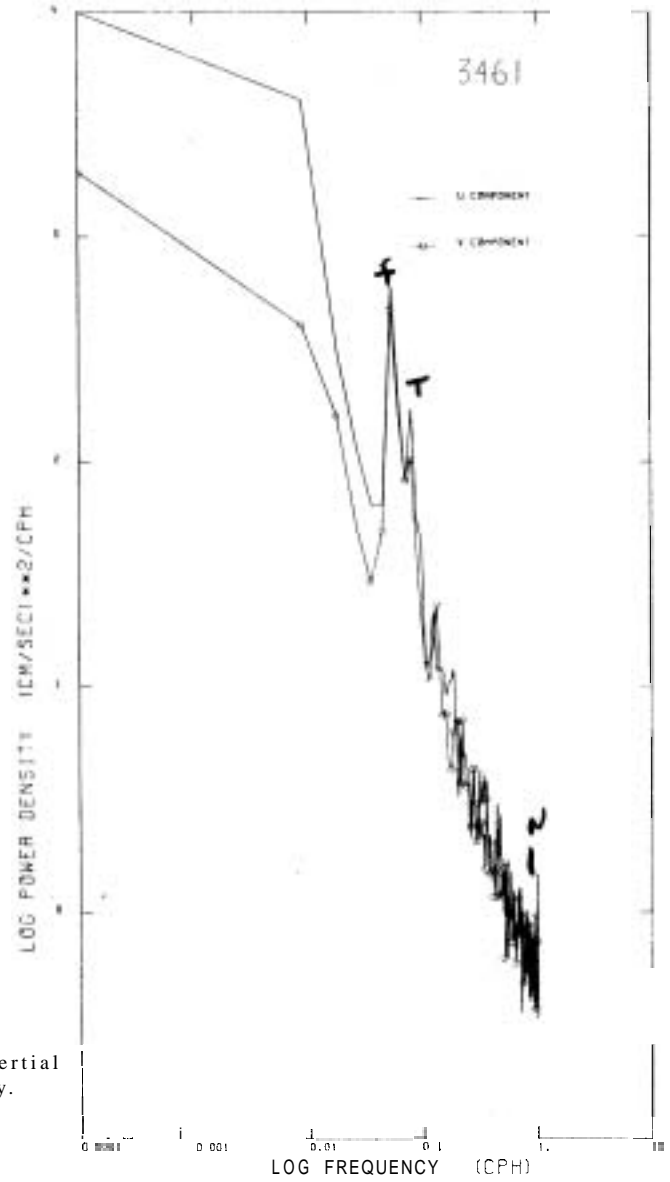


Fig.5 Spectrum of temperature made in the Sargasso Sea.

such spectrum, though it is that of a temperature time series. Many of the features it shows are the same, except that it does exhibit some cut-off at  $N$ . (It seems appropriate to remark that attempts to convert the temperature spectrum to vertical velocity spectrum have so far run afoul of the problem of unknown temperature microstructure introducing spurious energy at higher frequencies. A similar effect may contaminate the horizontal velocity.

Now, consider how such spectra might change from place to place or, time to time. First, changes in latitude should bring about a shift in the  $f$  peak. And, WKBJ internal wave theory predicts a scaling of horizontal and vertical velocities with  $N^{\frac{1}{2}}(\sigma)$  we expect a corresponding variation in the spectra versus density gradient changes. In fact these variations do appear. But after these effects are taken into account, what remains is remarkably spatio-temporally homogeneous. In addition, such spectra are nearly isotropic. Consequently we are led to the hypothesis that there is a universal deep ocean spectrum. Garrett and Munk examined this spectrum and have produced the empirical formula

$$\Phi(k, \sigma) = \frac{E(\frac{\sigma}{f})f}{2\pi(\sigma^2 - f^2)^{\frac{1}{2}}} \sigma^{-1} (\sigma^2 - f^2)^{-\frac{1}{2}} \text{ for } k_1 \leq k \leq \mu(\sigma).$$

where  $\mu(\sigma)$  is the band width of  $k$  present at any  $\sigma$ .

Finally, we may ask from where the energy in the deep ocean spectrum is coming. Sources which have been considered are:

- 1) surface wave interaction
- 2) direct wind effects
- 3) instabilities of currents
- 4) tide
- 5) Townsend's Mechanism (boundary layer radiating internal waves).

Notes submitted by  
Robert F. Bergholz  
and Michael N. Freese.

# TIME SERIES ANALYSIS

Carl I. Wunsch

## Lecture #1. Introduction to Practical Time Series Analysis

$t$  = time,  $s$  = frequency (circular frequency). Everything is invertible, in the sense that  $t$  can be substituted for  $s$ , and vice versa, Define

$$\hat{f}(s) = \int_{-\infty}^{\infty} f(t) e^{2\pi i s t} dt, \quad -\infty \leq s \leq \infty$$

$$\text{then } f(t) = \int_{-\infty}^{\infty} \hat{f}(s) e^{-2\pi i s t} ds$$

Selected theorems:

1. if  $f(t) = \pm f(-t)$ , then

$$\hat{f}(s) = 2 \int_0^{\infty} f(t) \begin{cases} \cos 2\pi s t \\ \sin 2\pi s t \end{cases} dt$$

2.  $f'(t) = \int_{-\infty}^{\infty} -(2\pi i s) \hat{f}(s) e^{2\pi i s t} ds$

so  $\mathcal{F}(f'(t)) = -2\pi i s \hat{f}(s)$

where  $\mathcal{F}(x)$  means Fourier transform of  $x$

3.  $\mathcal{F}(f(at)) = \frac{1}{|a|} \hat{f}\left(\frac{s}{a}\right)$  - stretching and contraction theorem.

4. Define  $\langle t \rangle = \frac{\int_{-\infty}^{\infty} t f^2(t) dt}{\int_{-\infty}^{\infty} f^2(t) dt}$

Same for  $\langle t^2 \rangle$ , etc.

Also  $\langle s^2 \rangle = \frac{\int_{-\infty}^{\infty} s^2 \hat{f}^2(s) ds}{\int_{-\infty}^{\infty} \hat{f}^2(s) ds}$

Assume  $\langle t \rangle = \langle s \rangle = 0$

Then  $\langle t^2 \rangle \langle s^2 \rangle \geq \frac{1}{4\pi^2}$  (uncertainty relation)

5.  $\mathcal{F}(f(t-a)) = e^{2\pi i a s} \hat{f}(s)$

shift in phase only

6. Suppose  $f(t)$  periodic in  $-\frac{T}{2} \leq t \leq \frac{T}{2}$

then  $f(t) = \sum_{n=0}^{\infty} \alpha_n e^{\frac{-2\pi i n t}{T}}$

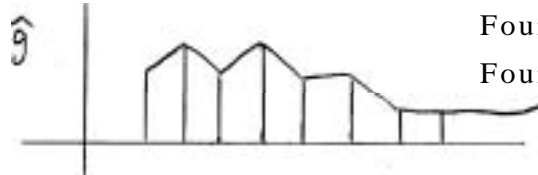
$$\alpha_n = \frac{1}{T} \int_{-\frac{T}{2}}^{\frac{T}{2}} f(t) e^{\frac{2\pi i n t}{T}} dt$$

7. Let  $g(t) = f(t)$  in  $-\frac{T}{2} \leq t \leq \frac{T}{2}$

$g(t) = 0$  - otherwise

$$\text{then } \hat{g}(s) = \int_{-\frac{T}{2}}^{\frac{T}{2}} f(t) e^{2\pi i s t} dt$$

$$\hat{g}(s_n) = T a_n, \text{ where } s = \frac{n}{T}$$



Fourier transform = F.T.  
Fourier series = F.S.

F.T. ( $= \hat{g}$ ) is equal to  $T x(\text{coefficients of F.S.})$

( $= a_n$ ) at the discrete values of  $s (= \frac{n}{T})$  where F.S. is defined.

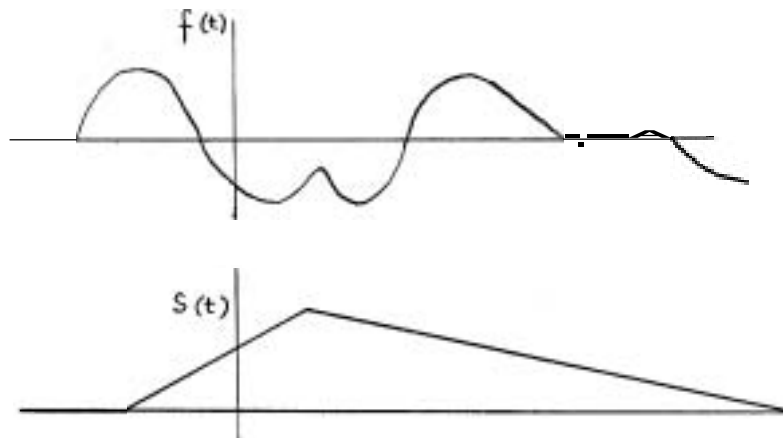
### 8. Convolution

Define 
$$h(t) = \int_{-\infty}^{\infty} f(t') g(t-t') dt' \quad (\text{written } h = f * g)$$

$$= \int_{-\infty}^{\infty} f(t-t') g(t') dt'$$

then  $\hat{h}(s) = \hat{f}(s) \hat{g}(s)$ , O.K. as long as you can interchange order of integration between  $t$  and  $s$ .

Example:



Convolution is a running average of  $f$ , weighted by  $g$ . So if  $g$  is a smoother function than  $f$ , convolution is a smoothing operation on  $f$ .

9. Corollary: define  $h(t) = \int_{-\infty}^{\infty} f(t) g(t+t') dt$

$$\text{then } \hat{h}(s) = \hat{f}^*(s) \hat{g}(s)$$

called cross correlation, not convolution. If  $f = g$ , called autocorrelation i.e.  $\hat{h}(s) = \hat{f} * f = |\hat{f}|^2$

Note  $h(t) = g \star f \neq f \star g$   
↙ cross correlation operation.

10.  $\delta$  function:

$$\hat{\delta}(s) = \int_{-\infty}^{\infty} \delta(t) e^{2\pi i s t} dt = 1$$

So  $\delta(t) = \int_{-\infty}^{\infty} e^{-2\pi i s t} ds$

integral looks funny, but it always works.

11. Define  $\Psi(t) = \sum_{n=-\infty}^{\infty} \delta(t-n)$

properties: periodic with period 1.  $\Psi(t+n) = \Psi(t)$

symmetric  $\Psi(t) = \Psi(-t)$

$$\hat{\Psi}(s) = \sum_{n=-\infty}^{\infty} e^{2\pi i s n}$$

This is the F.S. of the function  $\delta(s)$  over the interval  $-\frac{1}{2} \leq s \leq \frac{1}{2}$ .  
 So  $\Psi(t)$  is its own F.T., i.e.  $\hat{\Psi}(s) = \Psi(s)$ . Call  $\Psi(t)$  the sampling function.

12. Sample  $f(t)$  at discrete times  $t, t + \Delta t$ , etc.

$$f_{\Psi}(t) = f(t) \Psi(t/\Delta t)$$

$$= \Delta t f(t) \sum_{n=-\infty}^{\infty} \delta(t - n\Delta t)$$

What is  $\mathcal{F}(f_{\Psi}(t))$ ?

Do it directly:

$$(I) \hat{f}_{\Psi}(s) = \sum_{n=-\infty}^{\infty} f(n\Delta t) e^{2\pi i s n \Delta t} \quad (\text{its periodic})$$

Use convolution theorem:

$$(II) \hat{f}_{\Psi}(s) = \hat{f}(s) * \mathcal{F}\left[\frac{\Psi(t/\Delta t)}{\Delta t}\right]$$

$$= \hat{f}(s) * \sum_{n=-\infty}^{\infty} \delta(s - n/\Delta t)$$

$$= \sum_{n=-\infty}^{\infty} \hat{f}(s - n/\Delta t)$$

We want F.T. of unsampled function from the sampled function.

This works only if  $f(t)$  is band-limited (defined below). To show this,

consider (II)

$$\begin{aligned} \hat{f}_w(s) &= \hat{f}(s) + \hat{f}\left(s - \frac{1}{\Delta t}\right) + \hat{f}\left(s + \frac{1}{\Delta t}\right) \\ &\quad + \hat{f}\left(s - \frac{2}{\Delta t}\right) + \hat{f}\left(s + \frac{2}{\Delta t}\right) + \dots \\ &\neq \hat{f}(s) \text{ unless } \hat{f}\left(s \pm \frac{n}{\Delta t}\right) = 0 \\ &\qquad\qquad\qquad \text{for } n = \pm 1, \pm 2, \pm 3, \dots \end{aligned}$$

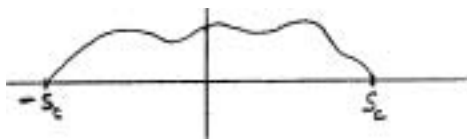
The simplest way to get this is  $\hat{f}(s) = 0$  for  $|s| \geq \frac{1}{2\Delta t}$ .

Then F.T. of unsampled function = F.T. of sampled function. Otherwise, the data sample is "aliased".

Define  $\frac{1}{2\Delta t} =$  Nyquist frequency.

If you have a band-limited function  $f(t)$  then you must sample at least at the Nyquist frequency in order to get F.T. of  $f(t)$  from sampling. On the other hand, there's no need to sample at frequencies greater than Nyquist frequency, if you have a band-limited function,

13. Suppose  $\hat{f}(s) = 0$  for  $|s| > s_c$



The sampling theorem asserts that it is sufficient to know  $f(n\Delta t)$  where  $\frac{1}{2\Delta t} = s_c$

Proof: define  $\hat{f}(s) = \sum_n c_n e^{-2\pi i s \Delta t}$ ,  $|s| \leq s_c$   
 $= 0$  otherwise.

Then  $c_n = \frac{1}{2s_c} \int_{-s_c}^{s_c} \hat{f}(s) e^{2\pi i n \Delta t s} ds = \frac{1}{2s_c} f(n\Delta t)$

So  $f(t) = \int_{-\infty}^{\infty} \hat{f}(s) e^{2\pi i s t} ds =$  work it out  
 $= \sum_{n=-\infty}^{\infty} f(n\Delta t) \frac{\sin \frac{2\pi}{2\Delta t} (t - n\Delta t)}{2\pi (t - n\Delta t)}$

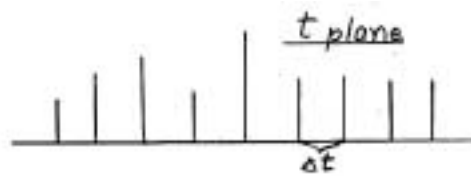
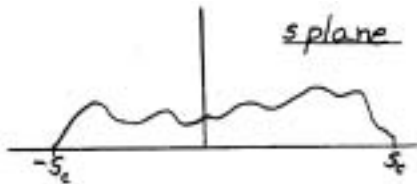
This says you can do a perfect interpolation from the sample points, if  $f(t)$  is band limited. However, you need all the sampled data from  $n\Delta t = -\infty$  to  $+\infty$ . There are better ways to interpolate, in practice, because  $\frac{\sin x}{x}$  dies off too slowly.

The above is called  $\left. \begin{array}{l} \text{Shannon's} \\ \text{Kotelnikov's} \\ \text{Whittaker's} \end{array} \right\}$  sampling theorem,

Aliasing occurs when high-frequency power (at  $|s| \geq \frac{1}{2\Delta t}$ ) appears at low frequencies, due to undersampling. In practice, if the high frequency power is small compared to the low frequency power, then sampling will give an accurate picture of low frequency processes.  
 (Notes taken by Andrew P. Ingersoll)

Wunsch Lecture #2.

If you have a band-limited process



can describe process completely by sampling at intervals  $\Delta t$ , where  $\Delta t = \frac{1}{2s_c}$ . Now consider problem posed by data record of finite length  $-\frac{T}{2} \leq t \leq \frac{T}{2}$  (ignore sampling problem for now)

$$f(t), -\infty \leq t \leq \infty$$

$$f_T(t) = f(t) \text{ in interval } -\frac{T}{2} \leq t \leq \frac{T}{2}$$

unspecified elsewhere (time limited function)

Use sampling theorem with  $s \rightarrow t$   
 Then  $t \rightarrow x$

$$s_c = \frac{T}{2} \text{ and}$$

$$\Delta s = \frac{1}{T} \quad \hat{f}(s) = \sum_{n=-\infty}^{\infty} \hat{f}(n\Delta s) \frac{\sin \frac{2\pi}{2\Delta s}(s-n\Delta s)}{\frac{2\pi}{2\Delta s}(s-n\Delta s)}$$

Given a time-limited process, it is sufficient to compute F.T. at a discrete set of points  $s \pm n\Delta s$ .

One can assume function  $f(t)$  is either zero, or periodic outside the interval. If periodic, the Fourier coefficient frequencies are

$$s_n = \frac{n}{T}, \text{ then}$$

$$f(t) = \sum_{n=-\infty}^{\infty} \alpha_n e^{\frac{2\pi i n t}{T}}$$

$$\alpha_n = \frac{1}{T} \int_{-\frac{T}{2}}^{\frac{T}{2}} f(t) e^{-\frac{2\pi i n t}{T}} dt = \frac{1}{T} \hat{f}\left(\frac{n}{T}\right)$$

Exercise: Assume  $\hat{f}(s) = \sum_{n=-\infty}^{\infty} \beta_n \frac{\sin \frac{\pi}{2AS} (s-nAS)}{\frac{\pi}{2AS} (s-nAS)}$

prove by contour integration that  $f(t)$  is zero outside

$$|t| \leq \frac{T}{2} = \frac{1}{2AS}$$

Define

$$f_T(t) = f(t) \pi \left( \frac{t}{T} \right)$$

$$\pi(x) = 1 \quad |x| \leq \frac{1}{2}$$

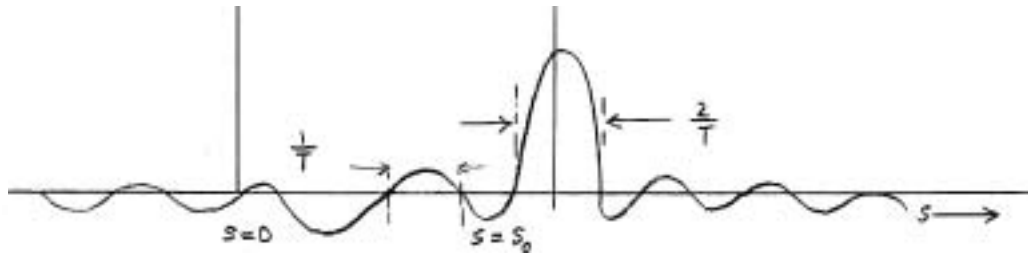
0 otherwise

$$\hat{f}_T(s) = \hat{f}(s) * \mathcal{F} \left( \pi \left( \frac{t}{T} \right) \right)$$

$$\hat{f}_T(s) = \hat{f}(s) * \frac{\sin \pi s T}{\pi s T}$$

Suppose  $\hat{f}(s) = \delta(s - s_0)$

then  $\hat{f}_T(s) = \sin \frac{\pi(s-s_0)T}{\pi(s-s_0)}$



Effect of sampling in finite interval is to spread energy out in  $s$  space.

If you have two spikes  $\hat{f}(s) = \delta(s - s_0) + \delta(s - s_1)$

then you can distinguish them if

$$|s_0 - s_1| \geq \frac{1}{T}$$

Increasing the data length increases the resolution in frequency space.

There is no point in interpolating to get  $\hat{f}(s)$  in between  $s = nAS$ , because you cannot resolve better than  $AS$  anyway,

Note that energy from  $s = s_0$  appears at frequencies  $s \neq s_0$  with contribution  $\frac{1}{|s - s_0|}$ . The exception is when the length of the record is a multiple of the period associated with  $s_0$ . Then there is no contamination at the frequencies  $s = \frac{n}{T}$ .

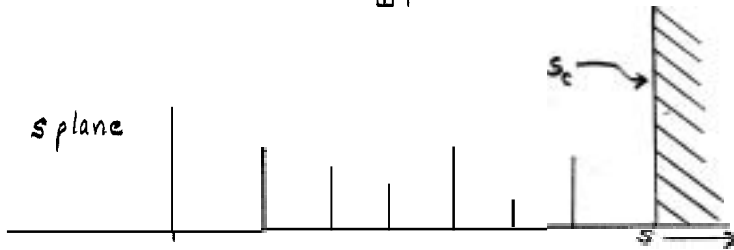
Now, both problems  $f_{\omega T}(t) = f(t) \omega(t) \pi \left( \frac{t}{T} \right)$

convolution says

$$f * g * h = (f * g) * h = f * (g * h)$$



1. Finite data: compute  $\hat{f}_{wT}(s)$  only at frequencies  $S = T$



2. Sampled data: look only at frequencies

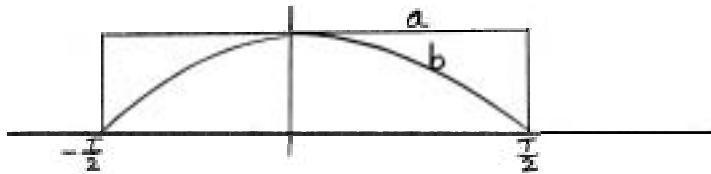
$$s = \frac{1}{\Delta t} - s_c$$

Note that sampling and finite record effects are independent. Also, if  $T = N\Delta t$ , then these are commensurable:

$$\frac{1}{2\Delta T} / \frac{1}{N\Delta T} = \frac{N}{2} = \text{number of data points from 0 to } s_c.$$

Each data point is two pieces of information (real and imaginary part). The information for  $s \leq 0$  is the same, since coefficients are complex conjugates of those at  $s \geq 0$  for real data.

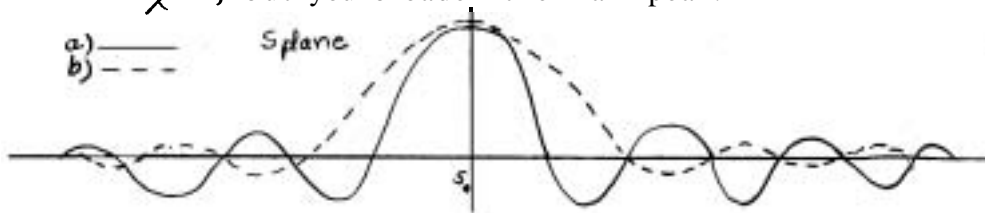
Question:  $\hat{f}\left(\frac{s}{T}\right) = T\alpha_n$ , do we compute  $\alpha_n$  or  $\hat{f}\left(\frac{s}{T}\right)$ ? If looking at pulses (non-periodic), better to use  $\hat{f}$ . If looking at periodic process, use  $\alpha_n$ , but either will do. How to improve your estimates - decrease the spreading?



a) give all data equal weight (gives much spreading)

b) give less weight to data near ends of the record.

We considered a) already. In going to b), you knock down the side lobes relative to  $\frac{\sin x}{x}$ , but you broaden the main peak.



From sampling  $f(n\Delta t) \rightarrow$  sequence  $f_n$   

$$\hat{f}(s = \frac{p}{T}) = \sum_{n=0}^N f_n e^{\frac{2\pi i n p}{N}} ; T = N\Delta t$$

$n, N, p$  are integers. These all look like  $\cos \frac{2\pi n p}{N}$  or  $\sin \frac{2\pi n p}{N}$ ,  $N$  points;  $2N$  multiplications and additions for each frequency.  $N$  frequencies  $s_p$  have about  $2N^2$  operations, which is prohibitive for  $N = 10^4$ .

Actually, there are a lot of duplicated operations, so number of operations actually goes as  $N \ln N$  using Fast Fourier Transform (FFT), i.e. for  $N = 6 \times 10^4$ , takes 2 minutes on modern computer using FFT. Now we deal with the discrete set  $\{f_t\}$  with F.T.  $\hat{f}(s) = \sum_t f_t e^{2\pi i t s}$  (setting now  $\Delta t = 1$ ). Compute F.T. only at  $s = \frac{p}{T} = \frac{p}{N}$   
 $\rightarrow$  because  $\Delta t = 1$

Convolution of sequences:

$$\hat{g}(s) = \sum_t g_t e^{2\pi i t s}$$

$$\hat{f}(s) = \sum_t f_t e^{2\pi i t s}$$

multiply these together, let  $m = n+r$

$$= \left( \sum_n f_n g_{m-n} \right) e^{2\pi i s m} = \sum_m h_m e^{2\pi i s m}$$

So if  $h_t = \sum_n f_n g_{t-n}$ , then F.T. of  $h_t$  is just product of F.T. (f) and F.T. (g).

Now let  $z = e^{2\pi i s}$

$$\hat{f}(s) = \sum_t f_t z^t ; \hat{g} = \text{etc.}$$

and

$$\hat{h} = \left( \sum_n f_n z^n \right) \left( \sum_p g_p z^p \right)$$

$$= \sum_q h_q z^q$$

Rules for multiplying polynomials can be used. The best way to take convolution is to take F.T. of each side, multiply these together, then invert F.T.

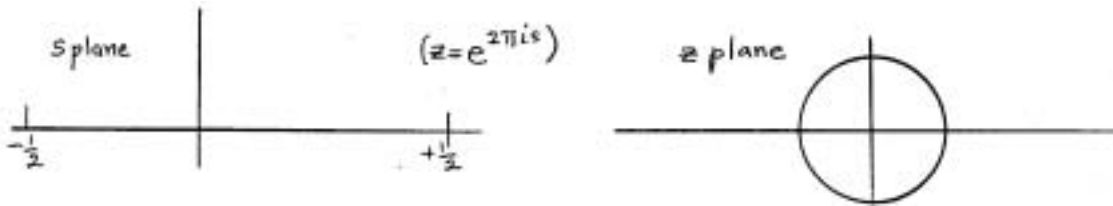
Suppose  $f_t = \cos \omega_0 t$  for  $t \geq 0$   
 $= 0$  otherwise

(sampled at  $t = 0, 1, 2, 3, \text{etc.}$ )

Then

$$\begin{aligned}\hat{f}(s) &= \sum_{t=0}^{\infty} \frac{e^{i\omega_0 t} z^t + e^{-i\omega_0 t} z^t}{2} \\ &= \frac{1}{2} \left\{ \begin{aligned} &1 + e^{i\omega_0} z + e^{2i\omega_0} z^2 + \dots \\ &+ 1 + e^{-i\omega_0} z + e^{-2i\omega_0} z^2 + \dots \end{aligned} \right\} \\ &= \frac{1}{2} \left[ \frac{2 - 2z \cos \omega_0}{1 - 2z \cos \omega_0 + z^2} \right]\end{aligned}$$

using fact that these F.T.'s are polynomials, can often sum the F.T. (an infinite series) and express in finite algebraic form



The upper half of s plane maps into interior of unit circle in z plane, and the real axis maps into the unit circle.

causality:  $f(t) = \int_{-\infty}^{\infty} \hat{f}(s) e^{-2\pi i s t} ds$

Suppose  $f(t) = 0$  for  $t < 0$  (defines a causal sequence).

This implies  $\hat{f}(s)$  has no poles in upper half of s plane, i.e. the interior of the unit circle in z plane.

So  $\hat{h}(s) = \sum_q h_q z^q$  is a Taylor series (not Laurent series) if  $f(t)$  is a causal sequence.

Write 
$$\begin{aligned}\hat{f}(z) &= + f_{-p} z^{-p} + f_{-p-1} z^{-p-1} + \dots \\ &\quad + f_0 + f_1 z + f_2 z^2 + \dots\end{aligned}$$

Consider  $\frac{1}{1-2z} = 1 + 2z + 4z^2 + \dots$  no good because pole at  $z = \frac{1}{2}$ . Also write

$$\frac{1}{1+2z} = -\frac{1}{2z} \left\{ 1 + \frac{1}{2z} + \frac{1}{4z^2} + \frac{1}{6z^3} + \dots \right\}$$

How to undo a convolution using this formalism?

Suppose  $h_t = \sum_n a_n f_{t-n}$  a is an averaging operation.

$$\hat{h}(z) = \hat{a}(z) \hat{f}(z)$$

i.e. can we get f, if we know h and a?

$$\hat{f}(z) = \frac{\hat{h}(z)}{\hat{a}(z)} \quad \text{depends on } a(n)$$

$\frac{1}{\hat{a}(z)} = \hat{b}(z)$ , express as Taylor-Laurent series in z.

Example:

$$a_0 = 1, a_1 = \frac{1}{2}, a_p = 0 \quad \text{otherwise}$$

$$h_t = f_t + \frac{f_{t-1}}{2}$$

$$\hat{f}(z) = \hat{h}(z) \hat{b}(z) = \frac{\hat{h}(z)}{1 + \frac{1}{2}z^{-1}}$$

$$\hat{h}(z) = [1 - \frac{z}{2} + \frac{z^2}{4} - \frac{z^3}{8} + \dots]$$

Note that  $b$  has a pole at  $z = -2$ , i.e.  $b$  is causal: only need prevfous values of  $h$  to get  $f$ , i.e.

$$\hat{f}(z) = \frac{h_0}{f_0} + \underbrace{\left(\frac{h_1}{2} + h_1\right)}_{f_1} z + \underbrace{\left(\frac{h_2}{4} + \frac{h_1}{2} + h_2\right)}_{f_2} z^2$$

every value  $f_n$  involves only

$$h_n, h_{n-1}, h_{n-2}, \text{ etc.}$$

So in this example, " $b$ " is a causal process (the response of the instrument to a pulse) and  $h_t$  is the output. You want to infer the input  $f_t$ . The theory just proved says that the value of  $f_t$  depends only on measurements of  $h_t$  from earlier times.

One can simplify further by noting that

$$f_n = \frac{f_{n-1}}{2} + h_n; \text{ do it recursively.}$$

Recursive filters,

Suppose you have a nearly resonant system (pole just outside unit circle) better to use reciprocal of  $\hat{b}(z)$ .

### Bibliography


Bracewell, Jenkins very useful, also Gold and Rader.

Wiener - makes functions proper.


(Notes taken by Andrew P. Ingersoll)


Wunsch Lecture #3.

Examples of Random Signals

(1)  $f(t) = \pm \sigma$  with equal probability  $f_t$  (i)   $\langle f_t \rangle = 0$

ergodic:  $\overline{\text{time average}} = \langle \text{ensemble average} \rangle$

(ii)   $\bar{f}_t = 0$

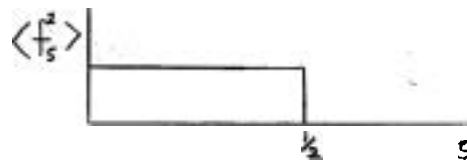
The Fourier Transform,  $f_s = \sum_t f_t \theta$  is random   $\langle f_s \rangle = 0$

hence, ~~so is~~  $|f_s|^a$

but  $\langle |f_s|^1 \rangle$  not random

$$\langle |f_s|^1 \rangle = \sum \sum \langle f_t f_q \rangle e^{2\pi i s(t-q)}$$

$$= N \sigma^2$$



$f_t$  is a non-Gaussian white noise process,

(2)  $f_t = \sum_n a_n \theta_{t-n}$   
 ↑ excitation  
 ↑ impulse response  
 (fixed sequence)

(very general decomposition, Wold)

where  $\langle \theta_t \rangle = 0$

$$\langle \theta_p \theta_t \rangle = \delta_{tp} \sigma^2$$

$$\text{then } f_s = \hat{a}(s) \hat{\theta}(s)$$

$$\langle \hat{f}(s) \rangle = \hat{a}(s) \langle \hat{\theta}(s) \rangle = 0$$

e.g. Example bell 



but  $\frac{1}{N} \langle \hat{f} \hat{f}^* \rangle = |\hat{a}(s)|^2 \sigma^2$ , so can find  $|\hat{a}_n|^2$  experimentally.

(3)  $f_t$  = Gaussian variates with zero mean, variance  $\sigma^2$ , finite duration T.

$$\hat{f}(s_p) = \sum_{n=0}^{N-1} f_n e^{2\pi i n s_p} \quad s = s_p \equiv \frac{p}{T}$$

$$= \sum_{n=0}^N f_n \cos 2\pi n s + i \sum f_n \sin 2\pi n s = a_p + i b_p$$

$$\langle \hat{f}(s) \rangle = 0 \quad \langle \hat{f}(s)^2 \rangle = N \sigma^2 \quad \langle a_p b_p \rangle = 0$$

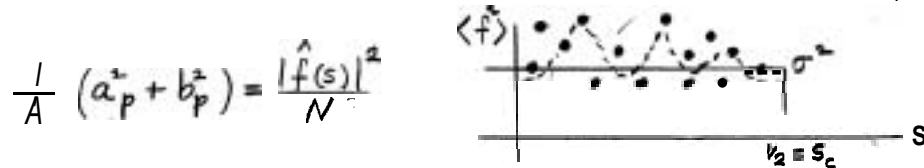
so  $\langle a_p^2 \rangle = \frac{N\sigma^2}{2}$      $\langle b_p^2 \rangle = \frac{N\sigma^2}{2}$   
 $\frac{1}{N} (a_p^2 + b_p^2) = \frac{|\hat{f}(s)|^2}{N}$

now  $\frac{a_p}{N^{1/2}}$  is Gaussian with zero mean,    let  $X = Y^{1/2}$

$$P\left(\frac{a_p}{N^{1/2}} = X\right) = \frac{1}{\sqrt{2\pi}\sigma} e^{-X^2/2\sigma^2} \Rightarrow P\left(\frac{a_p^2}{N} = Y\right) = \frac{1}{\sqrt{2\pi}\sigma^2} e^{-Y/2\sigma^2}$$

This

follows a Chi-squared distribution with 2 degrees of freedom,  $a_p$  and  $b_p$ ,  $\chi_2^2$ .



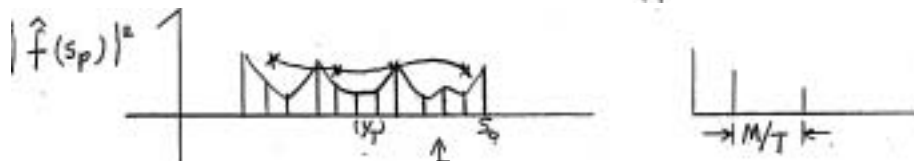
Note: variance about  $\sigma^2$  is  $\frac{\sigma^4}{2}$

(large and independent of N!) (N = sample size)

This is a periodogram, before averaging, and, periodogram = power spectrum. Imagine building ensemble of M records, (this Chi-squared with 2 M degrees of freedom).

Then variance =  $\frac{\sigma^4}{2M}$

$$\langle |\hat{f}(s_p)|^2 \rangle = \frac{1}{M} \sum_{n=1}^M |f_n(s_p)|^2 \equiv \bar{\Phi}_{ff}^{(M)}(s_p)$$



alternatively, average neighbors together:: say there are M neighbors averaged, then again have Chi-square distribution,  $\chi_{2M}^2$ . For highly tuned physical process (e.g.  $\omega = f$ ) keep resolution high, M small. The stability of the spectrum trades off against resolution. Chopping the record into several pieces, transforming, and averaging, gives equivalent increase in stability.

The correlation method is equivalent:

correlation theorem: let  $\phi_\tau = \sum_t f_t f_{t+\tau}$

then  $\langle \text{the Fourier Transform } [\phi_n] \rangle = \langle \hat{f}(s) \hat{f}^*(s) \rangle$

Calculations of  $\phi_\tau$  for large  $\tau$ , with finite data, are statistically poor, just like calculations of power spectra for small s.

If we truncate the autocorrelation, it is equivalent to using a spectral window

$$\pi(\tau/\varphi) = \text{[rectangle function]}$$

which is the averaged periodogram, using a  $\sin(s)/s$  window: not a good window, since side lobes can give negative energy density,  $\int_{-\infty}^{\infty} f f$ .

The advantage of the correlation method is that after truncation the Fourier Transforming is quicker. The FFT is so efficient as to make this method old-fashioned. An advantage of correlation functions is that

$\lim_{N \rightarrow \infty} \hat{f}(s)$  doesn't exist,

but  $\lim_{N \rightarrow \infty} \phi_{\tau}$  does exist ( $\phi_{\tau}$  is an estimate of  $\langle f_{\tau} f_{\tau+\tau} \rangle$ )

(The Wiener Khinchine relation  $\mathbb{I}_{Sf}(\sigma) = \text{F.T.}(\langle f_{\tau} f_{\tau+\tau} \rangle)$ ).

$$\text{F.T.}(\sum \phi_{\tau}') = \phi(s)^* \frac{\sin \pi s \varphi}{\pi s \varphi}$$

(Notes taken by Peter B. Rhines)

Wunsch Lecture #4

Note from last lecture:

The Power Density Spectrum

$$= N^{-1} \langle |\hat{f}(s)|^2 \rangle \quad (= \sigma^2 \text{ if process is white})$$

$$= \langle |\text{Fourier series}|^2 \rangle \div (1/N)$$

= the square of the Fourier 'coefficients' divided by the spacing used, Thus if M coefficients are averaged spacing is M/N.

Coherence

There are many ways in which this concept can be explained; the following is one of them. Suppose there are two random processes,  $x_t$  (an input) and  $y_t$  (a signal) related by the linear convolution

$$y_t = \sum_{p=-\infty}^{\infty} a_p x_{t-p} + n_t$$

where  $n_t$  represents noise.

Simple, perfect case:  $n_t \equiv 0$ . In this case  $\hat{a}(s)$  can be evaluated as  $\hat{y}(s)/\hat{x}(s)$ . But this can always be done with any two sets of data - wave heights on Bondi Beach and examination results in a Cambridge Mathematics

examination, for example - even if there is no real physical relationship between them. We hence wish to examine  $\hat{a}(s)$  closely and determine if it is of the sort that could come from a physical process.

Suppose  $x_t$  and  $y_t$  are Gaussian random variables with

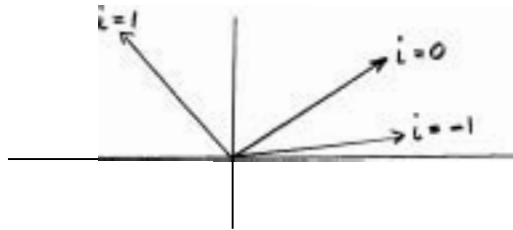
$$\hat{x}(s) = |\hat{x}(s)| e^{i\phi_x(s)} \text{ and } \hat{y}(s) = |\hat{y}(s)| e^{i\phi_y(s)}.$$

Then  $\phi_x(s)$  and  $\phi_y(s)$  are random variables, uniformly distributed in  $-\pi \leq \phi < \pi$ . Hence

$$\hat{a}(s) = |\hat{y}(s)| / |\hat{x}(s)| \exp \{ i [\phi_y(s) - \phi_x(s)] \}$$

will have a phase  $\phi_a(s) = \phi_y(s) - \phi_x(s)$  which is randomly distributed in  $(-\pi, \pi)$ . We now assert that if  $a$  comes from a physical system the phase of  $a$  is a smooth function of frequency.

What does "smooth" mean? Consider  $\hat{y}(s_p) \hat{x}^*(s_p)$  and compare it with  $\hat{y}(s_{p+i}) \hat{x}^*(s_{p+i})$  for  $i = \pm 1, \pm 2, \dots$



The vectors  $\vec{E}_i = \hat{y}(s_{p+i}) \hat{x}^*(s_{p+i})$ .

Define

$$\Phi_{yx}(s_p) = \frac{1}{M+1} \sum_{n=p-M/2}^{p+M/2} |\hat{y}(s_{p+n})| |\hat{x}(s_{p+n})| e^{i\phi_a(s_{p+n})}$$

If adjacent  $\vec{E}_i$ 's have close to the same phase  $\Phi_{yx}$  will be large while if adjacent  $\vec{E}_i$ 's are unrelated  $\Phi_{yx}$  will be comparatively smaller. An appropriate normalization is introduced by defining

$$\text{coh}_{yx}(s_p) = \frac{\Phi_{yx}(s_p)}{\sqrt{\Phi_{yy}(s_p) \Phi_{xx}(s_p)}}$$

where

$$\Phi_{yy}(s_p) = \left( \frac{1}{M+1} \sum_{p-M/2}^{p+M/2} |\hat{y}|^2 \right)^{1/2}$$

and there is a parallel definition for  $\Phi_{xx}(s_p)$ ,  $\text{coh}_{yx}(s_p)$  is called the coherence of  $y_t$  and  $x_t$  at frequency  $s_p$  (suitably averaged over the  $M$  adjacent frequencies). Using Schwartz's inequality we can show that



$$\text{coh}_{yx} \leq 1$$

Now, for  $\hat{y} = \hat{a}\hat{x}$  (perfect case)

$$\begin{aligned} \Phi_{yx} &= \langle \hat{y}\hat{x}^* \rangle \\ &= \hat{a} \langle \hat{x}\hat{x}^* \rangle \quad \text{because } a \text{ is not random,} \end{aligned}$$

$$\Phi_{xx} = \langle \hat{x}\hat{x}^* \rangle$$

$$\text{and } \Phi_{yy} = |\hat{a}|^2 \langle \hat{x}\hat{x}^* \rangle$$

Thus  $\text{coh}_{yx}$  has amplitude 1 and phase equal to the phase of  $\hat{a}$ .

Case with noise:  $n \neq 0$

Suppose that  $\hat{y} = \hat{a}\hat{x} + \hat{n}$ , where  $\hat{n}$  represents the noise which, by assumption is uncorrelated with  $\hat{x}$ . Then

$$\begin{aligned} \Phi_{yx} &= \langle (\hat{a}\hat{x} + \hat{n})\hat{x}^* \rangle = \hat{a} \langle \hat{x}\hat{x}^* \rangle, \\ & \quad (\langle \hat{x}\hat{n}^* \rangle = 0 \text{ by assumption}) \\ \Phi_{yy} &= |\hat{a}|^2 \langle \hat{x}\hat{x}^* \rangle + \langle \hat{n}\hat{n}^* \rangle \end{aligned}$$

$$\text{and } \Phi_{xx} = \langle \hat{x}\hat{x}^* \rangle,$$

Thus

$$\begin{aligned} (S_p) &= \frac{\hat{a}}{|\hat{a}| \left(1 + \frac{\langle \hat{n}\hat{n}^* \rangle}{|\hat{a}|^2 \langle \hat{x}\hat{x}^* \rangle}\right)^{1/2}} \\ &= \frac{\hat{a}}{\Phi_{aa} \left(1 + \frac{\Phi_{nn}}{\Phi_{aa} \Phi_{xx}}\right)^{1/2}} \\ & \quad | \ll \Phi_{nn} \gg \Phi_{aa} \Phi_{xx} \\ & \sim | \ll \Phi_{nn} \ll \Phi_{aa} \Phi_{xx} \end{aligned}$$

Thus we have a complex valued quantity, the coherence, whose phase equals the phase of  $\hat{a}$ , and whose amplitude approaches one if the power in the noise is suitably small and approaches zero if the power in the noise is large. In this statement lies its usefulness.

Having calculated the  $\Phi$ 's and the coherence, we can evaluate

$$\begin{aligned} \hat{a} &= \Phi_{yx} / \Phi_{xx} \\ &= \text{coh}_{yx} \sqrt{\frac{\Phi_{yy}}{\Phi_{xx}}} \end{aligned}$$

and hence  $\underline{a}$  itself. And from  $\underline{a}$ , since we have  $x$  and  $y$  we calculate  $n$ , the noise. In this calculation, using the relationship

$$\Phi_{yy} = \Phi_{aa} \Phi_{xx} + \Phi_{nn}$$

we find that

$$\Phi_{nn} = \Phi_{yy} (1 - \text{coh}_{yx}^2)$$

which is called the incoherent noise and


$$\Phi_{aa} \Phi_{xx} = \text{coh}_{yx}^2 \Phi_{yy}$$

which is called the coherent noise. Often the noise is of more interest than the signal in that it can give you an indication as to what else is happening.

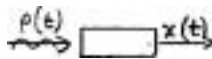
In practice, how do you average? This was discussed in the last lecture and we decided that either ensemble averaging or frequency band averaging was possible. Such finite methods lead to coherences which themselves are random variables. Goodman showed that the sample coherences follow a complex Wishart distribution which is now extensively tabulated, From these tables error bars for the coherence amplitude and phase determinations can be estimated. These errors will depend on M and the previously discussed payoff between resolution and accuracy is again encountered. It can easily be shown that sample coherence is biased, i.e. if  $\Upsilon$  is the true coherence, then  $\Upsilon$  is less than  $\langle \text{coh} \rangle$  for any finite N.

Notes taken by  
Herbert E. Huppert.

Wunsch Lecture #5

Model of an Instrument: 

$t/k$  = spring constant;  $x(t)$  = mass position;  $p(t)$  = forcing of spring  
then  $m\ddot{x} + \gamma\dot{x} + kx = mp(t)$



(model of a more general simple linear system)

Use Green's function approach:

$$m\ddot{g} + \gamma\dot{g} + kg = m\delta(t) \quad , \text{ take F.T.}$$

$$\hat{g}(s) = \frac{1}{(k/m) - (2\pi s)^2 + (b/m)2\pi i s}$$

$$|\hat{g}(s)| = \frac{1}{(k/m - (2\pi s)^2)^2 + \frac{b^2}{m^2} (2\pi s)^2}$$

phase

$$\hat{g} = -\tan^{-1} \left[ \frac{(b/m)(2\pi s)}{(k/m) - (2\pi s)^2} \right]$$

Then solution of original problem is

$$\hat{x}(s) = \hat{p}(s) \hat{g}(s)$$

Suppose there is noise: you measure  $y_t = x_t + n_t$

then  $\hat{y}(s) = \hat{p}(s) \hat{g}(s) + \hat{n}(s)$ ,

power spectrum  $\Phi_{yy} = \langle (\hat{p}\hat{g} + \hat{n})(\hat{p}\hat{g} + \hat{n})^* \rangle =$

$$= \hat{g}\hat{g}^* \langle \hat{p}\hat{p}^* \rangle + \langle \hat{n}\hat{n}^* \rangle \quad \text{since } \langle \hat{n}\hat{p}^* \rangle = 0$$

So  $\Phi_{yy}(s) = \Phi_{gg}(s) \Phi_{pp}(s) + \Phi_{nn}(s)$ .

Look at cross power between input  $p$  and output  $y$ .

$$\Phi_{yp}(s) = \langle \hat{y}\hat{p}^* \rangle = \langle (\hat{g}\hat{p} + \hat{n})\hat{p}^* \rangle = \hat{g}\Phi_{pp}(s)$$

so  $\hat{g}(s) = \frac{\Phi_{yp}(s)}{\Phi_{pp}(s)}$

; can find  $\hat{g}(s)$  of your instrument by putting a known input  $\Phi_{pp}(s)$  and measuring the cross spectrum  $\Phi_{yp}(s)$ .

Rewrite:

$$\hat{g}(s) = \sqrt{\frac{\Phi_{yy}(s)}{\Phi_{pp}(s)}} \text{coh}_{yp}(s)$$

Knowing  $\hat{g}(s)$  of the instrument, you can, in principle, find  $\Phi_{pp}$  once you know  $\Phi_{yy}$  (easiest to do in terms of  $z$  transforms).

For example above:

Suppose  $p_t$  is white noise:

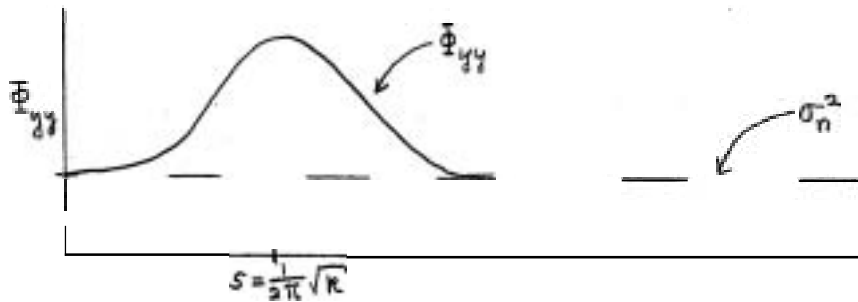
$$\Phi_{pp}(s) = \sigma_p^2$$

also assume  $\Phi_{nn}(s) = \sigma_n^2$

Define  $|\hat{g}|^2 = \frac{1}{B^2(s)}$ , set  $m = 1$  for convenience

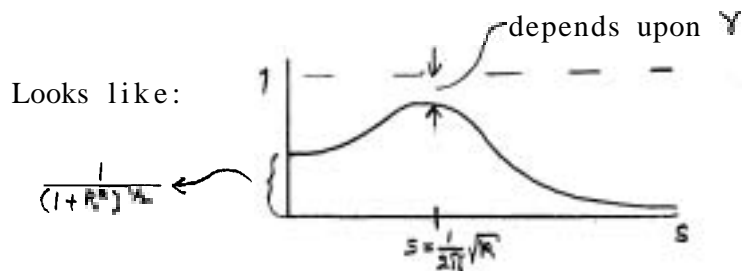
Then

$$\Phi_{yy}(s) = \frac{\sigma_p^2}{(k - (2\pi s)^2)^2 + \gamma(2\pi s)^2 + \sigma_n^2}$$



can separate noise  $\sigma_n^2$  from input  $\sigma_p^2$  if you know response of instrument.

$$\text{coh}_{yp}(s) = \left| \hat{g} \right| \sqrt{\frac{\Phi_{pp}}{\Phi_{yy}}} = \frac{1}{\beta(s)} \frac{\sigma_p^2}{(\frac{\sigma_p^2}{\beta^2(s)} + \sigma_n^2)^{1/2}} = \frac{1}{(1 + \frac{\sigma_n^2 \beta^2(s)}{\sigma_p^2})^{1/2}}$$



For large  $s$ , the coherence is low due to noise, Near resonance, the relative noise power is low. All information about the system is contained in the power spectrum and coherence.

Exercise (for the reader): given 2 waves

$$y_1 = A \cos(kx - \omega t), \quad y_2 = B \cos(k'x - \omega' t)$$

where  $\begin{cases} k' = k + \Delta k' \\ \omega' = \omega + \Delta \omega' \end{cases}$  compute coherence

between 2 points  $x = 0$  and  $x = \Delta x$ , where  $y(t, x) = y_1 + y_2$

Assume  $A \approx B$  and  $\begin{cases} \frac{\Delta k}{k} \ll 1 \\ \frac{\Delta \omega}{\omega} \ll 1 \end{cases}$

the result is  $\text{coh} \approx 1 - \frac{(\Delta x)^2 (\Delta k)^2}{2}$ ,

Example: relation between sea level  $f(t)$  and atmospheric pressure  $p(t)$

$$f(t) = a * p(t) * n$$

$$n(t) = f(t) - a(t) * p(t)$$

The noise is what was of interest. Carried out in detail in Wunsch, Rev. Geophys. 1972.

Signal extraction (filtering):

A linear filter is any operator  $a_p$  such that  $y_t = a + x$ .  
 Special example given:  $x_t = m_t + n_t$   
 ↙ signal (known)                      (mess age)                      ↘ noise

We want to suppress the noise as best possible, by use of a convolution filter.

$$\text{let } m_t = \sum a_p x_{t-p}$$

that is, we want  $(m_t - \sum a_p x_{t-p})^2 = e_t^2$  to be as small as possible ( $e_t$  is the error). Can we find such an  $a_p$ ? What is the best (optimal) filter  $a_p$  for realizations of the ensemble? Use least squares approach

$$\frac{\partial}{\partial a_q} \langle e_t^2 \rangle = 2 \langle x_{t-q} (\sum a_p x_{t-p} - m_t) \rangle = 0$$

$$\sum a_p \langle x_{t-q} x_{t-p} \rangle = \langle x_{t-q} m_t \rangle \quad \text{where } \langle \rangle \text{ denotes an ensemble average}$$

For stationary process,  $\langle x_{t-q} x_{t-p} \rangle = R(q-p)$

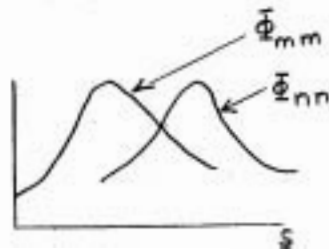
and  $\langle x_{t-q} m_t \rangle = Q(q)$ ;  $\sum a_p R(q-p) = Q(q)$  (linear simultaneous equations for  $a_p$ )

Take F.T.:  $\hat{a}(s) \hat{\Phi}_{xx}(s) = \hat{\Phi}_{xm}(s)$

$$\text{now } \hat{\Phi}_{xm}(s) = \langle (\hat{m} + \hat{n}) \hat{m}^* \rangle = \langle \hat{m} \hat{m}^* \rangle = \hat{\Phi}_{mm}(s)$$

$$\text{and } \hat{\Phi}_{xx}(s) = \langle (\hat{m} + \hat{n})(\hat{m} + \hat{n})^* \rangle = \langle \hat{m} \hat{m}^* \rangle + \langle \hat{n} \hat{n}^* \rangle = \hat{\Phi}_{mm}(s) + \hat{\Phi}_{nn}(s)$$

so 
$$\hat{a}(s) = \frac{1}{1 + \frac{\hat{\Phi}_{nn}(s)}{\hat{\Phi}_{mm}(s)}}$$

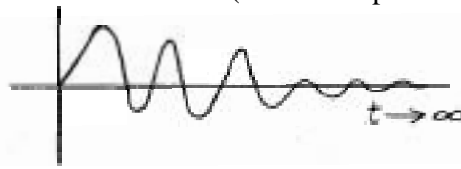


then the best filter is to suppress frequencies where

$$\frac{\hat{\Phi}_{nn}}{\hat{\Phi}_{mm}} = \frac{\text{noise power}}{\text{message power}} \text{ is high, and transmit frequencies}$$

where  $\frac{\hat{\Phi}_{nn}}{\hat{\Phi}_{mm}}$  is low.

Wiener Filter Problem:  $a_p = 0$  for  $p \leq 0$   
(causal operator)



can then solve matrix equation  $R \cdot A = Q$  where  $a_p \neq 0$  for  $p = 1, 2, \dots, N$  (truncating at  $p = N$  is O.K. because response of filter should die away after long time lags). Now consider a prediction problem: suppose we have  $x_{t-2}, x_{t-1}, x_t$  with  $\langle x_t \rangle = 0$ . What is the best estimate we can make for  $x_{t+1}$ ?

$$\hat{x}_{t+1} = \sum_{p=0}^N q_p x_t$$

Can determine  $q$  by least squares as above.  
causal operator. P

A more interesting approach: suppose  $x_t = \sum_{p=0}^{\infty} a_p v_{t-p}$ , where  $v$  is a white-noise process:

$$\langle v_t v_{t+\tau} \rangle = \sigma^2 \delta_{0\tau}$$

(can always do this for a stationary, regular process, i.e. no spikes in spectrum) Spectrum of  $x_t$  is  $\Phi_{xx}(s) = \Phi_{aa} \sigma^2$

Find  $a_p$  by first finding  $v_t$ : Suppose  $v_t = \sum_{p=0}^{\infty} b_p x_{t-p}$ ;

there is a  $b_p$  which turns  $x_t$  into white noise, in a least squares sense.

$$\langle (v_t - \sum_{p=0}^N b_p x_{t-p})^2 \rangle = \langle e_t^2 \rangle \text{ to be made as small as possible.}$$

$$\frac{\partial \langle e_t^2 \rangle}{\partial b_q} = 0 \text{ gives } \sum_{p=0}^{\infty} b_p \langle x_{t-q} x_{t-p} \rangle = \langle x_{t-q} v_t \rangle$$

what is  $\langle x_{t-q} v_t \rangle$ ? Use  $x_t = \sum_{p=0}^{\infty} a_p v_{t-p}$  so  $\langle x_{t-q} v_t \rangle = \sum_p a_p \langle v_{t-q-p} v_t \rangle = a_0 \sigma^2 \delta_{0q}$   
i.e. = 0 unless  $-q = p = 0$ , since  $q \geq 0$  and  $p \geq 0$ .

So matrix equation is

$$R \cdot B = \left\{ \begin{matrix} a_0 \sigma^2 \\ \vdots \end{matrix} \right\} \text{ where } R(p) = \langle x_t x_{t+p} \rangle \text{ as before.}$$

Normalization:  $a_0 = 1$

the  $x_t, x_{t-1}, \dots$  etc. are known.

Thus one can find  $b_p$ , for  $p = 0, \dots, N$ , where  $v_t = \sum_{p=0}^N b_p x_{t-p}$   
 i.e.  $v_t = b * x_t$ . But  $a * v = (a * b) * x_t = x_t$  so  $a * b = \delta_{t_0}$  or  $\hat{a}(s) \hat{b}(s) = 1$

$$\hat{a}(s) = \frac{1}{\hat{b}(s)} = \frac{1}{1 + b_1 e^{-2\pi i s} + b_2 e^{-2(2\pi i s)} + \dots}$$

do the long division ( $a_p$  causal implies no poles). Can get  $\hat{a}$ , hence  $a_p$ .

$$\text{so } \boxed{x_{t+1} = a_0 v_{t+1} + a_1 v_t + a_2 v_{t-1} + \dots}$$

we know  $v_t, v_{t-1}, v_{t-2}, \dots$  because  $v_t = b_0 x_t + b_1 x_{t-1}, \dots$  and the  $x_t, x_{t-1}, \dots$  are known. The only thing we do not know is  $v_{t+1}$ , but on the average we have  $v_{t+1} = 0$ . So the best prediction is

$$x_{t+1}^{(p)} = a_1 v_t + a_2 v_{t-1} + \dots$$

for which

$$\langle (x_{t+1}^{(p)} - x_{t+1})^2 \rangle = \langle v_{t+1}^2 \rangle = \sigma^2$$

is the expected prediction error. Best estimate says the system just "rings", where  $v_{t+1}$  is purely unpredictable.

$a_p$  is minimum phase operator  
 $b_p$  is prediction error filter.

Note

$$\left. \begin{aligned} \Phi_{yx} &= \Phi_{aa} \sigma^2 \\ \Phi_{xx} &= \frac{1}{\Phi_{bb}} \sigma^2 \end{aligned} \right\} \text{ because } |\hat{a}| = \frac{1}{|b|}$$

If estimate  $\Phi_{yx}$  by first getting  $\Phi_{bb}$ , then have what is called the maximum entropy spectrum. Can sometimes get a better frequency resolution than the normal Rayleigh limit.

(Notes taken by Andrew P. Ingersoll)

### Partial Bibliography on Time Series

Bracewell, R., The Fourier Transform and its Applications, McGraw Hill, N.Y.  
 Jenkins, G.M. and D.G.Watts, Spectral Analysis and Its Application, Holden-Day, San Francisco, 1969.  
 Hannan, E.J., Multiple Time Series, Wiley, N.Y. 1970.  
 Gold, B. and C.M.Rader, Digital Processing of Signals, McGraw-Hill, N.Y.  
 Lee, Y.W., Statistical Theory of Communications, Wiley, N.Y.  
 Davenport, W.B. and W.L.Root, Random Signals and Noise, McGraw-Hill, N.Y.

- Yaglom, A.M., An Introduction to the Theory of Stationary Random Functions, Prentice-Hall, N.J.
- Papoulis, A., The Fourier Integral and its Applications, McGraw-Hill, N.Y.
- Hannan, E.J., Time Series Analysis, Methuen, London and Wiley, N.Y.
- Blackman, R.B. and J.W.Tukey, The Measurement of Power Spectra, Dover, N.Y.
- Rosenblatt, M., Random Processes, Oxford U. Press.
- Bendat, J.S. and A.S.Piersall, Measurement and Analysis of Random Data, Wiley, N.Y. 2nd edition.
- Robinson, E.A., Introduction to Infinitely Many Variates, Griffin Monograph Series, London.
- Wiener, N., Extrapolation, Interpolation and Smoothing of Stationary Time Series, M.I.T. Press (Reprinted in paperback under title, Time Series).
- Wiener, N., Generalized Harmonic Analysis, M.I.T. Press, reprint.
- Cramér, H., Mathematical Methods of Statistics, Princeton U. Press, N.J.
- Jury, E.I., Theory and Application of the Z-Transform Method, Wiley, N.Y.
- Wainstein, L.A. and V.D.Zubakov, Extraction of Signals from Noise, Prentice-Hall, N.J.
- Freeman, H., Discrete Time Systems, Wiley, N.Y.
- Lighthill, M.J., Fourier Analysis and Generalized Functions, Cambridge U. Press.
- Middleton, D., Introduction to Statistical Communication Theory, McGraw-Hill, N.Y.
- Parzen, E. Stochastic Processes, Holden-Day, San Francisco.
- Wax, N. Selected Papers on Noise and Stochastic Processes, Dover, N.Y.
- Bartlett, M.S., An Introduction to Stochastic Processes with Special Reference to Methods and Applications, Cambridge U. Press.
- Applications, More Advanced Topics and Miscellaneous Papers
- Hasselmann, K., W.Munk and G.MacDonald, Bispectre of Ocean Waves, in Time Series Analysis, M.Rosenblatt, ed., Wiley, N.Y.
- M.I.T. Geophysical Analysis Group Reports, partially reprinted in Geophysics 32 (3), 1967,
- Special Issue of Institute of Electrical and Electronics Engineers Transactions on Audio and Electroacoustics, on the Fast Fourier Transform, Au-15, #2, 1967.
- von Neumann, Mathematical Foundations of Quantum Mechanics, Princeton U. Press, N.J.
- Slepian, D. and H.O.Pollak, Prolate Spheroidal wave functions, Fourier Analysis, and Uncertainty, Bell Syst.Tech.J. 40, and III Bell Syst.Tech.J. 41, 1961,



- Landau, H.S. and H.O.Pollak, Prolate spheroidal wave functions, Fourier Analysis, and Uncertainty II, Bell Syst.Tech.J. 40, and III Bell Syst. Tech.J. 41. 1961.1962.
- Peterson, D.P., D. Middleton, Sampling and reconstruction of wave-number limited functions in N-dimensional Euclidean Space, Information and Control, 5, 270-323, 1962.
- Wiggins, R. and E.A.Robinson, Recursive solution to the multi-channel filtering problem. J.Geophys.Res. 70, 1881-1891.
- Lacoss, R.T., Data adaptive spectral analysis methods, Geophysics 36: 661-675, 1971.
- Bach, H. and J.E.Hansen, Uniformly spaced arrays, Ch.5 of Collin and Zucker, Antenna Theory, Vol.1, McGraw-Hill, 1969.
- Haubrich, R.A., Array design, Bull.of the Seismological Soc.of America, 58, 977-991, 1968.
- Barber, N.S., Optimum arrays for direction finding, N.Zealand J.of Sci., 1: 35-51, 1956.
- Barber, N.S., Design of optimum arrays for direction finding, Elect.and Radio Engineer, 36: 222-232.
- Capon, J., R.Greenfield and R.J.Kolker, Multi-dimensional maximum likelihood processing of a large aperture seismic array, Proc.of the IEEE, 55: 192-211, 1967.
- Capon, J. and N.R.Goodman, Probability Distributions for estimation of the frequency wave-number spectrum, Proc.of the IEEE, 58: 1785-86, 1970.
- Schultz and Melsa, State functions and linear control systems, McGraw-Hill, 1967.
- Timothy, L.K. and B.E.Bena, State Space Analysis, McGraw-Hill, 1968,
- Sorenson, H.W., Controlability and observability of linear, stochastic, time discrete control systems, in Advances in Control Systems, 6, Academic Press, 1968.
- Rosenblatt, M. and J.W.van Ness, Estimation of the bispectrum, Annals of Math. Statist. 36: 1120-1136, 1965.
- van Ness, J.W., Asymptotic Normality of bispectral estimators, Ann.Math.Statist. 37: 1257-1272, 1966.

ABSTRACTS

LONG WAVES

David J. Benney

Consider the two dimensional time dependent motion of an inviscid homogeneous fluid under the action of gravity  $g$ . Let  $y = 0$  be the rigid bottom and  $y = h(x,t)$  the free surface. With  $u(x,y,t)$  and  $v(x,y,t)$  the horizontal and vertical velocity components, the equations for long waves are:

$$\begin{aligned}u_x + v_y &= 0, \\u_t + uu_x + vv_y &= -gh_x, \\v &= 0, \quad y = 0, \\h_t + uh_x - v &= 0, \quad y = h.\end{aligned}$$

A special nonlinear solution to this system, meaningful in the linear limit, is readily found by asking for a decomposition of the form

$$u = u(y,h),$$

where

$$h_t = -c(h)h_x,$$

so that the free surface deforms and propagates with speed  $c(h)$ . It follows that

$$v = -h_x \int_0^y u_h dy,$$

and substitution yields

$$\int_0^y u_h dy = -g(u-c) \int_0^y \frac{dy}{(u-c)^2},$$

where

$$\int_0^h \frac{dy}{(u-c)^2} = \frac{1}{g}.$$

The laws of conservation of mass, momentum and energy are well-known for inviscid fluids. In the present case they are

$$\frac{\partial h}{\partial \tau} + \frac{\partial}{\partial x} \left( \int_0^h u \, dy \right) = 0,$$

$$\frac{\partial}{\partial \tau} \left( \int_0^h u \, dy \right) + \frac{\partial}{\partial x} \left( \int_0^h u^2 \, dy + \frac{gh^2}{2} \right) = 0,$$

$$\frac{\partial}{\partial \tau} \left( \frac{1}{2} \int_0^h u^2 \, dy + \frac{gh^2}{2} \right) + \frac{\partial}{\partial x} \left( \frac{1}{2} \int_0^h u^3 \, dy + gh \int_0^h u \, dy \right) = 0.$$

It is possible to prove the system has an infinite number of conservation laws.

### A SIMPLE MAGNETOSTATIC MODEL OF SUNSPOTS

Friedrick H. Busse

Basically the reduction of temperature in sunspots can be explained by the inhibiting effect of a strong magnetic field on the convective heat transport. Concurrently the cooling of the sunspot gives rise to the density differences which produce the mechanical stresses capable of balancing the Lorentz forces. Thus an equilibrium can be attained which allows the establishment of a sunspot as a relatively permanent solar feature.

Since this explanation was first proposed by Burmann (1941) a number of theoretical models based on this idea have been investigated in detail (Schluter and Jemesvány, 1958; Deinzer, 1965; Dicke, 1970). However, the mathematical structure of the problem has not been investigated hitherto. Biermann's idea suggests that the problem is similar to an eigenvalue problem. In contrast to linear boundary problems leading to solutions at distinct eigenvalues of the relevant physical parameter, the magnetostatic equation

$$0 = -\nabla p + \rho \underline{g} + \frac{1}{\mu} (\nabla \times \underline{B}) \times \underline{B}$$

leads to a nonlinear problem which permits solutions only if the physical parameters satisfy certain inequalities. An analytical solution for a three-layer model is derived in the case when the heat transport in the middle layer depends on the square of vertical component of the magnetic field. The inequality which is to be satisfied for the existence of the

solution indicates that sunspots beyond a certain size cannot be realized. The closeness of the limit to the observed size of large sunspots suggests that a condition similar to that derived in the simple model may be the limiting factor for sunspots on the sun,

#### References

- Biermann, L. 1941 Vierteljahrsschrift der astron. Ges. 76: 194.  
Busse, F.H. 1973, submitted to Solar Physics  
Deinzer, W. 1965, Astrophys.J. 141: 548.  
Dicke, R.H. 1970 Astrophys.J. 159: 25.  
Schlüter, A. and Jemesváry, S. 1958, IAU Symposium No. 6, p.263.

#### TRANSITION TO TURBULENCE

Friedrick H. Busse

For a number of reasons convection in a layer heated from below is the best example to study the transition to turbulence. The gravitational mechanism of instability is the simplest among the causes for hydrodynamical instability. The physical conditions of the problem depend only on one dimension; with respect to the horizontal dimensions the problem is isotropic if lateral boundaries are sufficiently far away. No mean flow exists which would carry the convective eddies by the observer as in the case of pipe flow, thereby reducing observational difficulties.

Four distinct transitions have been investigated in detail as a function of Rayleigh- and Prandtl number and a few more are indicated by kinks in the curve of the heat transport as a function of the Rayleigh number (Malkus, 1954). The first transition is, of course, the instability of the static state leading to the onset of stationary convection in the form of rolls. The second transition introduces bimodal convection at Rayleigh numbers below 22,600 if the Prandtl number is large. (Busse, 1967; Busse and Whitehead, 1971.) The third transition introduces non-stationary convection for the first time. For  $Pr \leq 5$  this transition occurs below the second transition. The oscillatory instability of rolls is caused by the nonlinear terms in the equation of motion and has been investigated theoretically only for low Prandtl number (Busse, 1972). At high Prandtl number it is modified by the three-dimensional structure of the bimodal

cells and by the boundary structure of the convective layer. Hence at high Prandtl number the wavy oscillations transform gradually into blob oscillations which resemble the mechanisms discussed by Howard (1966) and Welander (1967). The oscillatory transition is followed by the collective instability which leads to large wavelength cells with a star-shaped convection pattern.

The importance of carefully controlled convection experiments with prescribed initial conditions originates from the fact that the complexities of normal turbulent flow are caused by the inhomogeneities of initial conditions and noise in the experiment as well as by the increasing complexity of the structure of the flow pattern at higher transitions. In fact, flows and other inhomogeneities in the convection pattern affect average properties like the heat transport as much as the transition to a new pattern. Convection experiments starting with random initial conditions do not allow the separation of these two effects. From this point of view the study of turbulence is similar to the study of solid matter in which effects due to phase transitions in the crystal lattice compete with effects of dislocations and other lattice impurities.

#### References

- Busse, F.H. 1972 J.Fluid Mech. 52: 97  
Busse, F.H. and J.A.Whitehead 1971 J.Fluid Mech. 47: 305  
Howard, L.N. 1966 Proc.of XI Int.Congr.Appl.Mech. p.1109, Berlin:Springer  
Malkus, W.V.R. 1.954 Proc.Roy.Soc. A225: 185  
Welander. P. 1967 J.Fluid Mech. 29: 17.

#### BIOCONVECTION

Stephen Childress

In the process of studying liquid cultures of swimming protozoa, biologists have frequently observed the formation of regular patterns of increased number density, reminiscent of classical **Bénard** convection cells<sup>1,2,3</sup> For a survey of the literature see Winet<sup>4</sup> and also Winet and Jahn<sup>5</sup>, who have carried out a systematic study of pattern forming by the ciliate *Tetrahymena pyriformis*. The phenomenon is observed for typical concentrations in the range  $10^4 - 10^6$  organisms/cc (the volume concentration of the organisms being only about .01) usually in suspensions whose

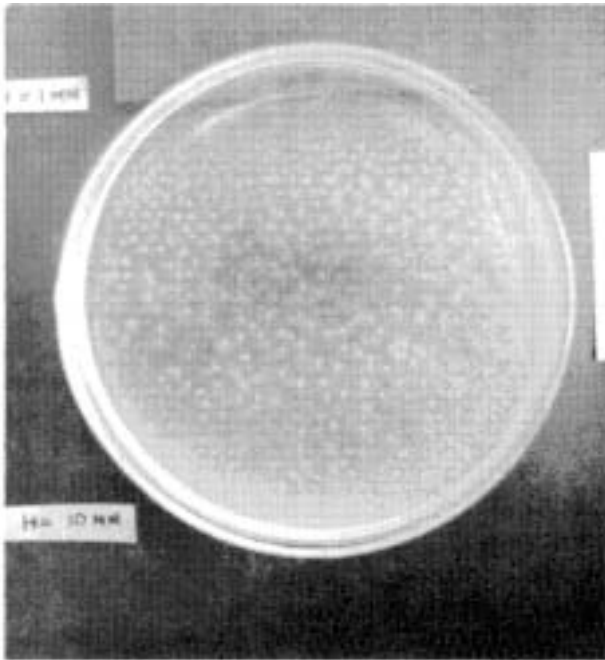


Fig. 1  
*Gyrodinium* at  $10^6$  organisms/cc  
in a tilted petri dish (diam.  
20 cm.). The depth of the  
layer varies from 1 mm. at  
the top to 10 mm. at the  
bottom,

depth exceeds 1.5 mm. With oblique lighting against a black background concentrations (or swarms) of organisms are seen as white, and the regularity of the patterns is often striking. Fig. 1 shows the variation of the pattern with layer depth for a culture of the dinoflagellate *Gyrodinium*. The pattern is initiated toward the top of the picture at a critical depth of about 1.5 mm, in a "polka-dot" form. In the deeper portion of the dish there is evidence of the so-called "reticulate" pattern<sup>3</sup>. In clearer cases this latter pattern consists of irregular but well-defined polygonal cells, separated by vertical sheets of descending swarms of organisms. A steady-state configuration of this type must then involve an upward flux of the organisms over the interior of the cells. Indeed, for *T. pyriformis* Winer and Jahn<sup>5</sup> have established that there is a preferential swimming against gravity (negative geotaxy), which is presumably due to the position of swimming effort relative to the mass distribution and the Stokes drag characteristics of the organism. A related mechanism for preferential swimming is available in phototropic organisms.

Platt<sup>2</sup>, noting the similarity to classical convection, reported an experiment of R. Donnelly in which the reticulate patterns persisted in a petri dish on ice, therefore presumably overcoming a stable mean temperature

gradient. Platt suggested that the pattern represented a dynamical instability and could be visualized as an instability in a cloud of small "hovering helicopters".

There appear to be at least two points of view leading to models of the phenomena of this kind, both of which require that the mean density of the organism exceed that of the suspending fluid, and that the organism be negatively geotactic. The preferential swimming can manifest itself as a mechanism whereby a relatively heavy upper layer of organism fluid is established over the lighter supporting fluid, a process that was actually observed for *T. pyriformis* by Winet and Jahn. The heavy layer will then go unstable by a viscous version of a Rayleigh-Taylor instability. A theory along these lines has recently been worked out by Plesset and Winet (unpublished). They report agreement between the horizontal wavelength of maximal growth rate (and its harmonics) with the peaks in the distribution curve for the node-to-node distances observed in deep cultures forming reticulate patterns,

A second point of view treats the vertical swimming and downwelling due to heavy local concentrations simultaneously. (A Rayleigh-Taylor instability could result from the organisms swimming to the top, then dying; the only role of swimming is to set up the heavy layer.) Recently the writer, in collaboration with M. Levandowsky and E. A. Spiegel, has examined a model of this second type. We find that such a model does predict an instability of the type envisaged by Platt; a given plane culture of fixed concentration will be stable below a certain critical depth, while cultures of the same depth will be stable below a certain critical volume concentration of the organism. While the model does thus give well-defined critical values (an analog of the Rayleigh number is involved) it does not, in the simplest form, give a finite horizontal wavelength at the onset of instability; disturbances of zero wave number are initiated first. We comment on this defect below,

The formulation is straightforward and involves three main assumptions: (i) the momentum density and the scalar viscosity of the mixture and the suspending fluid are approximately equal; (ii) the effect of inertia drift of the organism is negligible; (iii) the equation of the particles is taken to be

$$\frac{dc}{dt} + \underline{\nabla} \cdot \underline{J} = 0, \quad \underline{J} = c \underline{u} + c U(c) \underline{k} - D(c) \underline{\nabla} c \quad (1)$$

Here  $\underline{u}$  = fluid velocity,  $c$  = volume concentration of the organisms, and  $U(c)$  and  $D(c)$  are respectively the vertical swimming velocity and diffusivity for particles at a concentration  $c$ . Here (ii) has been used since the first convection term in  $\underline{J}$  represents convection by the fluid.

The equations of motion are then

$$\rho \frac{d\underline{u}}{dt} + \underline{\nabla} p - \mu \nabla^2 \underline{u} = -g \rho \alpha c \underline{k}, \quad \underline{\nabla} \cdot \underline{u} = 0 \quad (2)$$

where  $\alpha = \rho_0/\rho - 1$  is the relative excess density of the particles. The boundary conditions on the layer boundaries  $z = 0, H$  are obtained as in the Bknard problem, except that we must set the vertical flux of the organisms equal to zero there:  $J_z(0) = J_z(H) = 0$ . Since  $c$  is a rough analog of temperature in thermal convection, this last boundary condition represents an essential departure from the familiar convection problem, Insofar as the conditions on the velocity field are concerned we treat the boundaries as planes even though they may actually be free.

The linear stability of the equilibrium solutions of (1), (2), (i.e. solutions with  $\underline{u} = 0$  and  $c = C(z)$ ) can be carried out routinely. The exchange of stabilities holds for arbitrary positive  $U(c)$ ,  $D(c)$ , and a variational formulation of the stability problem can be given. For the special case  $U(c) = U_0 = \text{constant}$ ,  $D(c) = D_0 = \text{constant}$  [the exponential case) the neutral stability curves, which always have the form

$$R = \frac{g \alpha C_0 D_0^2}{\nu U_0^3} = R_c(\lambda, a), \quad c_0 = C(H), \quad \lambda = \frac{U_0 H}{D_0}$$

are characterized by

$$\min_a R_c(\lambda, a) = R_c(\lambda, 0),$$

so that perturbations of infinite wavelength are first unstable as  $R$  is increased. These curves are shown in Fig. 2.

For arbitrary choices of  $U(c)$ ,  $D(c)$  it is also true that there is instability if  $R$  exceeds a value computable by direct expansion in powers of  $a$ , corresponding to growth at zero wave number. It is not known whether or not this value is smallest critical value for arbitrary  $U(c)$ ,  $D(c)$ , and



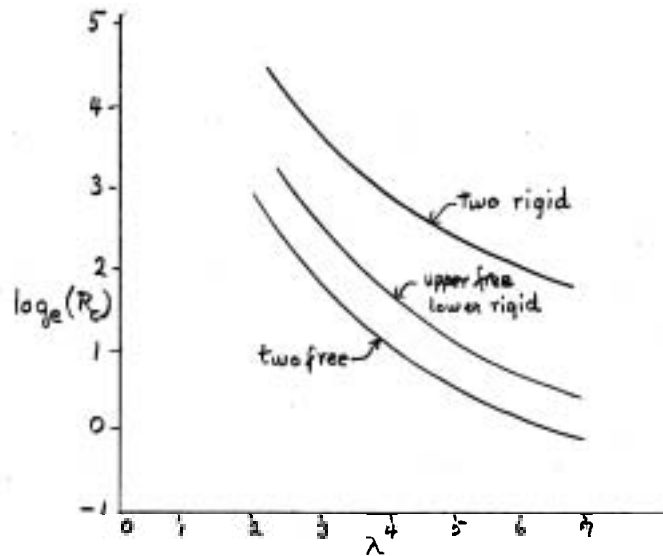


Fig.2 Critical values of  $R$ , exponential case.

$\lambda$ . Reasonably good agreement with the experimental values of  $R_c$  for *T. pyriformis* have been obtained, using indirect means to compute a value of  $D_0$  and assuming the constancy of  $U$  and  $D^*$ .

The polka-dot pattern clearly represents a finite-amplitude phenomenon. If the flow field is taken to be steady-state and two-dimensional, and if the diffusion of the organism fluid is neglected ( $D \equiv 0$ ), a possible flow model can be drawn as in Fig.3.

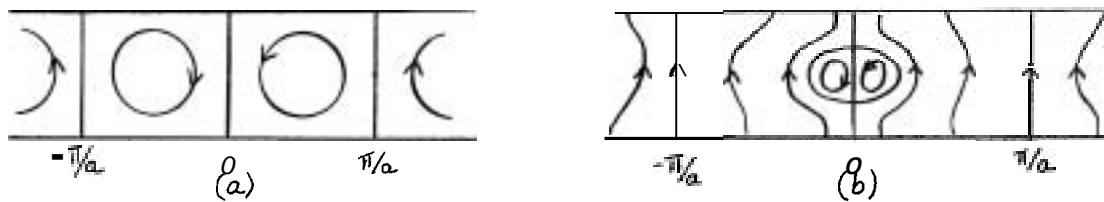


Fig.3 Two-dimensional diffusion-free pattern, (a) Streamlines. (b) Organism trajectories.

Taking  $U$  to be constant, one sees that these streamlines and organism paths are related by the addition of a uniform current. The region of closed organism trajectories is a region where the organisms may be placed without intersecting the boundary. We can, for simplicity, choose

As  $\lambda \rightarrow 0$  (thin layer limit) it can be shown that the model becomes a mathematical analog of Bénard convection between walls of zero thermal conductivity. In that case our results for  $R_c(\lambda, a)$  agree with those of Hurle, Jakeman, and Pike<sup>6</sup>.

to make  $c$  constant there. This region then will act as an "impeller" to drive the flow, shown. The resulting streamfunction must then be compatible with the region over which the organisms are distributed. Another possible configuration for the streamlines (obtainable from that of Fig.3(b) by a deformation) is shown in Fig.4. The three-dimensional version of Fig.4 gives a toroidal swarm of organisms. We have observed, in dense cultures of *Gyrodinium*, "polka dots" which were both spheroidal and toroidal, in either case arranged in a near hexagonal array, positioned roughly midway through the layer and having a diameter of perhaps a half of the layer thickness,

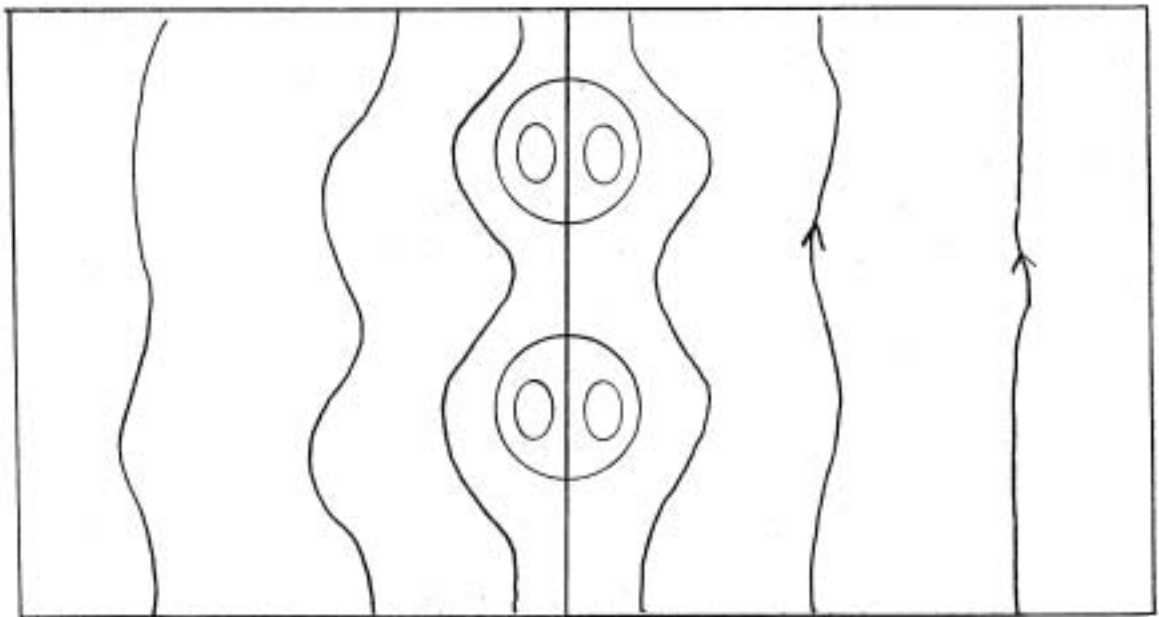


Fig.4 Alternative configuration for streamlines,

Mathematically, calculation of diffusion-free steady states involves a free-boundary problem for Stokes' equations, in which the domain over which the forcing term acts depends in a highly nonlinear (structural) way upon the flow field. Truncated eigenfunction expansions appropriate to the biharmonic operator have been used to generate some highly approximate results. Somewhat surprisingly the observed packing density of polka dots is closely predicted by minimizing the appropriate Rayleigh number (no longer  $R$ ) with respect to wavenumber,

assuming hexagonal cells and two stress-free boundaries. The result however depends upon the assumption that the experimental mean particle density within the dot is independent of its size, and it is not known whether or not such a limiting density is actually obtained.

We now consider the question of securing a finite critical wavelength. In the first place the expansion in powers of  $a$  predicts that the mode of maximal growth for  $R$  above  $R_c$  does occur at positive  $a$ , tending to zero as  $R$  tends to  $R_c$ . However this only suggests that a small modification of the model may be sufficient to make  $a_c$  small but positive; it does not explain the onset of instability in a tilted petri dish, at the critical depth, as a pattern with finite wavelength. It would appear that one or both of the following enlargements of the model may be necessary: (Note that if  $a_c$  remains small, then critical curves of Fig.2 should remain valid in the modified model.) (1) No conditions have been incorporated which take into account the presence of the upper boundary on the swimming (and hence on the vertical drift and diffusion). A reasonable representation of these effects would require that  $U$  depend upon  $z$  as well as upon  $c$ , and that diffusion should be non-isotropic with diffusivities depending upon  $z$ . (2) When the upper boundary is free, the correct condition is not exactly  $w = 0$ . The correct linearized condition is, once horizontal dependence is separated out,

$$\frac{\partial^3 w}{\partial t^2 \partial z} + 3v\alpha^2 \frac{\partial^2 w}{\partial t \partial z} - v \frac{\partial^2 w}{\partial t \partial z^2} + \alpha^2 g w = 0 \text{ on } z = H, \quad (3)$$

which introduces a quadratic dependence upon the growth rate. Incorporation of (3) brings with it an aspect of the Rayleigh-Taylor instability and may therefore be relevant to the wavelength at critical.

The author wishes to thank Melvin Stern and John Whitehead for comments,

#### References

1. Loeffler, J.B. and R.B.Mefferd 1952 The Amer.Naturalist **86**(830): 325-329.
- Platt, J.R. 1961 Science **133**: 1766-1767.

3. Wille, J.J. and C.F.Ehret 1968 J.Protozool. 15(4): 792-795.
4. Winet, H. 1969 Doctoral Thesis, Univ.of California at Los Angeles.
5. Winet, H. and T.L.Jahn 1972 Biorheology 9: 87.
6. Hurle, D.T.J., E.Jakeman and E.R.Pike 1967 Proc.Roy.Soc. A296:469-475.

## PERTURBED TURBULENCE AND EDDY VISCOSITY

Russ Davis

The perturbation of a turbulent shear flow by an organized wave-like disturbance is examined using a dynamical, rather than phenomenological, approach. On the basis of the assumption that an infinitesimal perturbation results in a linear change in the statistics and that the turbulence is either weak or that the turbulent perturbations are quasi-Gaussian, a method of predicting the perturbation turbulent Reynolds stresses is developed. The novel aspect is that the dynamical equations are solved before the information-losing process of averaging is accomplished.

When applied to long wave organized disturbance it is the perturbation turbulent shear stress which is of primary importance and this stress is determined primarily by the principal component of mean shear  $\partial u_1 / \partial z$  where the primary mean flow is  $U_1(z)$ . The shear stress is related to the velocity shear through a relation which depends on the spectrum of the turbulent velocity component parallel to  $\hat{z}$ . The constitutive equation relating the shear stress and mean shear is visco-elastic in nature and depends on how well the turbulent components obey Taylor's hypothesis that phase velocity equals the mean flow velocity. Theoretical and experimental results are used to estimate the spectrum of the turbulent components parallel to  $\hat{z}$  and this leads to a constitutive equation which is in agreement with the known behavior of a constant stress boundary layer.

## DUST DEVILS - Movies and Slides

Daniel E. Fitzjarrald

Movies were shown which were taken in the Mojave Desert of southern California to illustrate the qualitative aspects of flows within atmospheric thermal vortices. A great number of examples of these flows were seen, and several distinct features were noted.

Correspondence of the natural flows with films of an experiment designed to simulate thermal vortices was shown. In particular, several of the qualitative aspects of the laboratory flows, including regions of positive and negative vertical velocity and the turbulent vortex structure, were seen to be quite similar to real dust devils.

Based on measurements of velocity and temperature, (Fitzjarrald, 1973), dynamic similarity was indicated between the experiment and natural vortices. The nature of the data available precluded any exact comparison, but the agreement was good within reasonable limits.

### References

1. Fitzjarrald, D.E. 1973 A laboratory simulation of convective vortices, J.Atmos.Sci., July, 1973.
2. Fitzjarrald, D.E. 1973 A field investigation of dust devils. J.Appl.Meteorol., August, 1973.

## PLANE WAVE SOLUTIONS TO REACTION-DIFFUSION EQUATIONS

Louis N. Howard

The temporal evolution of the concentrations  $C_i$  in a chemically reacting system with diffusion is usually modelled by equations of the form

$$\frac{\partial C_i}{\partial t} = F_i(C_1, \dots, C_n) + \sum_j k_{ij} \nabla^2 C_j \quad (1 \leq i \leq n) \quad (1)$$

The (typically nonlinear) functions  $F_i$  describe the chemical kinetics, or an approximation thereto appropriate to the time scale under consideration, and the matrix  $K=(k_{ij})$  of diffusivities is symmetric and positive definite.

Under certain conditions such equations can have wave-like solutions, and these appear to be of interest in connection with the attempt

to understand the formation of certain spatially heterogeneous concentration distributions which occur sometimes in the Belousov-Zhabotinskii reaction. This reaction, an oxidation of malonic acid by bromate catalyzed by cerous ions, proceeds when stirred in an oscillatory manner with an overall duration of an hour or more but exhibiting regular nearly periodic variations in certain concentrations having a period of the order of half a minute. Thus in a mathematical model of this reaction like (1), appropriate to time scales of the order of the oscillation period, one would expect that the autonomous system

$$\frac{d\underline{c}}{dt} = \underline{F}(\underline{c}) \quad (2)$$

approximately describing the spatially homogeneous chemical kinetics would have a stable limit cycle among its solutions. [Unfortunately the chemical kinetics of the Belousov reaction is not yet completely known, but the available evidence supports this conjecture.] N. Kopell and I have recently found methods for showing the existence of plane wave-like solutions to (1) under the assumptions either that (2) has a limit cycle solution or that it has a critical point which is unstable by growing oscillations. These methods, which are adaptable to numerical computation of the plane wave solutions, were sketched in the lecture.

By a plane-wave solution of (1) we mean one in which

$$c_i(\underline{x}, t) = y_{\underline{c}}(\sigma t - \underline{\alpha} \cdot \underline{x}),$$

the vector  $\underline{y}$  being a  $2\pi$ -periodic function of its argument. Such solutions exist if the ordinary differential system

$$\sigma \underline{y}' = \underline{F}(\underline{y}) + K|\underline{\alpha}|^2 \underline{y}'' \quad (3)$$

has  $2\pi =$  periodic solutions. Using the Hopf bifurcation theorem we show the existence of a one-parameter family of such solutions  $\underline{y}_{\underline{\epsilon}}, \sigma(\underline{\epsilon}), |\underline{\alpha}|^2(\underline{\epsilon})$  [where the parameter  $\underline{\epsilon}$  may be regarded as a measure of the amplitude of the oscillations]. This is done assuming  $K$  is sufficiently close to a scalar matrix, and in the neighborhood of a critical point of (2) which has an unstable conjugate pair of complex eigenvalues. Such weakly nonlinear waves can be computed by expansions of the solution, its frequency  $\sigma$  and wave number  $|\underline{\alpha}|$  in powers of the amplitude,

With the assumption that (2) has a limit cycle, and no special hypotheses about the diffusion matrix, we can show also the existence of

such a one-parameter family of solutions in a neighborhood of the limit cycle. This is done by proving the convergence of an iterative process (which appears well-adapted to numerical purposes) for the construction of the solution, which in this case may be a large amplitude wave of highly non-sinusoidal form. It appears that these plane waves are unstable, as solutions of (1), when they are of small amplitude and near the unstable critical point of (2), but are stable in a neighborhood of the limit cycle.

(Further details can be found in the paper "Plane wave solutions to Reaction-Diffusion Equations" by N. Kopell and L.N. Howard, which will appear shortly in Studies in Applied Mathematics.)

## THE EFFECT OF BOTTOM TOPOGRAPHY IN ROTATING STRATIFIED SYSTEMS

Herbert E. Huppert

Three model problems were discussed. The thread linking these problems was that the intuition gained from I could be coupled with II to examine critically III.

### I. Flow of a Stratified Fluid over Arbitrary Bottom Topography in a Rotating Channel with Vertical Side Walls (Huppert and Stern, 1973).

Vertical walls are an essential feature of this problem and are the natural constraints for a laboratory experiment. While the oceans have shallower sloping walls similar effects are to be expected there, though maybe slightly less dramatic. The problem is essentially ageostrophic, even at vanishingly small Rossby number, and indicates the existence of effects that can not be investigated by the usual small Rossby number expansion procedure,

The geometrical setup of Fig.1 was first considered for the simpler case of: i) non-rotation, when steady lee waves exist because a quiescent, stratified fluid has wave motions whose upstream phase velocity can equal the downstream flow velocity; and ii) non-stratified, shallow water flow down a channel with vertical walls separated by a distance  $L$  for which the nonlinear conservation of potential vorticity equation

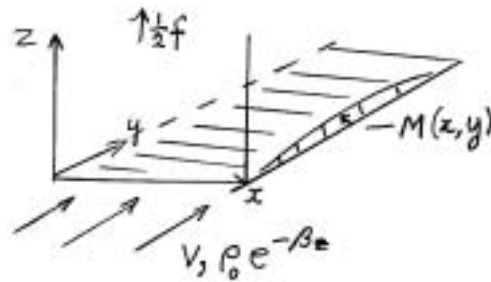


Fig. 1

$$\frac{D}{Dt} \left( \frac{f + \zeta}{H - h} \right) = 0$$

can be integrated exactly. Here  $\zeta$  is the relative vorticity,  $H$  the channel depth for upstream and  $H-h$  channel depth at any particular position, with  $H-h_0$  the final downstream value with  $h_0 \geq h$ . The integration indicates that the flow will be blocked somewhere, in the sense that no streamline originating upstream enters this region if

$$h_0/H > F(R) = [1 - (1 - 8R)^{1/2}] / 2$$

$$\sim 2R + 4R^2 \quad (R \rightarrow 0),$$

where the Rossby number  $R = v/fL$ .

The full problem was then analysed by linearizing about the mean flow  $V$ . The solution is a combination of: a modified quasi-geostrophic flow incorporating many of the features of the flow discussed in ii) except that the modified flow decreases like  $e^{-\pi N z / (fL)}$ ; and a Kelvin wave trapped to the left-hand wall with decay  $e^{-vz/f}$  and vertical wavelength  $2 \hat{\lambda} V / N$ . The strength of this flow was discussed by two examples: a) Suppose  $R = 0$ . Then the statement  $u = 0$  at the wall implies, assuming quasi-geostrophy, that  $P = 0$  at the wall. But since  $P_z = -N^2 M$  at the bottom of the wall, if  $M$  is non-zero there  $P_z \neq 0$  there. This paradox can only be broken if the assumption of quasi-geostrophy is incorrect, i.e. the quasi-geostrophic calculation is singular, leading to infinite velocities. b) From the analysis the normalised maximum height of the topography can be calculated for which blocking will not occur. The result is shown in Fig. 2.



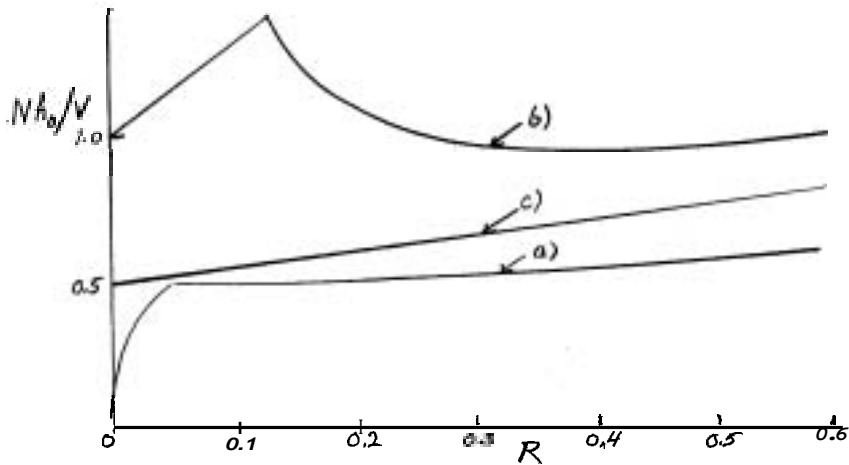


Fig. 2

Fig.2 The critical value of  $Nh_0/V$  versus Rossby number for stratified flow in a rotating channel

$$a) M(x, y) = h_0 \left[ 1 + (\epsilon y/L)^2 \right]^{-1}, \quad 0 < x < L.$$

$$b) M(x, y) = h_0 \sin(\pi x/L) \left[ 1 + \epsilon y/L^2 \right]^{-1}, \quad 0 < x < L.$$

$$c) M(x, y) = h_0 e^{-\pi x/2} \left[ 1 + (\epsilon y/L)^2 \right]^{-1}, \quad 0 < x < \infty, \text{ with } \epsilon \ll 1.$$

In case a) and b) the blocking is due almost entirely to the modified quasi-geostrophic component of the flow for  $R \leq R_c$  and entirely to the Kelvin wave for  $R > R_c$  with  $R_c = 0.048$  for case a) and  $R = 0.135$  for case b). The blocking occurs at the bottom of the right-hand wall for  $R \leq R_c$  and at the top of the left-hand wall for  $R > R_c$ . For case c) the blocking is entirely due to the Kelvin wave for all  $R$  and occurs at the top of the left-hand wall.

## II. The Initiation of a Taylor Column over an Isolated Obstacle in a Homogeneous Fluid.

The approach of Ingersoll (1969) was reviewed and the stagnation condition

$$h_0/H = \min_r \left( \frac{r}{\int_0^r x h(x) dx} \right) R \quad (II.1)$$

was derived for a circularly symmetric obstacle of shape  $h_0 h(r_*/L)$ . It was argued that while a top-hat  $[h(r) = H(1-r)]$  obstacle gave an adequate representative streamline pattern for non-stagnant conditions, it may be very special when  $h_0$  exceeds the value given by (II.1). This is because once a vortex line has been compressed the amount  $h_0$ , it can move

over a flat plateau without further compression. This will not be true for general obstacles.

It was indicated that each closed streamline shape corresponded to a different obstacle shape and the problem of determining some streamline patterns when stagnation occurs was suggested as a useful summer project.

III. The Initiation of a Taylor Column over an Isolated Obstacle in a Stratified Fluid. (Huppert, 1974)

Adding stratification of constant  $N$  to II and assuming the obstacle to be of infinitesimal height leads to the stagnation condition

$$h_0/H = \min_r \left( \frac{\sigma \int_0^1 t \coth \sigma t J_0(tr) \hat{h}(t) dt}{r} \right) R, \quad (III.1)$$

where  $\sigma = NH/fL$  and  $\hat{h}(t) = \int_0^1 r h(r) J_0(tr) dr$  (III.2)

In contrast to (II.1), (III.1) can yield  $h_0/H = 0$ , and does so for a top-hat obstacle. That is, a Taylor column is always formed over a top-hat and this is hence always an atypical obstacle in a stratified fluid.

Evaluating (III.1) for the lens  $h(r) = (1-r^2)H(1-r)$ ,  $\hat{h}(t) = 2t^{-2}J_2(t)$ , we obtain Fig. 3.

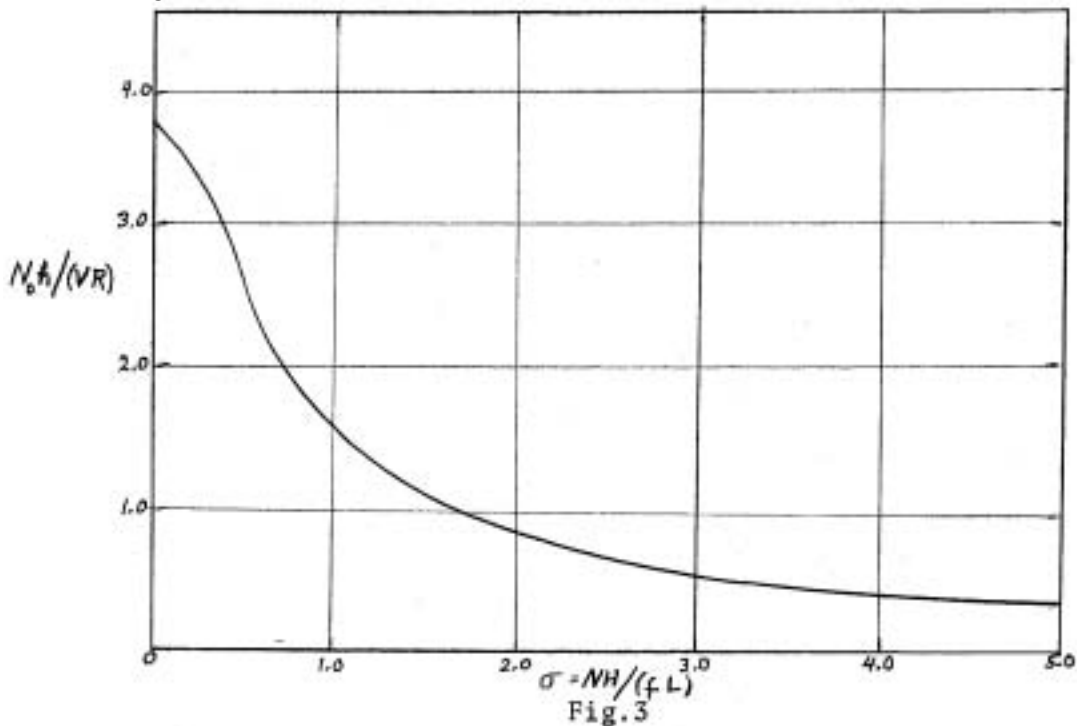


Fig.3 The critical value of  $h_0 R^{-1}$  versus  $\sigma$  for stratified flow over the cylindrical lens  $h(r) = h_0(1-r^2)$ .

## References

- Huppert, H.E. 1974 Some remarks on the initiation of inertial Taylor columns. J.Fluid Mech. (*sub judice*)
- Huppert, H.E. and M.E.Stern 1973 Ageostrophic effects in rotating stratified flow, J.Fluid Mech. (*sub judice*)
- Ingersoll, A.P. 1969 Inertial Taylor columns and Jupiter's Red Spot. J.Atmos.Sci. 26: 744-752.

### JUPITER'S GREAT RED SPOT: A FREE ATMOSPHERIC VORTEX?

Andrew P. Ingersoll

The Great Red Spot (GRS), like all other visible features on Jupiter, is a large cloud system. On the earth, such cloud systems are either migrating weather systems whose lifetime is 1-2 weeks or quasi-permanent features directly forced by the distribution of continents and oceans. Since the GRS has existed for at least 100 years, it is tempting to assume that it is the result of direct forcing by the solid parts of Jupiter. However, there are difficulties with this explanation. First, Jupiter may not have a solid surface; any solid surface must be thousands of km below the visible clouds, and it is not clear that atmospheric motions can couple over such a great range of depth. Second, the rotation rate of the GRS is less than that of the magnetic field, which might be expected to rotate with the solid planet. Moreover, the rotation rate of the GRS varies erratically on a long time scale, while that of the magnetic field appears to be constant. While these difficulties are not insurmountable, they lead one to consider models in which there is no interaction with the solid parts of Jupiter. I shall call these free or unforced flows, as opposed to forced or driven flows.

The new result presented here is that free, steady-state solutions of the governing hydrodynamical equations exist with many of the flow features of the GRS and the neighboring currents. If, as assumed here, the GRS does not have a special forcing mechanism, it should have many dynamical properties in common with other major flow features in Jupiter's atmosphere. Accordingly, I also discuss the observations which bear on this question, and show that the GRS is dynamically similar to the zones, which, together with the darker belts, comprise Jupiter's axisymmetric banded structure,

## RAY THEORY OF WAVE PROPAGATION

Joseph B. Keller

The ray method of analyzing wave propagation is presented. First straight rays in homogeneous media are introduced, followed by reflected, refracted, edge diffracted, vertex diffracted, surface diffracted, and complex rays. Then the phase on a ray is described, and it is evaluated in terms of the optical length of a ray. Next the amplitude on a ray is introduced, and it is shown to be determined by a conservation law involving energy flow in a tube of rays. In addition coefficients of reflection, refraction edge diffraction, vertex diffraction and surface diffraction are introduced. Furthermore the orientation or polarization of the field at each point on a ray is defined. By combining all these quantities, the field at each point on a ray of any kind can be found. Then the total field at any point is determined as the sum of the fields on all rays through the point. This field is the sum of the leading terms in the short wave asymptotic expansion of the field on each ray.

For wave guides, or waves in layered media, each mode of the cross section can be described by a ray theory of the type just described. This is the case, for example, for internal waves in an ocean or atmosphere. The rays are then curves in the horizontal plane.

### Bibliography

1. Keller, J. B. "Geometrical Theory of Diffraction" J.Opt.Soc.Amer., 1962 52: 116-130,
2. Keller, J. B. "Diffraction by an Aperture". J.Appl.Phys., 1957 28: 426-444.
3. Keller, J. B., Lewis, R. M. and Seckler, B. D. "Diffraction by an Aperture. II." J.Appl.Phys. 1957 28: 570-579.
4. Keller, J. B. "A Geometrical Theory of Diffraction" Calculus of Variations and its Application, Math.Soc., L. M. Graves, Ed., McGraw-Hill, New York, 1958.
5. Keller, J. B., Lewis, R. M. and Seckler, B. D, "Solution of some Diffraction Problems". Comm Pure Appl.Math. 1956 9: 207-265.

## ASYMPTOTIC THEORY OF WAVE PROPAGATION

Joseph B. Keller

A method for obtaining the short wave asymptotic expansion of any problem of linear wave propagation is presented. The method is based upon a suitable asymptotic representation of the solution in terms of waves. Each wave is characterized by a phase function and an amplitude vector. The phase is shown to satisfy a first order partial differential equation of the Hamilton-Jacobi form. It is solvable in terms of characteristics or rays. The amplitude is shown to satisfy a transport equation along the rays. Reflected, refracted and diffracted waves of various kinds are also introduced. The leading terms of the resulting expansion are found to agree with those given by the ray method. It is also shown how to avoid the singularities of the expansion at caustics, shorelines, etc. by means of uniform asymptotic expansions.

## FORCED PERIODIC VIBRATIONS OF NONLINEAR SYSTEMS

Joseph B. Keller

A response diagram of a vibrating system is a graph of the amplitude of some particular mode of vibration as a function of the vibration frequency, for a fixed forcing amplitude. When the forcing amplitude is zero, the graph shows the free vibrating amplitude as a function of its frequency. A method is presented for finding the forced vibration curves for a nonlinear system in terms of the corresponding free vibration problem in terms of the modes, or nonlinear eigenfunctions, of the nonlinear free vibration problem. Thus it is analogous to a procedure widely used for forced linear vibration problems, and is an extension of that method to nonlinear problems.

When the forcing occurs through a boundary condition, a slight modification of this method is used. It is illustrated by applying it to finite amplitude sound waves produced by a piston in a tube of finite or infinite length. The cases of forcing frequency near the cut-off frequency and near a free vibration frequency of a closed tube, are examined

in detail. The resulting amplitude is shown to be large and finite in both cases, and not infinite as linear theory would predict.

### AN EXPERIMENT ON "HEAT ISLAND" CONVECTION

Ryuji Kimura

#### 1. Introduction

The average temperature near the ground in cities is usually higher than that of the rural areas, This is caused mainly by artificial heat production in cities and is called the "urban heat island effect".

A laboratory experiment which is simple enough for a G.F.D. approach was made to observe convective motions due to the heat island effect.

#### 2. Model and problem

Consider a viscous fluid layer stably stratified (with constant temperature gradient) and bounded below by a horizontal plane which has an infinite thermal conductivity (Fig.1).

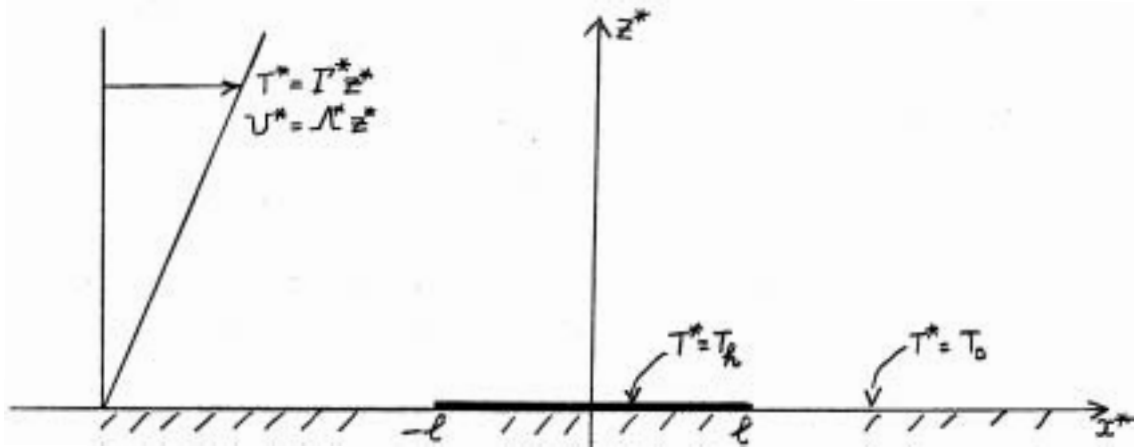


Fig. 1

Problem 1: What kind of motions do we have in the steady state, when the boundary condition for the temperature at the lower boundary is given by

$$T^* = T_h \text{ (const.) for } -\ell \leq x^* \leq \ell$$

$$T^* = T_o \text{ (const. } < T_h) \text{ otherwise?}$$

Problem 2: How does this flow pattern change, if a basic current with vertical shear is added in the situations stated in Problem 1?

### 3. Dynamical properties for Problem 1.

The basic equations scaled by  $\ell$ ,  $\Delta T (\equiv T_h - T_o)$ ,  $U (\equiv \sqrt{\alpha g \Delta T \ell})$  show that the flow dynamics is controlled by three non-dimensional parameters:

$$Re = \frac{U \ell}{\nu} \text{ (square root of Grashoff number)}$$

$$Pr = \frac{\nu}{\kappa} \text{ (Prandtl number)}$$

and  $\Gamma = \frac{\ell}{\Delta T} \Gamma^*$  where  $\Gamma^*$  is the temperature gradient of the basic state.

Non-dimensional temperature is expressed as

$$T(x, z) = \bar{T}z + T_1(x, z) + T'(x, z)$$

where  $T_1$  is the temperature deviation from the basic state due to heat conduction from the "city" and  $T'$  is the temperature deviation which accompanies the convective motions. From the equation of heat conduction we obtain

$$T_1 = \frac{1}{\pi} \left( \tan^{-1} \frac{z}{x-1} - \tan^{-1} \frac{z}{x+1} \right).$$

Notice that we have an unstably stratified region above the "city" when  $\Gamma$  is small, but  $\frac{d}{dz} (\bar{T}z + T_1) > 0$  everywhere when  $\Gamma$  exceeds a critical value ( $\sim 0.63$ ).

### 4. Experimental arrangement.

A circular channel with a rectangular cross section is used as the fluid container. The scale of the container is shown in Fig. 2. The stable stratification of the fluid layer is maintained by keeping the temperature of the top and bottom of the container constant ( $T_{\text{top}} > T_{\text{bottom}}$ ).

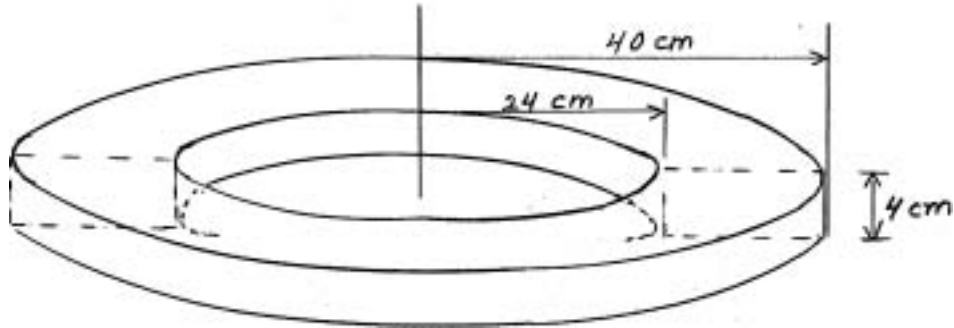


Fig. 2

A flow with a vertical shear is produced by rotating the top boundary of the container. The convective motions are generated by putting a heater at the bottom of the container.

5. Results (qualitative)

(for Problem 1)

We have two kinds of flow regimes by changing  $\Gamma$  as sketched in Fig. 3.

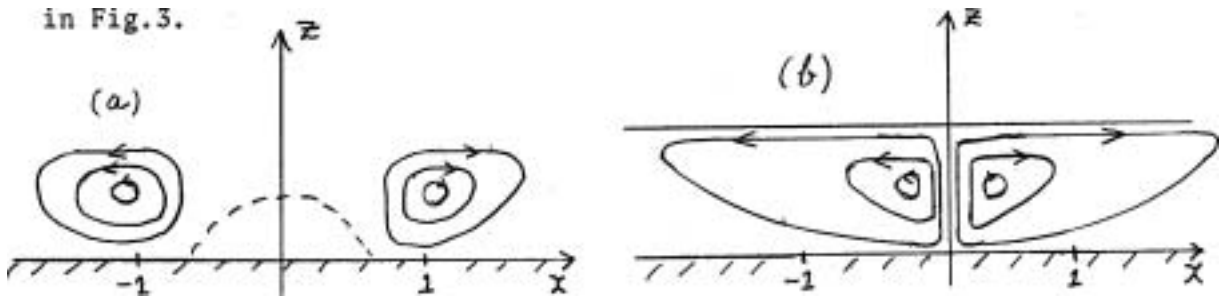


Fig. 3

When  $\Gamma$  is large, the circulation is most intense near the edges of the "city", and the central part of the "city" is stagnant (a). When  $\Gamma$  is small, a narrow vertical jet is formed at the center of the "city" (b). The heights of the maximum penetration are plotted as a function of  $\Gamma$  in Fig. 4.

(for Problem 2)

1) When we add the vertical shear flow with moderate intensity, the flow pattern remains stationary, but

- i) the position of the jet at the ground shifts downstream,
- ii) the jet axis inclines downstream,



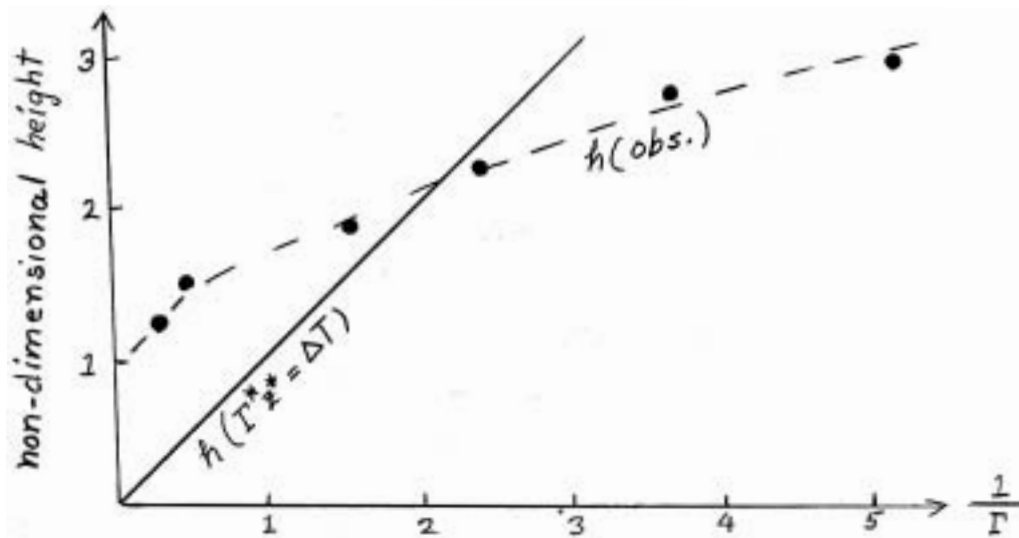


Fig.4

iii) the overshooting of the jet increases.

2) When the vertical shear exceeds a certain value, the internal waves associated with the overshooting of the jet are no longer stationary.

3) We have a region where the flow is very weak (blocking region) in the upstream side of the jet.

## CUMULUS CONVECTION AND EQUATORIAL WAVES IN THE ATMOSPHERE

Richard S. Lindzen

CISK (conditional instability of the second kind) is examined for internal waves where low level convergence is due to the inviscid wave fields rather than to Ekman pumping.

It is found that CISK induced waves must give rise to mean cumulus activity (since there are no negative clouds), and it is suggested that this mean activity plays an important role in the finite amplitude equilibration of the system. The most unstable CISK waves will be associated with very short vertical wavelengths ((0(3 km)) in order to maximize (in some crude sense) subcloud convergence. Thus the vertical scale, in turn, determines the dispersive relations between horizontal and temporal scales. It is found that there exists a wave-CISK mode

which is independent of longitude, and hence independent of the mean zonal flow. Because of this independence, the period of this oscillation should form a prominent line in tropical spectra. This period turns out to be about 4.8 days which is indeed a prominent feature of tropical spectra. It is shown, that due to longitudinal inhomogeneities in the tropics (such as land-sea), the above oscillation must be accompanied by travelling disturbances whose period with respect to the ground will also be 4.8 days and whose longitudinal scales will typically be from 1000-3000 km depending on the mean zonal flow. It is further shown that the existence of the above oscillatory system has two additional implications:

- i) The above system is, itself, unstable with respect to gravity waves with horizontal scales on the order of 100-200 km. Such waves may be associated with cloud clusters.
- ii) The above system leads to maximum low level convergence (and hence, a tendency toward mean cumulus activity) in regions centered about  $\pm 6 - 7^\circ$  latitude, thus providing a possible explanation for the position of the ITCZ.

#### MACRODYNAMICS OF PLANETARY DYNAMOS

W. V. R. Malkus and M. R. E. Proctor

#### Abstract

Past study of the large scale consequences of forced small scale motions in electrically conducting fluids has led to the ' $\alpha$ -effect' dynamos. Various linear kinematic aspects of these dynamos have been explored, suggesting their value in the interpretation of observed planetary and stellar magnetic fields. However, large scale magnetic fields with global boundary conditions can not be force-free and will cause large scale motions as they grow. In this paper the finite-amplitude behavior of global magnetic fields and their induced large scale flows in rotating systems is investigated. In general, both viscous and ohmic dissipative mechanisms have ranges of importance in determining the amplitude and structure of the evolved flows and magnetic fields. In circumstances

where ohmic loss is the principal dissipation, it is found that determination of the zonal flows is an essential part of the solution of the basic stability problem. Nonlinear aspects of the theory include meridional flow amplitudes which are independent of rotation and a total magnetic energy which is directly proportional to rotation. Constant  $\alpha$  is the simplest example exhibiting the various dynamic balances of this stabilizing mechanism for planetary dynamos. A detailed analysis is made for this case to determine the initial equilibration of fields and flows in a rotating sphere.

### Resume

Many large scale features of planetary and stellar magnetic fields may have their origin in geometric and rotational constraints. Even the periodicity of field reversals may be insensitive to the structure of the underlying motions responsible for magnetic regeneration. In this study an exploration is begun of the finite amplitude balance of large scale fields and flows in rotating fluid spheroids based upon the ideas of mean field magnetohydrodynamics (Steenbeck, Krause, and Radler 1966, 1969, 1970). Related to earlier work by Parker (1955) and Braginskii (1964), mean field electrohydrodynamics supposes that the magnetic and velocity fields in a conducting fluid may exist at two widely different length scales ( $L$  and  $\ell$  say, where  $\ell \ll L$ ). Then the induction equation for the large scale, or mean, magnetic field,  $\mathbf{B}$ , may be written

$$\frac{\partial \mathbf{B}}{\partial t} = \nabla \times (\mathbf{U} \times \mathbf{B}) + \nabla \times (\overline{\mathbf{U}' \times \mathbf{B}'}) + \lambda \nabla^2 \mathbf{B} \quad (1.1)$$

where  $\mathbf{U}$  is the mean velocity,  $\lambda$  is the magnetic diffusivity and  $\mathbf{U}'$  and  $\mathbf{B}'$  are small scale velocity and magnetic fields. The bar denotes an average over volumes large compared to  $\ell^3$ . The principal problem addressed in past work has been the determination of small scale fields which would lead to regeneration of the large scale field  $\mathbf{B}$  through the interaction term  $\overline{\mathbf{U}' \times \mathbf{B}'}$ . A recent successful study by Moffatt (1970, (a,b), 1972) restricts attention to forced quasi-linear processes (e.g. small amplitude inertial waves). Moffatt concluded that to a first approximation

$$\overline{\mathbf{U}' \times \mathbf{B}'} = \alpha_{ij} B_j \mathbf{e}_i \quad (1.2)$$

where  $\alpha_{ij}$  is a symmetric tensor which is a function of the spectrum of the mean 'helicity' ( $\equiv \overline{U' \cdot \nabla \times U'}$ ) of the small scale flow. At large amplitudes  $\alpha_{ij}$  will depend also upon the mean fields  $\underline{B}$  and  $\underline{U}$  in a complicated manner. In his 1972 paper, Moffatt finds a finite-amplitude equilibrium for  $\underline{B}$  in a homogeneous unbounded medium due to this dependence of  $\alpha_{ij}$  on  $\underline{B}$ .

An alternate mechanism which can restrict the growth of unstable magnetic fields is the concomitant development of large scale velocity fields. In a global geometry such velocity fields must exist because all finite magnetic fields compatible with global boundary conditions will produce Lorentz forces. The dynamical equation for the mean fields in an incompressible rotating fluid is written

$$\frac{\partial \underline{U}}{\partial t} + \underline{U} \cdot \nabla \underline{U} - \frac{1}{\mu \rho} \underline{B} \cdot \nabla \underline{B} + 2\Omega \times \underline{U} + \nabla P = \nu \nabla^2 \underline{U} - \frac{\partial}{\partial x_j} (\overline{U'_i U'_j} - \mu \rho \overline{B'_i B'_j}), \quad (1.3)$$

where  $\Omega$  is the angular velocity of the frame of reference,  $\nu$  is the kinematic viscosity,  $\mu$  is the magnetic permeability,  $\rho$  is the density,  $P$  is the effective pressure, and the mean terms on the right are the Reynolds stresses due to the small scale process. Anticipating that the principal balance of forces for the evolved fields will be the magnetostrophic balance between the Lorentz force, the Coriolis force, and the pressure, we will scale the variables so that these are the leading terms in Eq. (1.3). To satisfy the fluid boundary conditions, the viscous term must be retained as a singular perturbation. The determination of a finite-amplitude solution consistent with this scaling justifies the magnetostrophic balance, if in addition it can be established that the Reynolds stresses (and any other large scale body forces) are small compared to the Lorentz force.

Hence we visualize an equilibration of the growing magnetic field by "back e.m.f.'s" (i.e.  $\underline{U} \times \underline{B}$ ) and increased ohmic dissipation resulting from the magnetostrophic velocity field.

The basic stability problem posed in Eq. (1.1) has been solved in a kinematic sense for a variety of assumed  $\alpha_{ij}$ . Recent numerical work by Roberts (1972) explores the (linear) structure of growing magnetic fields compatible with global boundary conditions for  $\alpha_{ij}$  and  $\underline{U}$  prescribed

as smooth functions of position. However, we will find that the solvability conditions for magnetostrophic balance impose conditions on the field  $\underline{u}$  which markedly alter this entire class of kinematic problems.

The complexity of global magnetic fields as exemplified by Roberts' numerical models suggests that analytical study of the mechanisms of finite amplitude balance will be possible only for the simplest choices for  $\alpha_{ij}$ . However, the finite amplitude problem for arbitrary  $\alpha_{ij}$  is formulated and certain general conclusions are drawn concerning the role of dissipation and the conditions for subcritical instability\*. In order to establish that finite amplitude solutions with and without finite viscous effects indeed exist, the example of constant  $\alpha$  (i.e.  $\alpha_{ij} = \alpha \delta_{ij}$ ) is then studied. The linear eigenvalue problem has been solved by Krause and Steenbeck (1967). Here certain self-adjoint aspects and degeneracies of the linear problem are outlined before proceeding to the nonlinear problem. It is found that the first equilibration of the unstable magnetic field is achieved by viscous dissipation of the induced flow, Ohmic dissipation and 'back e.m.f.'s' finally determine the balance in the next order of the finite amplitude expansion. Most significantly, the appearance of zonal flows due to zonal Lorentz torques requires that parts of the problem be reordered to treat the important case of small viscosity. This reordering is done so that the finite-amplitude fields and flows become independent of the viscosity for vanishingly small viscosity. In general this is possible only if a zeroth-order zonal flow is determined so that the initially unstable magnetic field produces no mean zonal torques. Fortunately the constant  $\alpha$  case leads to no zeroth-order zonal flows and the finite-amplitude problem can be approximately closed at third order. To do so requires the determination of the meridional flows from which an upper bound on magnetic field amplitude is found without requiring solutions for the magnetic field distortions or second order zonal flows,

The intricate interplay of fields and flows needed to achieve a nonlinear macrodynamical dynamo balance is reassessed in a conclusion. A final topic discussed is the parameter range in which the macrodynamical

restraints on dynamo growth are likely to be more important than restraints on dynamo growth due to the reduction of  $\alpha \omega$  by the mean fields.

#### WIND-INDUCED INTERNAL WAVES IN A STRATIFIED OCEAN

Martin T. Mork

Using linear dynamics and an eddy viscosity coefficient which is inversely proportional to the static stability the response is derived with aid of series expansion in eigenfunctions. The eigenfunctions which contain the vertical dependency are the same as in the nonviscous case of free internal waves. The internal response is weak in a laterally unlimited ocean with flat bottom, but is increased by a factor of 10 when a lateral boundary is introduced. When the ocean is made up of a deep and a shallow region the internal modes are effectively excited as a result of the transformation of the forced surface mode. In a practical example the displacement in the interior is found to be more than 1000 times that of the surface.

#### MODELS OF EDDIES AND WAVES

Peter B. Rhines

Computer experiments with a two-layer ocean (or atmosphere) show what happens when two-dimensional turbulence is subjected to a number of geophysical effects: stratification,  $\beta$  (the northward gradient of Coriolis parameter,  $f$ ), isolation (intermittency), and bottom topography. The tendency of geostrophic eddies to cluster and increase in size (and to avoid turbulent dissipation) without limit can be defeated by any of the above effects:  $\beta$  halts the migration to large scale,  $L$ , when  $L^2$  reaches  $2U/\beta$ , where  $U$  is the rms particle velocity; isolation of a patch of eddies halts the cascade when  $L$  approaches the size of the patch; rough topography causes a cascade to small scales if  $\delta > U/fL_h$ ,  $\delta$  being the rms roughness height scaled by the ocean depth,  $L_h$  its dominant scale. Intensification of the currents can then occur

near the ocean bottom. Smooth topographic slopes limit the size as does

$\beta$  Finally, stratification allows a cascade from large scales to small via baroclinic instability. If, however, one starts with a field of baroclinic eddies smaller than the internal deformation radius, they evolve into larger eddies coherent in the vertical: that is, the turbulence can quickly convert energy from baroclinic to barotropic flow, while increasing  $L$ .

Estimates show that both the atmosphere and ocean are in states near to those occurring in the experiments.

#### ARCHIMEDEAN INSTABILITIES IN TWO-PHASE FLOWS

Edward A. Spiegel

The equations for two-phase flows contain the description of a number of interesting natural phenomena in different limits. The prototype of such flows is the fluidized bed for which a laboratory demonstration was given. Such beds are frequently unstable as a result of differential buoyancy forces. The relation to solutal convection, Childress' bioconvection equations, and the flow of radiation through matter was discussed starting from the basic two-fluid equations. Under appropriate conditions each of these flows exhibits an Archimedean instability and the nonlinear development of such instabilities in the different cases was speculated on.

#### DIABATIC AND WIND STRESS ADJUSTMENTS OF ROTATING CURRENTS

Melvin E. Stern

There are many studies of the influence of spatially varying wind stress and heating functions upon the ocean, the most familiar being the Sverdrup circulation and the theory of wind-generated internal waves. But a horizontally uniform wind stress or surface cooling can also generate interesting internal motions, provided they act upon a "pre-existing" vorticity in the ocean. A motivating example for the discussion of the latter effects is provided by recent (MEDOC)

observation of the formation of Mediterranean bottom water when the cold-dry mistral blows in winter. Here the preexisting vortex has a relatively high surface salinity (and relatively low static stability) at its center. With the onset of the mistral the thermocline at the center of the eddy is eroded, and cold water is eventually supplied to the Mediterranean abyss. Convection from the surface to the bottom only occurs, however, in such isolated regions, whereas the major portion of the sea does not overturn in winter.

Thus the question is raised as to the geostrophic adjustments in the vortex during the cooling process, but prior to the time of mixing from top to bottom of the ocean.

Various models have been explored in order to parameterize the diabatic effects and to examine the resulting dynamical consequences. For example, we have considered a two-layer model containing a geostrophic jet in the upper layer. We then allow the density of the upper layer to change in time, these density changes being (somehow) related to the thermodynamic effects produced by surface heating or cooling. If the heating function varies rather rapidly (diurnally) in time then inertia oscillations can be generated and resonantly amplified (at the inertia frequency) by interaction with the undisturbed jet. With regard to the slower geostrophic adjustment problem, we plan to devise a model for a uniform rate of surface cooling, and in which horizontal variations in density will be allowed in a modified two-layer system. From such models we may determine the vortex conditions, such that the internal interface surfaces before the entire thermocline becomes gravitationally unstable.

#### THERMOCLINE IN A ROTATING ANNULUS

Melvin E. Stern

We investigate the steady, laminar, and axial symmetric circulation in a semi-insulated annulus of height  $H$  and width  $L$ , when a uniform radial temperature gradient  $\Delta T/L$  is imposed on the rigid upper surface. The rotation rate  $f/2$ , the viscosity  $\nu$ , and the conductivity  $\kappa$  are restricted to a range such that all of the radial heat transport is



accomplished in an upper Ekman layer, the thickness  $(\nu/f)^{1/2}$  of which is small compared to the vertical scale depth  $h$  of the thermocline. The horizontal velocity in this region of the thermocline is geostrophic, and the downward diffusion of heat is completely balanced by upwelling from a lower Ekman boundary layer. We find that the maximum depth of the thermocline is equal to a numerical constant multiplied by

$$h = L \left[ \frac{K^{1/2} f^{3/2}}{g \alpha \Delta T} \right]^{1/2} \left( \frac{K}{\nu} \right)^{1/4} \ll H$$

The thermocline regime is similar to that which H. T. Rossby found in a nonrotating experiment, insofar as the cold sinking motions are confined to an isolated region of very weak static stability, but the detailed solution for this sidewall boundary layer is not considered here. Our solution differs from previous oceanic thermocline theories because meridional barriers and  $f$ -variations are absent. Moreover, this relatively simple thermocline theory is also crucially dependent on the rigid upper boundary, a condition which is of course absent in the real ocean. Nevertheless the regime is experimentally realizable, and such experiments should complement related work in a heated rotating annulus (Hide). The latter employ heating and cooling at the sidewalls of an annulus, whereas we want to investigate the case where the heat sources and sinks occur on the same level (top) surface. Despite this difference in boundary conditions we expect that the symmetric thermocline will become baroclinically unstable and geostrophic eddies will form, as is the case in Hide's experiment. It would be most interesting to observe the effect of such eddies on the value of the thermocline depth,

#### MODEL OF WORLD OCEAN CIRCULATION

George Veronis

In preparation for a more comprehensive study the present analysis develops a picture of steady global ocean circulation as it would appear if the ocean were driven only by the wind stress at the surface. The spherical geometry is retained but bottom topography is neglected and the lateral boundaries of the different basins are segments of parallels

of longitude or latitude. The observed zonal wind stress is zonally averaged for each basin and the stratification is represented by two homogeneous layers which are dynamically uncoupled, i.e., there is no stress transfer across the interface or thermocline,

Outside of boundary layers geostrophic flow is modified only by wind stress. The downstream flow in boundary layers is geostrophically balanced but the momentum balance of the cross stream flow is not specified. The requirement that the net transport across a latitude circle must vanish then suffices to yield most of the gross features of the circulation.

A simple argument is put forth to show that eastern boundary layers are required as part of the general circulation. Several types of eastern boundary currents arise. At mid-latitudes the California, Peru and Portugal-Canary Currents form one class. The Benguela serves a different function. The Norwegian, Alaska and Cape Horn Currents form a third class. The Flinders Current, actually a zonal boundary current in the Great Australian Bight, also falls in a separate class. All of these boundary currents affect the separation of the western boundary currents from the coast by imposing requirements on the amount of water that must be carried by the latter. However, the mechanism differs from class to class.

An analysis is presented for the manner in which a western boundary current separates from the coast, follows an open ocean path and penetrates through the normal "barrier" formed by the vanishing of the wind stress curl. The western boundary current ends up as a relatively narrow poleward current in the subpolar eastern side of the ocean. In this sense the Norwegian is part of the Gulf Stream, the Alaska is part of the Kuroshio and the Cape Horn is part of the East Australian-New Zealand Current.

The Agulhas separates from the coast at the south tip of Africa and reenters the Indian as the Return Agulhas Current. If the wind stress curl in the Indian were weaker, the Agulhas could round the Cape of Good Hope and transport a massive amount of warm Indian water into the South Atlantic. It is suggested that the transient winds in the Indian probably lead to periods when there are such leaks of Agulhas water into the Benguela Current.

The (cold water) flow between South America and Antarctica appears to be blocked by meridional barriers to zonal flow. The Antarctic Convergence is identified as the eastward jet that forms because of the presence of these barriers.

A rough classification of western boundary currents is offered to explain the different behavior exhibited by the several currents. Finally, it is shown that the different Convergences serve very specific functions and that the presently used classification attaches the same name to Convergences that serve different functions.

### OCEANIC MICROSTRUCTURE

Andrei S. Monin

Microstructure of the ocean is significant especially because of the importance of its vertical stratification, including in it the presence of thin quasi-horizontal layers with sharp vertical gradients of thermodynamic parameters. So microstructure appears evidently to be a special property of stably stratified liquids in general.

Microstructure appears in the form of steps in measurements with fast response probes of vertical profiles of temperature, conductivity and sound speed (in the last case, it appears especially sharp). It appears also in profiles of salinity computed from temperature and conductivity and evidently should appear on profiles showing refraction; but on profiles of density "steps" it usually appears equal to the experimental and numerical error levels,

Microstructure appears sometimes also in the so-called "mixed" surface layer of the ocean, is more diffused at the thermocline and evidently takes place in all the water masses to the bottom. It is encountered in the ocean almost everywhere, but apparently is more intense in the zones of significantly horizontal non-uniformity (for example, in currents), and evidently should be absent in regions of winter convection.

The lifetime of microstructure layers has a lower limit of the order of many hours. Microstructure layers are generally hydrostatically

stable, although distinct layers with inverted density occasionally appear (with lifetime of the order of 10's of minutes).

The thickness of microstructure layers varies from 10's of meters to millimeters. Their statistics are still inadequately studied. Examples exist of computed spectra of vertical gradients of temperature in microstructure.

The following hypotheses exist for the generation mechanism for microstructure: (a) double diffusion, i.e. different coefficients of heat and salt diffusion (however microstructure appears also in the fresh water lake Loch Ness; the possibility of double diffusion of heat and momentum in the presence of currents has not yet been investigated); (b) instability of internal waves or their breaking; (c) lateral currents in the condition of horizontal inhomogeneity, produced by isopycnal (isentropic flow) or internal and inertial waves with approximate vertical wave vectors.

Measurements by a series of authors of microstructure have appeared also on the vertical profiles of horizontal current velocity. Evidently it often correlates with the temperature microstructure and in it appear tendencies to variations with inertial periods.

Turbulence in the presence of microstructure is weak, having a small Reynolds number (i.e. not developing and not having a universal statistical structure) - for fluctuations of conductivity the last is true down to the minimal spatial scale and does not show any kind of characteristic dependence on depth.